Transport of Atmospheric Aerosols Above

the Sierra Nevada Slopes

Final Report on Research Contract A4-127-32

L. O. Myrup

R. G. Flocchini

Diane Ewell

Department of Land, Air and Water Resources

University of California

Davis, CA 95616

January 15, 1989

Disclaimer

The statements and conclusions in this report are those of the contractor and not necessarily those of the California Air Resources Board. The mention of commercial products, their source and their use in connection with material reported herein is not to be construed as either an actual or implied endorsement of such products.

ABSTRACT

The general objective of this program was to document the boundary-layer transport of aerosol pollution into Sequoia National Park. To accomplish this, four measurement programs were carried out: (1) Tethersonde profiles of temperature, humidity, and wind velocity, (2) tethered balloon measurements of aerosol concentrations, (3) Pibal wind measurements at three sites in the park, and (4) measurement of surface meteorological parameters at the pibal wind sites. These data were collected during July and August 1985 at Emerald Lake, Wolverton Meadow, and Ash Mountain. The following conclusions are drawn from the data: 1) When averaged over the entire concentration period, the concentration of all fine elements reported is higher in upslope conditions than in other conditions; 2) the fluxes of most elements also exhibit similar behavior; 3) the concentration of certain coarse elements shows a strong tendency to increase upward in the lower 200 m during the nighttime hours; 4) the potential for "smog front" phenomena seems to exist in the lower regions of the park, due to convergence in the meso-scale wind field, 5) The upslope/downslope boundary-layer, meso-scale, and large-scale winds seem to interact in a complex fashion to produce the observed transport.

4

Table of Contents

*Note that the apendices are numbered beginning with page 1. This is
because the thesis is viewed as an independent document that is added to
this report to aid the reader and to provide depth and breadth to the
material presented.

List of Tables

List of Figures

I.   INTRODUCTION

Sequoia National Park, located east of the San Joaquin Valley in central California, is noted for its unique panoramic vistas and as a primary location for an extensive acid deposition research program. This research program encompasses wet and dry deposition effects on vegetation, soil, lakes, and streams. This report summarizes measurements we made during summer 1985 of pibal winds aloft and surface meteorological parameters at three locations (Ash Mountain, Wolverton Meadow, and Emerald Lake) and vertical profiles of temperature, humidity, winds, and particulates using tethered balloon techniques at Wolverton.

II. MEASUREMENTS

A.   Introduction

During this study, we collected data at three sites in Sequoia National Park during two ten-day intensive sampling periods in July and August of 1985. The data from the July period are incomplete because of equipment problems. At all three sites we released single theodolite-tracked pilot balloons 4 times a day and twice nightly 50 percent of the time. The calculated ascent rate was 3 meters per second (30 gram free-lift weights). Observations were recorded every 30 seconds, yielding wind observations every vertical 90 meters. The Atmospheric Science Department of Fresno State University also released 4 balloons per 24-hour period in Fresno at times which roughly corresponded to the release times used in the park.

At all three sites 23 setup ground weather stations with instrumentation measuring wind speed, wind direction, relative

humidity, and temperature at five meters and temperature again at two meters. Every 30 minutes, mean relative humidity, temperature, wind speed, mean wind vector magnitude, wind direction, and standard deviation of direction were recorded.

Additionally, we operated dual tethered balloons were operated at the middle elevation site. On one balloon a meteorological sounding package (tethersonde) was attached which measured pressure (change), dry- and wet-bulb temperatures, wind speed and wind direction. On the tether line of the other balloon, two-staged stacked filter unit aerosol samplers were attached at intervals of 50 meters up to 250 meters above the ground. The filters were analyzed for elements heavier than sodium using an alpha particle induced x-ray emission (PIXE) technique developed at the Crocker Nuclear Laboratory at the University of California, Davis (Cahill et al. 1976). Elemental mass is measured above a threshold value which is determined by the filter characteristics, particle loading, and sensitivity of the x-ray detector. In addition, the filters were weighed using a Cahn electrobalance and the fine filters were analyzed for carbon soot and elemental hydrogen.

This study was the first time we employed the aerosol sampling balloon system in the field. The system was tested, however, prior to the present study at the University of California, Davis, for short periods. We made a total of 5 morning, 9 afternoon, and 3 evening aerosol profiles during the August field period. We made a total of 7 morning, 15 afternoon, and 7 evening meteorological profiles as well. Table 1 shows the schedule for the July and August field periods.

Table 1   Schedule of tethered balloon runs. For samplers, time indicates when the first pump began and total minutes indicate the longest sampling time, usually corresponding to the sampler at the highest level (except where indicated). The levels 0, 1, 2, 3, 4 and 5 correspond to 0, 50, 100, 150, 200, and 250 meters, respectively. For each level, the sampling time was 5 minutes on average less than the level above it. If, for example, all 5 levels were in operation, then the sampling time difference between the lowest and highest level would have been approximately 20 minutes. The sounding schedule also shows the starting time and indicates the duration of the up and down soundings. Also listed are Fresno temperature (T), dewpoint temperature (DT), and station pressure (P).

DATE	TIME	SAMPLERS TOT. MIN.	LEVELS	TIME (PDT)	TETHERSONDE MIN. UP	MIN. DOWN	FRESNO °C T	DT	mb P
7/25	0934	59	0,1,2	1005	34	--	30.0	17.8	997.8
7/26*	0920	70	0,2	0959	23	__	28.3	16.7	1001.2
7/26	1242	72	0,1,2,3	1300	09	__	35.6	15.0	1000.2
7/26*	1426	34	0,4	1440	09	__	36.7	15.0	999.2
7/27				1354	08	17	37.8	12.8	999.2
7/28				0838	26	18	26.7	13.9	999.8
7/28				1101	15	08	31.7	12.8	999.5
7/28				1143	12	05	33.9	11.1	999.2
7/28				1220	12	10	36.7	10.0	998.8
7/28				1647	22	14	38.3	8.9	996.4
7/28				1818	17	15	37.8	8.3	996.1
7/28				2224	22	14	26.7	13.9	997.5
7/29				0411	13	10	18.9	10.6	998.5
7/29				0624	27	20	16.7	11.1	1000.5
7/29				0746	20	15	17.8	11.1	1001.2
7/29				0857	20	12	19.4	11.7	1001.5
7/29				1132	09	12	26.1	11.1	1001.2
7/29				1255	18	13	28.9	10.0	1000.8
7/30				0743	17	17	17.2	12.2	1002.5
7/30				0855	19	12	20.0	12.8	1002.9
7/30				1114	17	27	23.9	12.8	1003.2
7/30				1510	13	18	30.6	12.8	1001.5
7/30				1805	14	11	31.7	10.6	999.5
7/30				2208	14	09	25.0	12.2	999.8
7/31				0727	12	07	17.7	11.7	1002.5
7/31				1138	13	16	25.0	12.2	1003.2
8/13	1020	83	1,2,3				23.3	12.2	1003.9
8/14	1416	92	1,2,3	1445	37	17	32.2	01.6	1000.8
8/15	0902	96	1,2,3	0845	45	16	22.2	12.2	999.5
8/15*	1446	97	1,2	1450	16	13	33.9	11.7	997.0
8/16	0859	128	1,2,3,4	0923	11	24	23.9	13.3	997.1
8/16				0958	25	20	23.9	13.3	997.1
8/16	1643	134	1,2,3,4	1649	18	17	34.4	12.8	994.4
8/16				1656	16	15	34.4	12.8	994.4
8/16				1811	17	20	33.9	12.2	994.1
8/17				0824	28	28	17.8	13.9	1001.5
8/17	1627	134	2,3,4,5	1629	46	40	29.4	15.6	1000.8

DATE	TIME	SAMPLERS TOT. MIN.	LEVELS	TIME (PDT)	TETHERSONDE MIN. UP	MIN. DOWN	°C T	DT	mb P
8/17				1755	16	17	29.4	15.6	1000.5
8/18	0936	134	2,3,4,5	0954	22	30	20.0	12.8	1006.3
8/18				1127	27	28	25.0	15.0	1005.9
8/18	1648	102	2,3,4,5	1640	25	13	31.7	14.4	1003.2
8/18	2301	109	2,3,4,5	2324	21	17	22.8	11.7	1003.2
8/19				0002	39	22	22.8	11.7	1003.2
8/19	1443	115	1,2,3,4,5	1148	29	35	30.6	12.8	1003.2
8/20	1002	106	2,3,4,5	1056	38	32	26.7	14.4	1003.2
8/20				1206	26	30	29.4	13.9	1002.9
8/20*	1638	106	2,3,4,5	1639	31	20	33.3	10.6	1000.2
8/20				1730	22	06	33.9	9.4	999.8
8/21*	0406	112	1,2,3,4	0414	20	23	18.9	8.9	1002.5
8/21				0457	22	21	18.3	8.9	1002.5
8/21				1402	48	28	32.8	12.2	1003.6
8/21	1656	112	2,3,4,5	1704	31	40	34.4	11.1	1001.9
8/21				1900	43	29	33.3	11.7	1001.5
8/21	2216	121	1,2,3,4	2053	36	29	28.9	13.3	1002.2
8/21				2251	43	33	25.6	12.2	1002.9
8/22*	1349	114	2,3,4,5	1456	22	15	35.0	10.6	1002.9

* 7/26: (0920) 100m batteries exploded at unknown time, 70 minutes estimated.
 7/26: (1416) 200m batteries exploded at unknown time, 29 minutes estimated.
 8/15: (50m sampler brought down early due to high windspeed, total time was 32 minutes.
 8/20: 250m intake tube came off at unknown time, 106 minutes estimated.
 8/21: 50m batteries quit at unknown time, 97 minutes estimated.
 8/22: 100m batteries quit at unknown time, 102 minutes estimated.

B.   Sites

The three experimental sites were located at or near Sequoia National Park's long-term primary acid deposition research sites established in 1982 through funding from the congressionally mandated 10 Year National Acid Precipitation Assessment Program. Figure 1 is a map of the study area. For the study, the lower elevation site at Ash Mountain was 125 meters northwest of and 30 meters above the Park Headquarters area at 560 meters elevation. The site was located on a east-southeasterly facing slope in the chaparral community vegetation. The mid-elevation site, Wolverton, was 1.5 kilometers southwest of the Lodgepole campground and 1 kilometer from the General's Highway by road at 2222 meters elevation. Balloons were launched in the middle of Wolverton Meadow, which is surrounded by mixed-conifer community vegetation.   The upper elevation site, Emerald Lake, was 3.5 kilometers east of the Lodgepole campground along the Marble Fork west of Pear Lake at 2719 meters elevation. The site was located on a flat granite area sparsely vegetated with sub-alpine community species. The weather stations were located near the balloon release sites. At Ash mountain, the weather station was located at the Park Headquarters area.   The instrumentation was located at ten and seven meters on the park's meteorological tower instead of at five and two meters above the ground as at the other two stations because of the tall oak trees surrounding the area.   The weather station at Wolverton was near a maintenance road directly across Wolverton Meadow from the ski resort/trail head parking lot and was surrounded by low-lying meadow vegetation.   At Emerald Lake, the weather station was located on a large granite outcrop, using a dead standing tree as the instrument
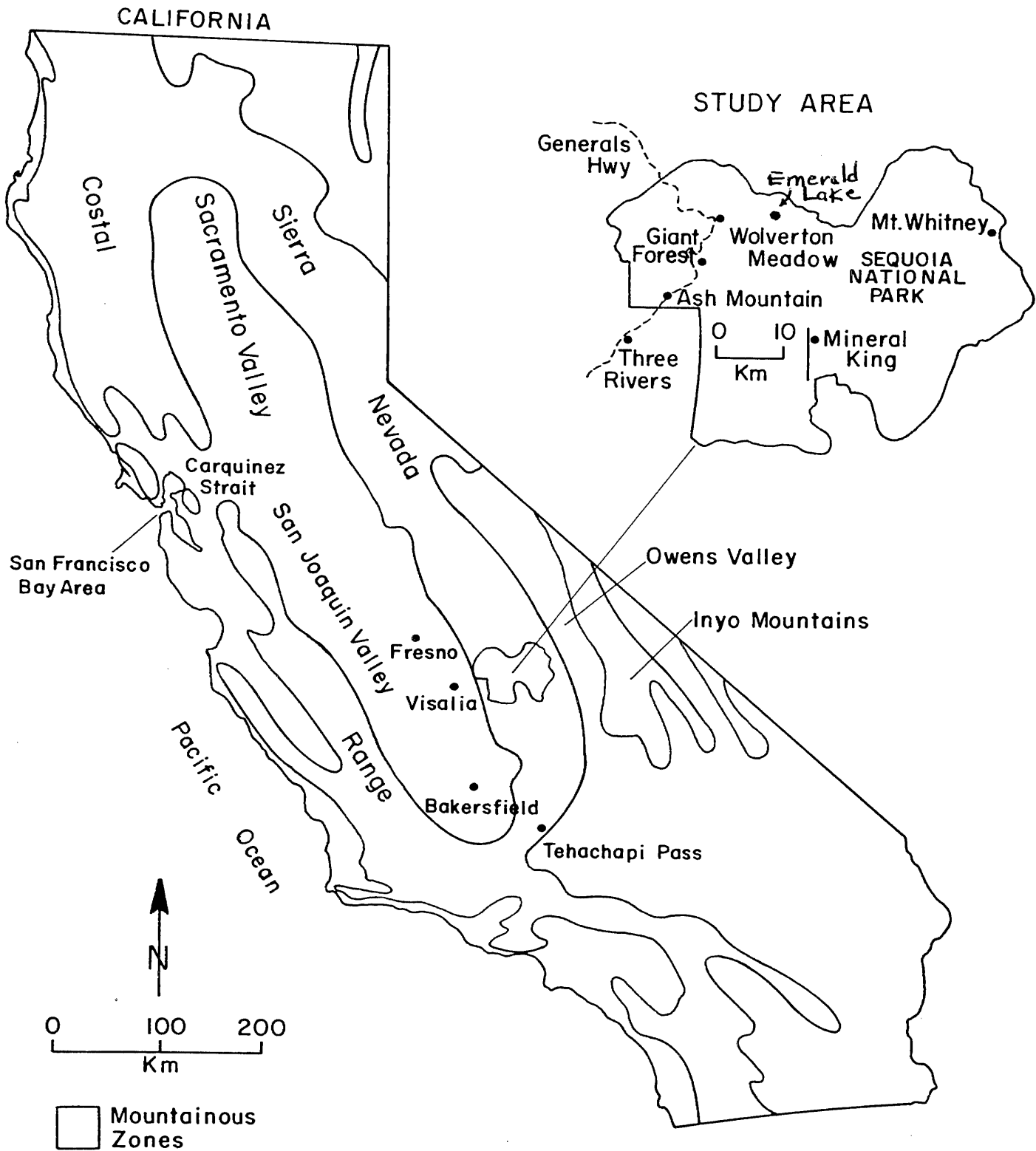
Figure 1. Map of Study Area

tower. The data were recorded on CR21 microloggers (Campbell Scientific, Inc., Logan, Utah) and transcribed manually twice a day.

The special requirements of the tethered balloon systems, namely storage area and electricity, greatly limited the possible locations for the mid-elevation site. Electricity was not required but was convenient for charging the 12-volt batteries needed for the winch operation and was used to operate the receiver and printer ground station. For these reasons the Wolverton site was chosen and as a result, the features of this location are slightly different from those at the park's research site in Log Meadow. The other two sites are more comparable to the Park research sites. The Wolverton Meadow is in a bowl that faces to the north and is used as a ski area during the winter season. Localized inversions are frequent and break up in late morning. The topography has more gradient and is more complex than in the gently rolling Giant Forest area.

The topographic features for the three sites are presented in Table 2. Fresno is included for comparison. The values were estimated using 15-minute quadrangle maps. Directions are from true north and indicate the direction toward the specified parameter. For example, the up-valley direction for Emerald Lake is 90 degrees. This indicates that the Marble Fork Valley rises toward the east near the Emerald Lake site. Since the topography is variable and does not follow a straight line, an imaginary line was drawn perpendicular to the valley axis and through the site, representing a cross section of the valley at the site. The direction of a line perpendicular to this at the valley floor was the recorded up-down valley direction. Valley floor width was measured by the distance between the two intersection

points of the lowest contour line and the cross section line. The distance between the first contour above and below the valley axis line was used to measure the valley floor slope. Distance ridge to ridge was measured by a cross section of the valley perpendicular to the orientation of the highest ridges on either side of the valley, which was not always the same as the cross section through the site. To determine the general slope orientation surrounding the site, the ground weather station wind directions were also considered in addition to the maps. Slope inclination was then calculated by a line drawn from the site to the second 400 foot contour line above the site using the up-slope direction. For Fresno, the valley floor was approximated by the distance between the beginning of the coastal range to the west and the foothills to the east at the 1000-foot contour levels. The distance ridge to ridge was taken along the same line but extended to the Fresno County line on either side. The slope of the San Joaquin Valley was considered approximately zero.

C. Equipment

1. Aerosol Sampling Unit

The weight of each sampling unit including batteries, and filter cassettes assemblage was less than one kilogram. A review of the aerosol sampling system may be found in Flocchini (1984).

a. Filter cassette assemblage

The stacked filter cassette design is described in Cahill, et al. (1977). The only differences in the configuration for this study were that an intake manifold was not used and the filter cassette hung downwards toward the ground from the tether line. For the coarse and fine particle modes, 8.0-micron coated nuclepore filters and 3 micron

TABLE 2: TOPOGRAPHIC FEATURES

	EMERALD LAKE	WOLVERTON	ASH MOUNTAIN	FRESNO STATE
Longitude	118.68	118.73	118.83	119.75
Latitude	36.62	36.60	36.50	36.93
Township	15S	15S	16S	13S
Range	30S	30E	29E	20E
Section	24W	29NE	33E	5SE
Elevation (m msl)	2719	2222	560	100
Height Above Valley Floor (m)	10	200	50	0
Up/Down Valley (degrees)	90/270	080/260	020/210	135/315
Valley Floor Width (m)	250	100	125	100 km
Ridge Height (m msl)	3400 SE 3400 NNW	2750 SE 2450 NW	1900 E 1080 W 1600 NW	1200 W 4000 E 2000 SE
Ridge Height Above Site (m)	767 SE 767 NNW	528 SE 228 NW	1340 E 520 W 1040 NW	1100 W 3900 E 1900 SE
Distance Ridge To Ridge (km)	5 N-S	10.9 NNW-SSE	7.4 NW-SE	200 SW-NE
Valley Floor Slope (%)	5	6	7.5	0
Upslope/Downslope (degrees)	150/130	135/315	300/120	090/270
Slope Inclination (%)	18	10	23	

teflon filters were used, respectively, which were both 25 millimeters in diameter. The manufacturer's filter specifications are listed in Table 3.

b. Motor and pump assemblage

Astro Challenger Cobalt 05 motors designed for model airplanes by Astro Flight were employed to drive the modified GAST rotary vane vacuum pumps. They were powered by two lithium cell batteries (50 ampere-hour) which lasted approximately 3 to 4 hours without an appreciable decline in output.

Table 3: Membrane Filter Specification

Filter Type	Mfg. Code	Pore Dia. μm	Pore Dens. pores/cm	Filter Thick. μm	Por- osity %	Filter Dia. mm	Filter Area cm^2
Teflon[1]	PTFE	3	1 x 10	25	75-85	25	1.1[2]
Nuclepore[4]	N800	8	--	10[3]	5	25	3.8

1. Gelman Science, Ann Arbor, Missouri.
2. Masked filter area.
3. Values are for uncoated filters. Apeizon-L grease coated filters (lot 51A8B2) were used during this study which increased the thickness by 30 to 65 μm (actual value unknown).
4. Nuclepore Corp., Pleasanton, California. ampere-hour) which lasted approximately 3 to 4 hours without an appreciable decline in output.

During the July field program, we discovered that the pumps were rotating too fast; we reduced the speed by one third for the August field program. This reduced the average flow rate from 11.9 ± 1.7 to 1.05 ± 1.8 liters per minute but improved the battery performance remarkably, resulting in only one case of battery explosion during the August period compared to a 30+ percent failure rate during the July period.

Flow rates were measured at the beginning and end of each sample, and flow volumes were estimated as described in Appendix II-B. The cut-point between fine and coarse collection stages was between 1.0 and 1.5 microns aerodynamic diameter. The coarse filter probably had no practical upper cut-point due to the high face velocity (46 centimeters per second) and the absence of an intake manifold. The calculated upper cut-point was approximately 123 microns aerodynamic diameter. This includes most coarse particles suspended in the atmosphere!

2. Tethersonde

Specifications for the tethersonde package and balloons are contained in the Appendix II-C. The meteorological package is described in Morris, et al. (1975). Since barometric pressure at the site was not measured, pressure was calculated using Fresno airport hourly station pressure observations and the hydrostatic equation. The equation for this calculation as well as equations for calculating potential temperature, mixing ratio, absolute humidity, and other secondary meteorological parameters are presented in the Appendix II-D.

D. Filter Analysis

The fine teflon filter was used with a mask to decrease the sample area by 70 percent, thus increasing the sensitivity of the elemental analysis. The samplers were run from one to two hours, allowing detection of major elements present at higher concentrations in the atmosphere. Minor elements such as lead and vanadium were frequently below the sensitivity threshold. The accuracy of the PIXE elemental analysis, determined by regular re-analysis of filters, is reported as 4 percent for sulfur, 6 to 9 percent for silicon, potassium, calcium,

iron and zinc and 10 to 15 percent for copper, lead and bromine. A new analytical method, proton elastic scattering analysis (PESA), was used to analyze the fine filters for elemental hydrogen as well. The current accuracy for this method is approximately 15 percent.

Filters were analyzed for gravimetric mass and carbon soot (fine filters only) using a Cahn 25 electrobalance and a laser integrating plate method, respectively (Cahill et al. 1984). The uncertainty associated with the Cahn electrobalance is on the order of 2 micrograms, which would correspond on average to a 6 and 7 percent uncertainty for the fine and coarse gravimetric mass concentrations, respectively. An additional uncertainty associated with weight gain is discussed below. For the carbon soot calculation, an absorption efficiency of 10 m^2/g is used to convert the coefficient of optical absorption to carbon soot concentration. The uncertainty of the measurement technique is approximately 6 to 7 percent. Table 4 lists the averages and associated errors for the fine and coarse elemental, gravimetric mass, and carbon-soot data. Table 4a gives a more detailed analysis in which average values for all afternoon (upslope) and all evening and/or morning (downslope) soundings are shown separately.

To investigate artifact weight gains, filter blanks were prepared and treated identically to the filters used for sampling, except that they were not loaded into the filter cassettes. A small weight gain was observed. It is possible that the major weight gain for the teflon filters is through interaction with the plastic material of the filter cassettes (Feeney et al. 1984). Weight gain from contact of the teflon filters with the O-ring was avoided by using filter masks. The weight

Table 4: Elemental concentrations averaged over all profiles and heights for August 13th through 22nd, 1985.

	FINE						COARSE				
Al	1	2	Fe	1	2	Al	1	2	Fe	1	2
avg.	189	139	avg.	71	69	avg.	1217	982	avg.	543	575
s	87	46	s	45	25	s	1050	391	s	839	202
err	21	11	err	22	10	err	39	16	err	24	12
s	10	<1	s	10	<1	s	17	2	s	11	<1
up	19	9	up	34	9	up	29	9	up	34	9
down	11		down	25		down	19		down	27	
Si	1	2	S	1	2	Si	1	2	S	1	2
avg.	260	268	avg.	630	713	avg.	1786	2234	avg.	320	89
s	136	90	s	299	123	s	1223	781	s	146	16
err	19	10	err	14	10	err.	25	11	err.	68	82
s	9	<1	s	8	<1	s	10	<1	s	22	7
up	33	9	up	33	9	up	33	9	up	8	2
down	28		down	29		down	27		down	6	
K	1	2	Mass	1	2	K	1	2	Mass	1	2
avg.	61	143	avg.	36	14	avg.	284	262	avg.	27	14
s	33	29	s	33	2	s	259	71	s	19	3
err	33	10	err	6	1	err	51	18	err	7	1
s	19	<1	s.	--	--	s	17	3	s	--	--
up	33	9	up	34	9	up	19	9	up	33	9
down	26		down	15		down	22		C-S	1	2
avg.	1119	420									
s	616	108									
err	7	7									
s	--	--									
up	33	9									
down	27										

1. Avg. = average concentration; s = standard deviation of the concentration; err = average error for concentration; g = standard deviation of the error; up = number of afternoon concentrations in average; down = number of morning and/or evening concentrations in average.

2. mass = (μg/m^3)

    elements and carbon-soot = ng/m^3

3. 1 = Tethered Balloon.

    2 = Giant Forest 24 hour data.

Table 4a: Elemental concentrations averaged for all afternoon (upslope) and all morning and/or evening profiles (down slope) for the period 13 August through 22 August, 1985.

	afternoon			morning & evening			
Element	mean	s	n	mean	s	n	df
FINE							
Mass	39.1	19.3	34	33.1	11.0	29	61
S	849.5	191.9	33	380.8	179.4	29	60
K	73.3	33.8	33	45.9	26.3	28	59
Si	304.7	148.9	33	207.0	96.3	28	59
C-S	1474.3	705.6	33	684.7	434.7	27	58
Ca	33.2	16.6	22	34.0	13.7	15	35
Fe	84.3	50.8	34	52.5	23.7	25	57
Pb	61.7	37.0	12	58.1	30.5	11	21
H	580.9	155.0	33	386.6	146.8	26	57
Al	152.9	65.1	34	140.0	62.2	30	62
COARSE							
Mass	27.9	14.4	33	25.7	15.0	30	61
Si	2137.2	1524.7	33	1356.1	521.3	27	58
K	332.6	247.7	27	211.9	67.7	21	46
Ca	312.1	234.4	30	218.6	101.2	22	50
Fe	636.2	634.9	34	426.1	342.8	27	59
Al	1333.9	958.8	29	1037.7	620.8	19	46

df-degrees of freedom, s-standard deviation, n-number of data points, NS-not significant.

gain has been found to increase over time. The filters used for sampling were in the cassettes for no longer than a day and usually fewer than three hours. Over this period, the weight gain was found to be negligible and thus no corrections were made to the gravimetric mass values. The weight gain, in general, is less for the nuclepore filter than it is for the teflon filter so corrections for the nuclepore gravimetric mass were also considered negligible.

E. Sources of Error

In this section we will discuss the various sources of error related to the pilot balloon observations and tethersonde data. These sources of error can be discussed only in light of findings from other studies since no attempts have been made here to quantify them. We also discuss the problems associated with the aerosol sampling balloon and the possibility of contamination of the aerosol filters by the carbon vane pump.

1. Pilot Balloons

Wind speed error associated with single theodolite-tracked pilot balloon observations was investigated by Swanson, et al. (1981), using data from a study conducted in the Delta and the Sacramento Valley of Northern California. Variations in ascent rate for the 4-, 8- and 12-minute observations from 169 double theodolite profiles showed that some but not all releases had significant variability in ascent rates. The investigators did not explain why some of the releases showed more variability than others. Wind speed profiles were calculated using both theodolite observations and observations from just one of the theodolites and plotted in the same figure. It was evident that the

single theodolite profiles showed areas of large, fictitious wind speed shear when the ascent rate was not constant. Some of the windspeeds were three to six times higher than the double theodolite-calculated windspeeds. The ascent rate used for the single theodolite calculations was calculated from the computed height of the last double theodolite observation divided by the total time so that the error was minimized for the single theodolite computation. The ascent rate of 1.5 meters per second from the assumed constant ascent rate as presented by Swanson, et al. would be the lower limit in most cases. Wind direction error was not investigated.

2. Tethersonde Balloon

There has been some investigation of balloon-borne instrumentation error. Whiteman used the same meteorological package as does this study to investigate breakup of inversions in Colorado mountain valleys (1980, 1981). He conducted a series of tests at the National Center for Atmospheric Research (NCAR) facilities in Boulder, Colorado. The instrument package was tested in a wind tunnel and some attempts were made to simulate the conditions that might occur while the package was suspended from a balloon. The standard instrument specifications from the testing are included here in Appendix II-A and will not be discussed here. One test was to tilt the package 10, 20, and 30 degrees from the vertical and compare the resulting measured wind speed to the true wind speed. As expected from theory, the package windspeeds were consistently lower than the true air speed by approximately the cosine of the tilt angle. The balloon used for the project was a lightweight (1.5 kilogram) 3.25 cubic meter blimp-shaped balloon (Follmer Model 115). Field observations were presented that

give insight into the possible errors. They observed that when the wind speed was greater than 5 meters per second, the balloon drifted downwind, causing a low wind speed on the ascent and a high wind speed on the descent. A further complication was that on the descent, the balloon maintained its elevation until nearly above the winch, at which point it would descend straight down. For this reason, Whiteman did not average the up and down soundings in the data analysis. The balloon's response to changes in wind direction were discussed in view of its dimensions. The balloon was very responsive to light winds, pointing into the wind even when the cup-anemometer was stationary. It was theorized that the balloon would not respond to directional eddies smaller than half the length of the balloon. The balloon was observed to respond slowly to large stepwise changes in the wind direction, especially a 180-degree directional change. During turbulent convective conditions, it was observed that the tethersonde package swayed as much as 20 degrees away from the balloon orientation. It was summarized that the accuracy was a complex function of the "response time and damping coefficient of the balloon, the response time of the tethersonde compass, the angle of attack of the sonde and the swinging and twisting of the tethersonde relative to the balloon."

The package was suspended below the tail of the balloon to achieve a 25-degree angle of attack under calm conditions. This positioning was necessary so the balloon would be relatively level at higher altitudes with stronger winds since the tail expands with the increased inside pressure (Morris et al. 1975).

During our study, we used balloons purchased from Pie in the Sky (San Mateo, California). The balloon used for the tethersonde package

weighed 6.8 kilograms with a volume of 10.2 cubic meters (see Appendix B). Because of its different characteristics, its response was probably slower than the lightweight Follmer balloon. However, there were several reasons why we chose this balloon. During the July field season, we used the Follmer balloon for the tethersonde package. The balloon was very susceptible to damage, especially if moisture remained on the plastic for any length of time. For this reason as well as the problem of diffusion of air into the balloon, the balloon required constant recharging with helium and often became deflated during a profile. The Pie in the Sky balloons, although heavier, were not as susceptible to damage and required little recharging. We also suspended the tether package immediately below the front of the balloon because of the different lead-line configuration. The problem of being in the wake of the balloon was avoided, and the package was much more stable because of the reduced length of the suspension lines. Since the lift was greater than the Follmer balloon and the tether line came from the center of the balloon, the balloon was relatively level under calm conditions, and the front end tilted slightly upwards at higher altitudes because the expansion cords were located toward the front end of the balloon.

A study in Florida compared data from balloon-borne (metal-cable tether) and from tower-mounted instrumentation including the mean horizontal wind speed and direction and the fluctuating components of the horizontal winds, vertical winds, and temperature (Gaugen and Kaimal 1975). The instrument package on the balloon was attached to a vane which kept the instrumentation pointed into the wind. The blimp-shaped balloon was much larger (1300 cubic meters) than the balloons

used during the present study but some salient findings are of interest. The dominant motion of the balloon was lateral oscillation and this motion increased with increasing height above the ground. The sensors were located at 500 and 1000 feet with the balloon position varied at 1200, 2000, 3000, and 4000 feet above ground level. The mean horizontal wind speed was overestimated by the balloon instrumentation by 7 and 11 percent at 500 and 1000 feet, respectively. The balloon motion was tracked by two theodolites simultaneously. The average ratio of the standard deviation of the lateral motions of the cable at the two heights (500 and 1000 feet) and the ratio of the horizontal wind speed discrepancy were very close, indicating the overestimate of horizontal wind speed was largely attributable to the lateral motions of the balloon. It was stated that the effect of the lateral motion could be minimized by increasing the balloon-probe separation. Ryan, et al., 1979, recommended a spacing of 100 to 300 meters between the instruments and the balloon when measurements were taken close to the ground since they observed the instruments swayed as much as 15 to 20 meters from an imaginary centerline when the balloon was close to the ground. During the present study, the balloon acted as the wind vane, and it was not possible to increase the distance from the package to the balloon.

3. Aerosol Sampling Balloon

The balloon used for aerosol sampling during the August field study was a spherical-shaped Pie in the Sky balloon which had more lift than the blimp shaped JK20 balloon used in July (the same balloon used for the meteorological package during August). The JK20 balloon lifted

only 3 aerosol packages whereas the spherical balloon lifted 5 packages. The only problems encountered with the aerosol sampling balloon was at the point of attachment of the sampler on the tether line. During the July period, a JK20 balloon was lost because the line was cut by the edge of the plate on which the pump and motor were mounted. In August, the samplers were attached in such a way that the plate could not contact the tether line. Another added feature in August was attachment of the exhaust line to the tether line away from the filter inlet to avoid contamination from the pump exhaust. The aerosol samplers were placed every 50 meters along the tether line. Much calmer conditions prevailed during the morning and at night so that the tether line was nearly vertical.

4. Filter Contamination

A test was run connecting the exhaust of the pump to the filter inlet to determine if "blow-by" contamination was occurring. Data from one 33-minute sample were used to obtain the ratio of each major element (and carbon-soot) to silicon. In Table 5 are the ratios from the exhaust filter (test), balloon data (1), and 24-hour particle samples (2) collected during the same time at Giant Forest (Cahill et al. 1986a). Elements that are not listed but that occurred in the exhaust sample are fine Mg, Mn, Zn, Br, Cl, and Pb and coarse Mg, Mn, Cu, Zn, Cl, and Br. These elements are not presented because they were not included in the data analysis and because most of their concentration errors were larger than 50 percent since they were trace elements in the atmosphere. The 24-hour samples were from a similar stacked filter unit which was operated at a lower face velocity. The

TABLE 5

		FINE	
	K/SI	Al/Si	Fe/Si
Test	.261	.207	8.867
1-Balloon	.248(58)	.640(30)	.279(58)
2-Cahill	.582(9)	.527(9)	.254(9)
Soil	.070	.335	.200
Crust	.074	.292	.200

	C-S/Si	H/Si	S/Si
Test	2.159	.156	.433
1-Balloon	5.222(58)	2.359(57)	3.061(60)
2-Cahill	1.790(9)	2.017(9)	2.850(9)
Soil	--	--	.009
Crust	--	--	<.001

		COARSE		
	Al/Si	S/Si	Ca/Si	Fe/Si
Test	.621	.141	.099	5.352
1-Balloon	.657(46)	.207(14)	.151(52)	.294(59)
2-Cahill	.465(9)	.051(9)	.120(9)	.257(9)
Soil	.365	.021	.053	.192
Crust	.292	<.001	.147	.200

Dashes indicate the numerator is not present in soil.

coarse filter collected particles between 2.5 and 15 microns and the fine filter collected particles smaller than 2.5 microns. The sampler height was approximately 2 meters above ground level. The data are presented as ratios to render the data directly comparable. The exhaust sample was concentrated exhaust whereas the data collected in the field, if contaminated, would show values including the ambient air as well. The values in parentheses are the number of measurements that were averaged. Also presented are soil and average crustal ratios. The soil ratios are from a soil sample collected near the Giant Forest area which was analyzed for elemental concentrations. The crustal values were taken from a report by S.R. Taylor (1964).

The ratio for fine carbon soot (C-S) is higher for Wolverton than Giant Forest such soot may be a contaminant from the exhaust.

For the coarse particles, the ratios for sulfur and aluminum appear to be higher for Wolverton than Giant Forest. Since the test ratio for aluminum is so close to the Wolverton and Giant Forest ratios, it is not possible to determine whether the aluminum is a contaminant or not. The difference in the sulfur ratios between Wolverton and Giant forest may be due to the different cut-points. The coarse filters used for the balloon samplers collected particles larger than 1 micron whereas the coarse filters used at Giant Forest collected particles between 15 and 2.5 microns. The fine sulfur ratios agree fairly well which indicates that the discrepancy may be due to larger sulfur-containing particles. Since the test sulfur ratio is so much smaller than the Wolverton ratio, if there is contamination, it is probably small. As with the fine carbon-soot concentrations, the standard deviation for the Wolverton coarse sulfur concentration is

nearly half the average. The standard deviation of the sulfur/silicon ratio is 0.11, which indicates it is not significantly different from the Giant Forest ratio.

III. BOUNDARY-LAYER PROFILES

A. **Meteorological parameters.** As described in the Measurement section, a Tethersonde was operated at Giant Forest during the Sequoia program. Detailed profiles of temperature, absolute humidity, wind speed, and direction were obtained over the lower few hundred meters. Six soundings were made over the period 27-28 July and twenty-three in the August 14-22 period.

A bulk Richardson number, R_B, was computed for each sounding,

$$RB = \frac{g}{T} \frac{\Delta\theta\Delta Z}{\bar{u}^2}$$

where ΔZ was chosen as the lower 200m, $\Delta\theta$ was taken as the potential temperature difference, and U-bar as the average wind speed over the same height interval. In principle, the bulk Richardson number should be based on measurements taken over the entire boundary layer. However, the thickness of the boundary layer exceeded the vertical range of the Tethersonde system in many cases. Adopting a fixed Δz allows comparison between soundings but may not allow universal comparisons with measurements at other sites and in the laboratory. Table 6 gives average values of R_B for different periods of the day. The Richardson numbers demonstrate that the Afternoon, Late Afternoon, and Night periods correspond to three distinct regimes: (1) $R_B = -0.68$, slightly unstable - near neutral, (2) $R_B = 88.83$, stable, (3) $R_B = 23.30$, very stable. The value for the morning Richardson number,

43.46, would seem to indicate that the data from this period would fall in the same category as the late afternoon. However, this is a time of rapid change with the latter half of the period being unstable. Therefore, we advise caution when comparing these two periods. The Richardson number and related similarity parameters are highly useful in boundary-layer studies. When presented in non-dimensional form, most boundary-layer variables display universal relationships that can be used in practical applications. However, in the case of air quality data, Barone, et al. (1983) showed that when pollutant concentrations are significantly influenced by distant sources, vertical distributions depart markedly from the similarity relationships found for local ground-level sources.

Table 6. Average values for the bulk Richardson number for various periods of the day.

Period	Time(PDT)	Average R_B
Afternoon	(13 - 17)	-0.68
Late Afternoon	(18 - 20)	+88.83o
Night	(21 - 07)	+223.30
Morning	(08 - 12)	+43.46

Appendix II-E shows plots of all the tethersonde data. In each diagram the vertical distribution of absolute humidity, virtual potential temperature, and the wind vector are shown. Some conclusions can be made from inspection of these diagrams: in most cases, there is no sign of an upper limit to the boundary layer; that is, the boundary-

layer is thicker than the vertical extent of the tethersonde. The local influence of Wolverton Meadow is obvious on several soundings, resulting in a layer 100 to 200m thick with properties significantly different from the remainder of the sounding. In the morning, the "meadow influence" amounts to a local inversion while in the afternoon, the meadow causes a local unstable layer. Most of the tethersonde temperature soundings show largely neutral profiles above the surface layer. This may be due to the influence of the rough terrain of this site. In practical terms this may mean that the air from, say, 100 to 500m above the ground is always well mixed. The upslope/downslope wind regime is well represented in the tethersonde data. In most cases, however, this circulation extends to greater heights than those reached by the tethersonde.

The relationship between stability, as measured by the Richardson number, and the vertical structure of the wind flow is discussed in the next section.

B. Hodograph Analysis.

Hodographs (the x-component of the wind plotter against the y-component) which display average conditions for afternoon, late afternoon, transition downslope/night, and upslope/morning periods are shown in Figures 2-6. The first four periods correspond to the Richardson number categories previously discussed.
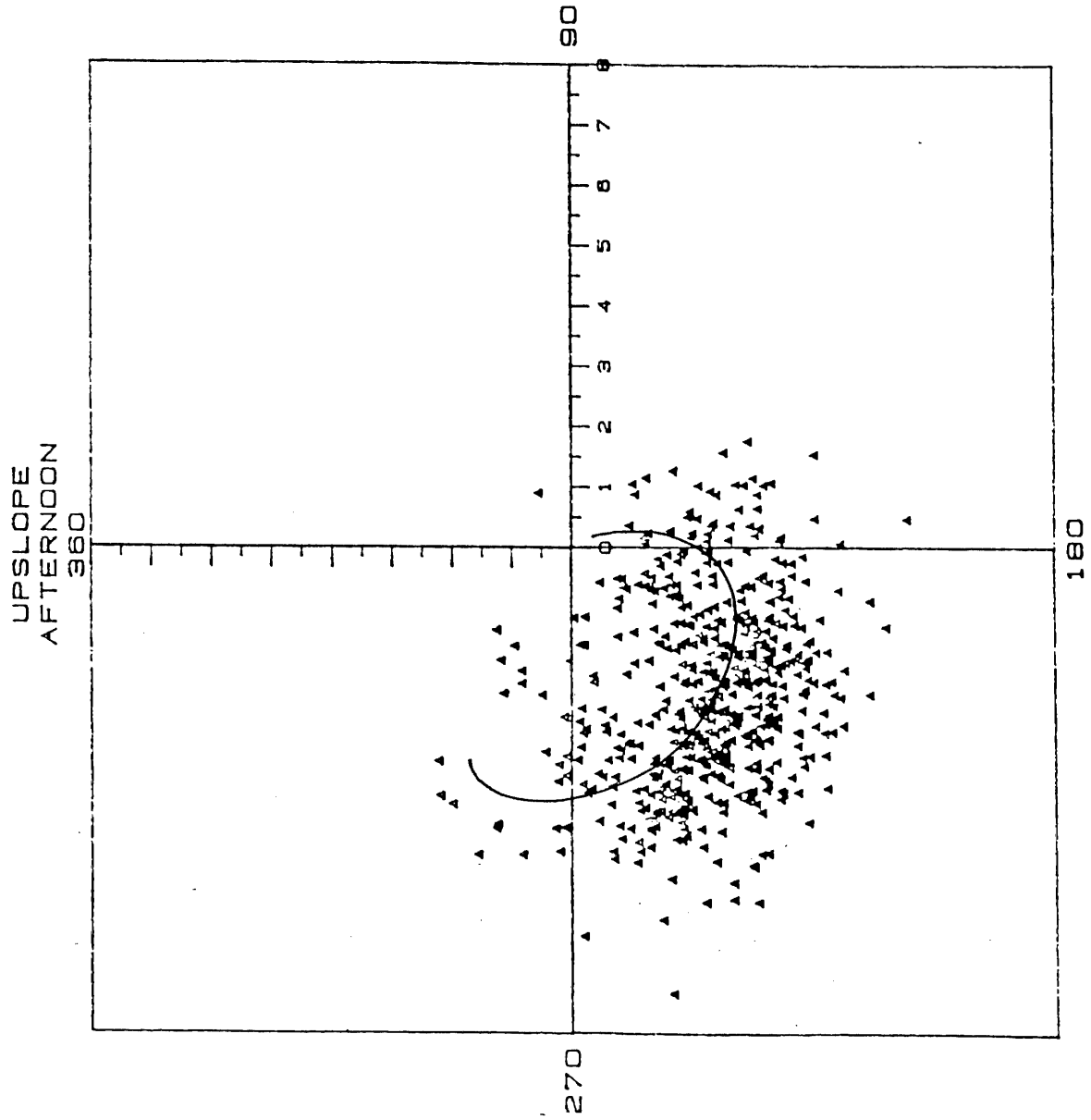
Figure 2. Hodograph of Upslope Afternoon Winds
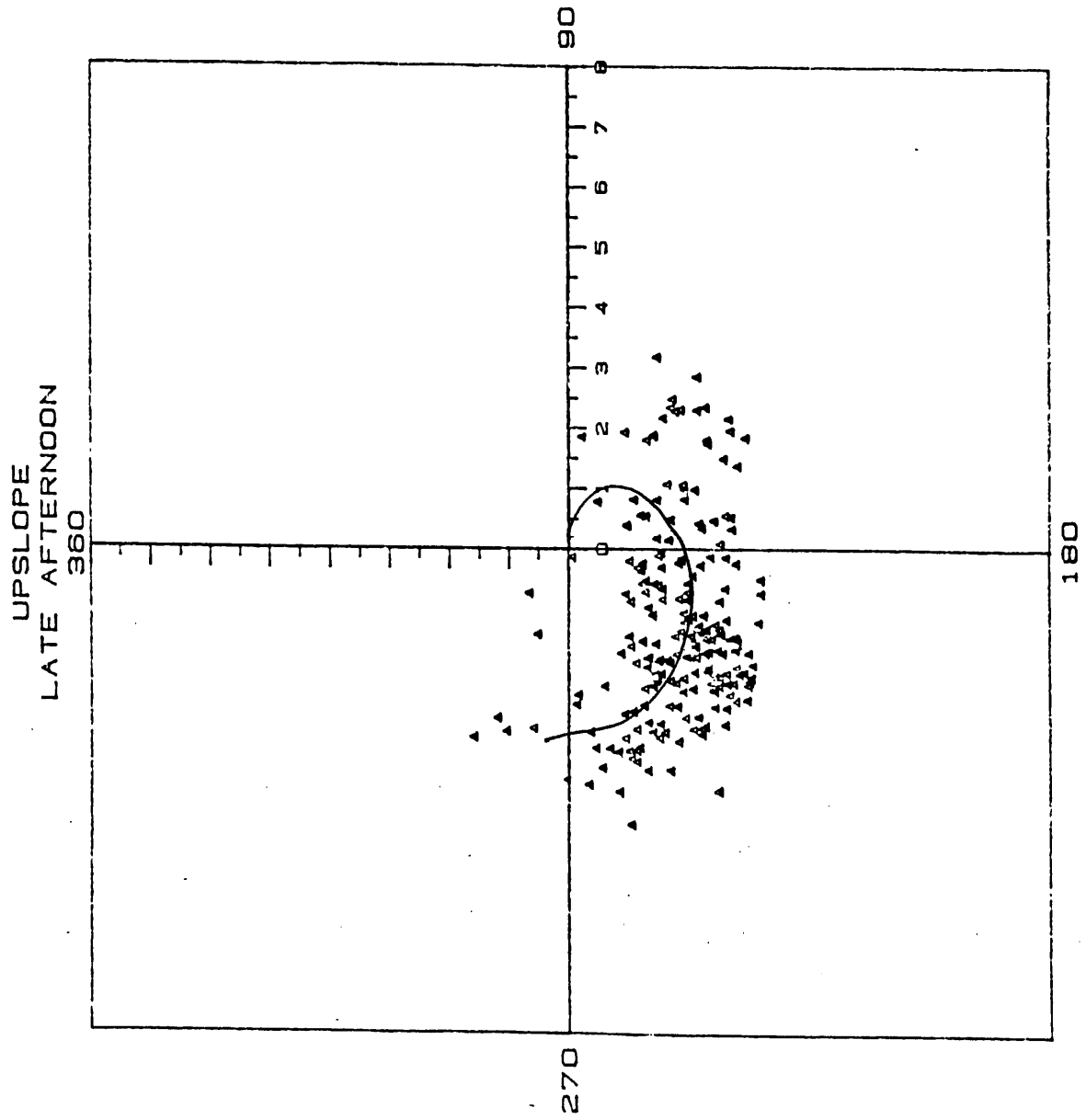
Figure 3. Hodograph of Upslope Later Afternoon Winds
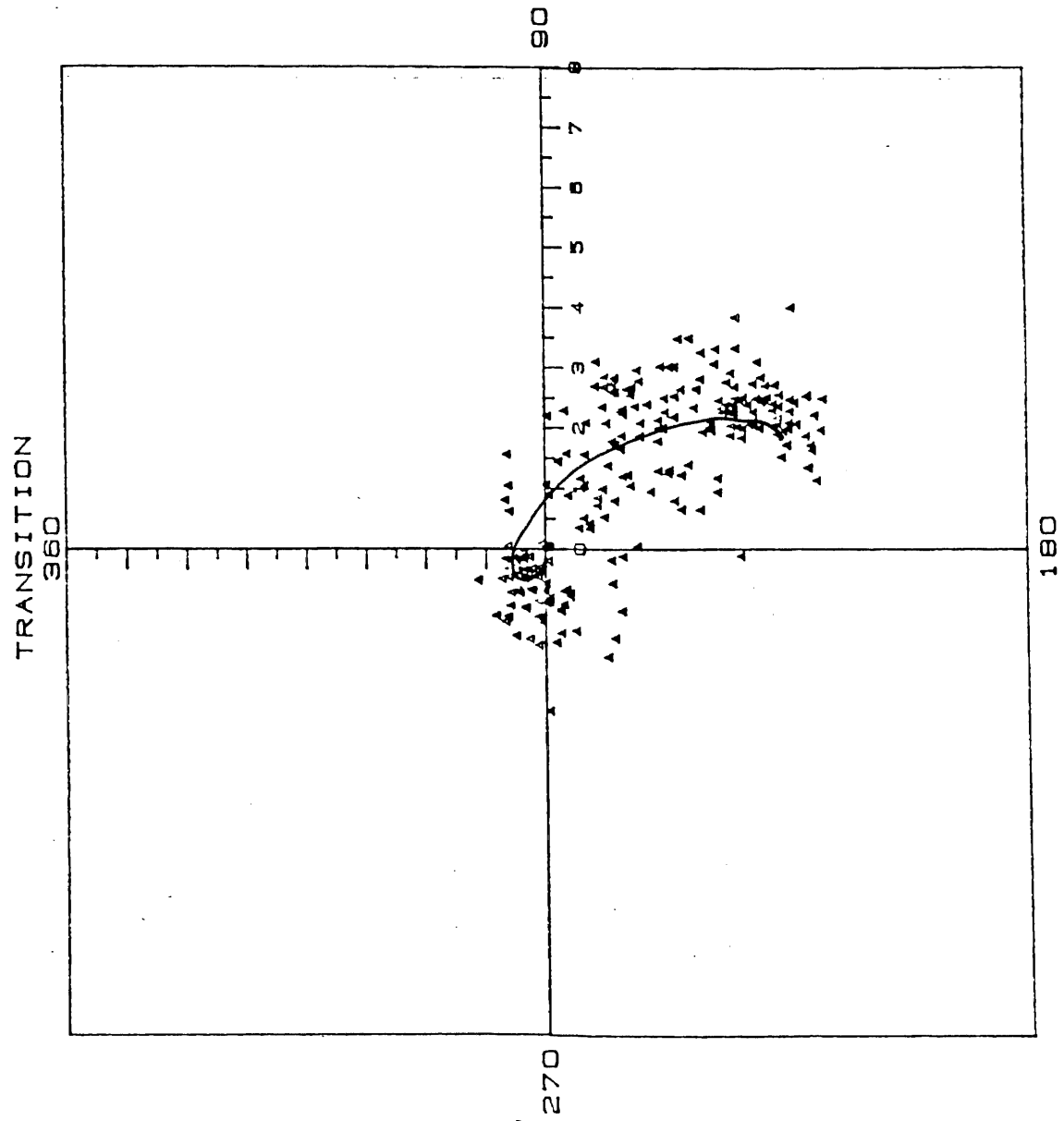
Figure 3. Hodograph of Winds During Transition Period
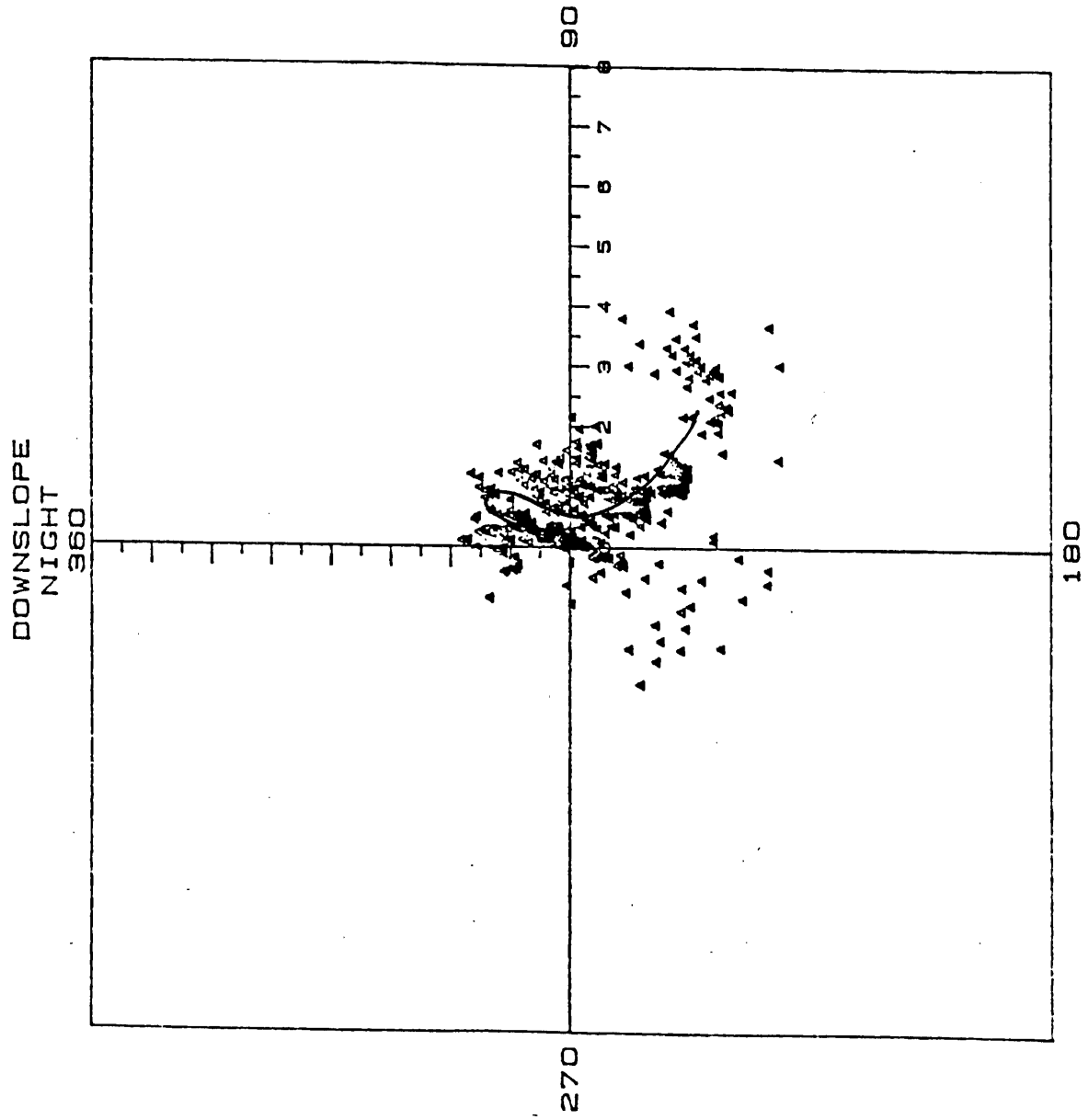
Figure 5. Hodograph of Downslope Night Winds
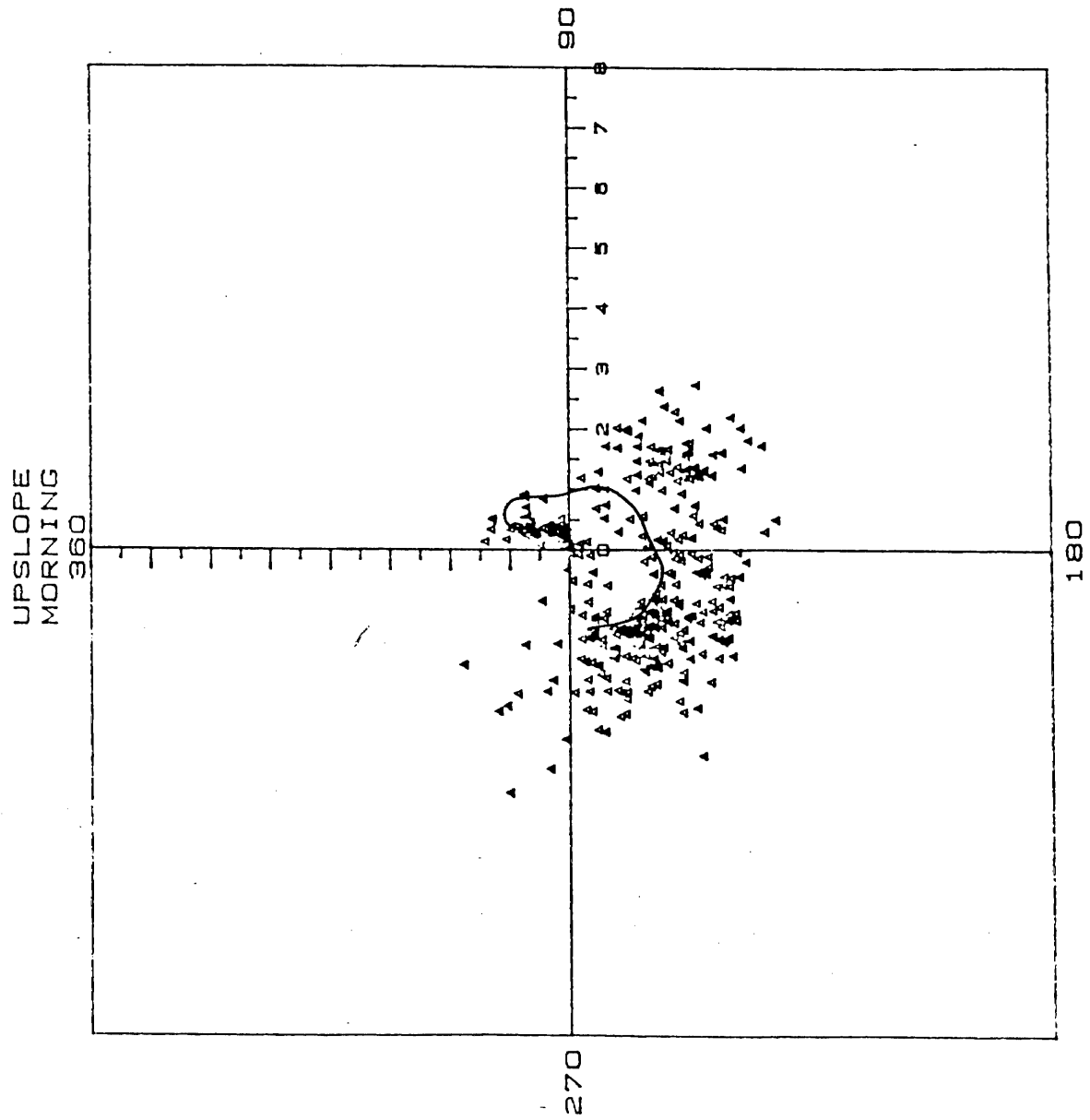
Figure 6. Hodograph of Upslope Morning Winds

These diagrams show the upslope flow to consist of a layer of vigorous westerly to southwesterly winds, which can be seen from the tethersonde profiles to be at least 300 m thick. Examination of the corresponding tethersonde temperature data shows that the virtual potential temperature was approximately constant in the upslope layer during this period. This indicates that the layer was well mixed by turbulence. Similarly, examination of the hodographs and the tethersonde plots shows no appreciable turning of the wind vector with height during the afternoon period. The data suggest that the wind vector may have a tendency to become more southerly at the highest levels but most of the upslope flow is solidly westerly to southwesterly.

Figures 2 and 3, in which all afternoon (1300-1700 PDT) and late afternoon (1700-2000 PDT) wind data are plotted show much the same features discussed above, except that general weakening of the flow is evident on the later data and a slight tendency to shift towards the south. Figure 4 shows a hodograph for the transitional period between the afternoon upslope and nighttime downslope regimes. Only two tethersondes were taken in the narrow transitional time period. The diagram shows a shift towards the southeast during this period. In contrast to the upslope period, there is considerable wind direction shear apparent in the transition period. This is to be expected since the classical behavior of thermally driven diurnal wind regimes is for changes in wind direction to occur first at the surface, then later at higher elevations. This structure can be seen in the tethersonde wind data for August 21, 1985, at 2100 PDT where the downslope winds have begun near the surface while the upslope winds persist aloft. Figure 5 shows the composite hodograph for the nighttime downslope period. The

data generally show weak easterlies in this period but with considerable dispersion in wind direction. There is greater wind direction shear at night than in the afternoon but the data are insufficient to be more specific. Figure 6 shows the composite diagram for the morning (0700 - 1200PDT) upslope period. The structure of the wind is similar to the afternoon period except that the wind direction is shifted somewhat to the southeast.

C. Aerosol Profiles

The aerosol profiles are the unique portion of the meteorological data set (Figures 7 and 8). To our knowledge, these are the first such measurements in mountainous terrain. All individual soundings, collected together for the morning, afternoon, and night periods, are given in Appendix I. Figures 7 and 8 show the profiles for selected elements averaged for the same three periods.

The most striking feature of the data collected by the tethered particulate sampler is the behavior of fine sulfur. The concentration is markedly higher during afternoon conditions. Since this is also the period of strongest upslope winds, substantial upslope transport of the fine sulfur aerosol occurs. The same feature is apparent for all the elements although not to the same degree and not necessarily at all levels.

In general, most of the vertical profiles are relatively constant with height, indicating good mixing by turbulence. The nighttime coarse elements are an exception. Most of these show a noticeable minimum at the lowest measurement level. We believe this is a reflection of surface deposition of these elements.
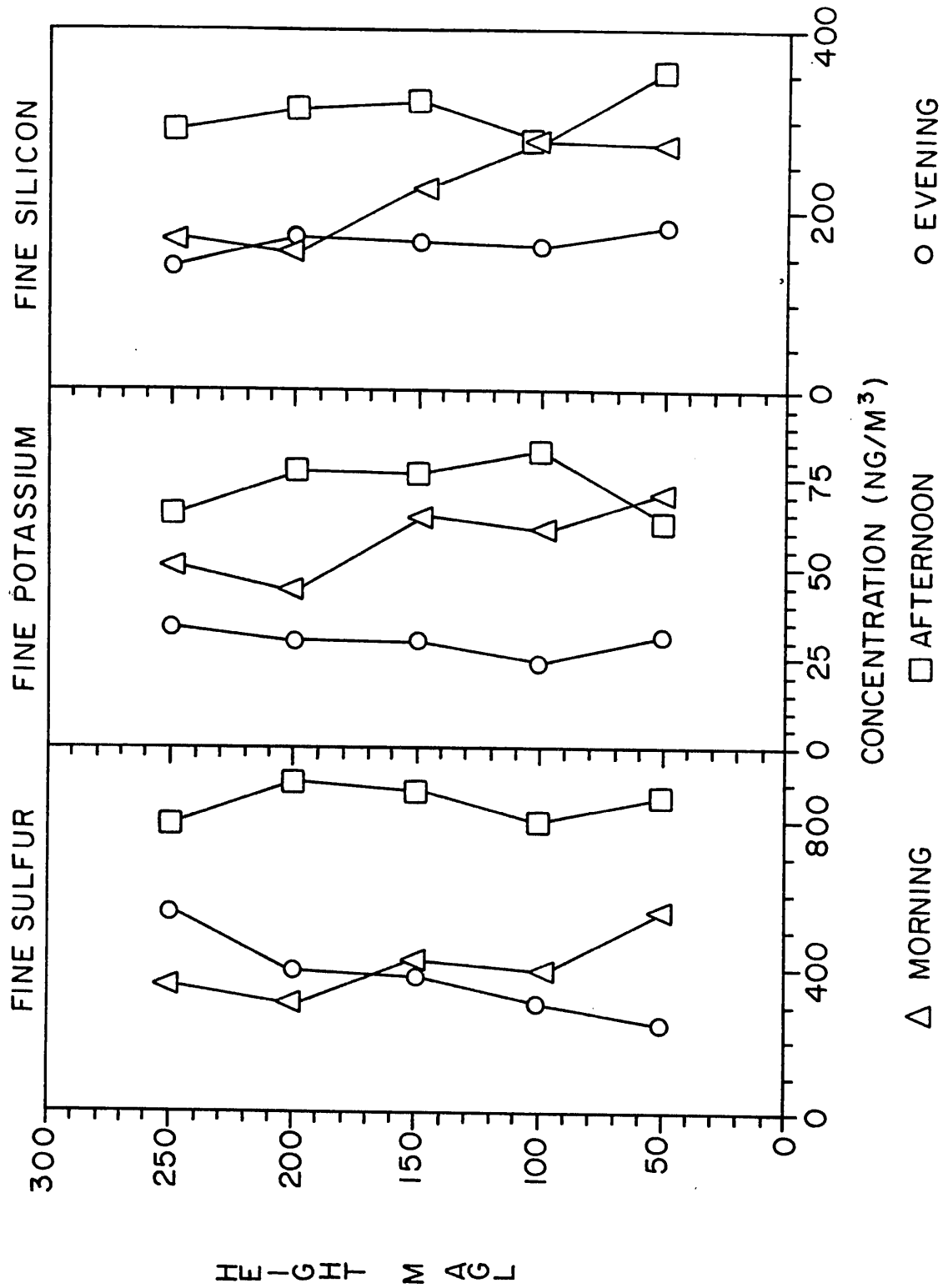
Figure 7. Aerosol profiles at Wolverton
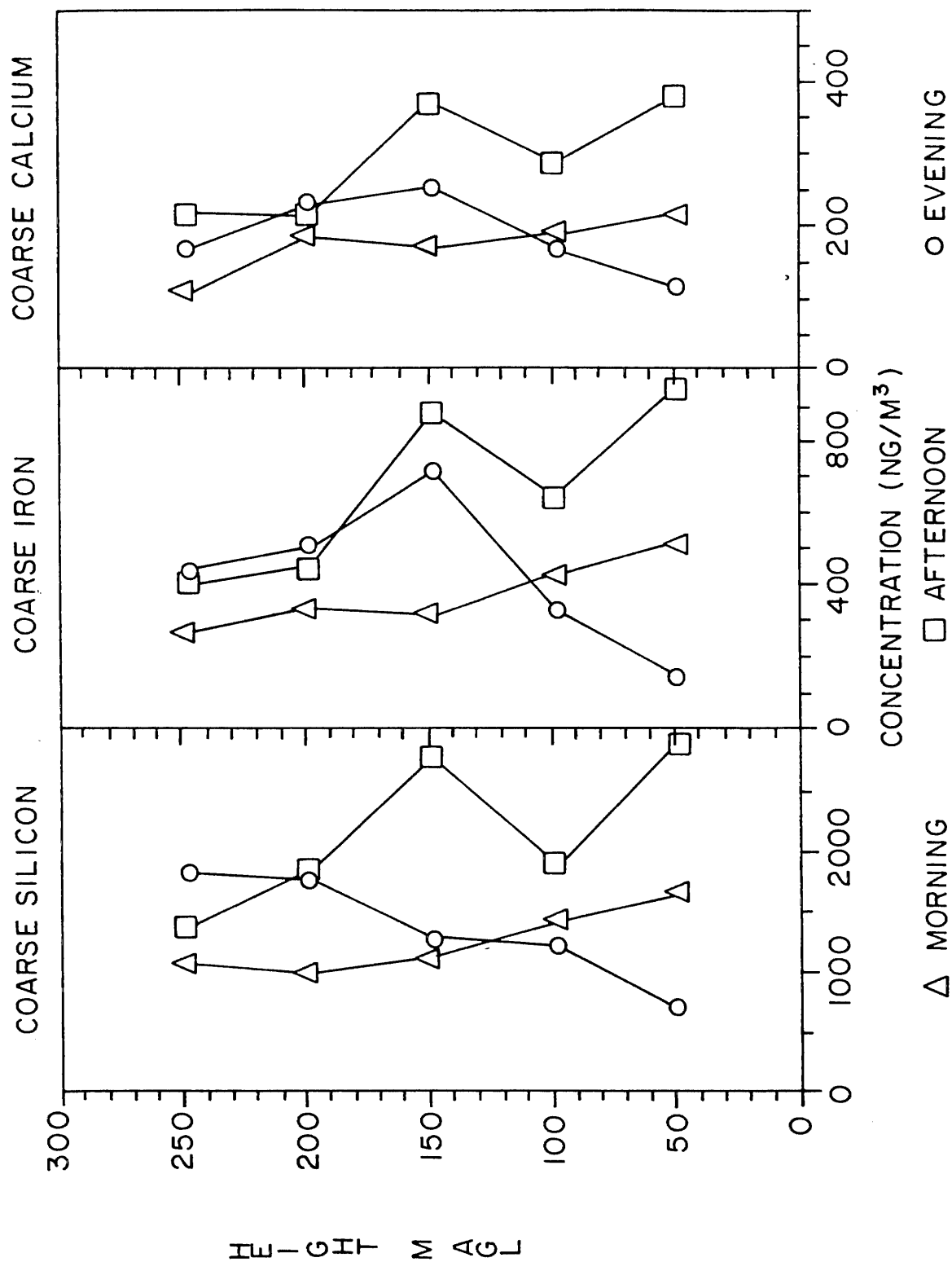
Figure 8. Aerosol profiles at Wolverton
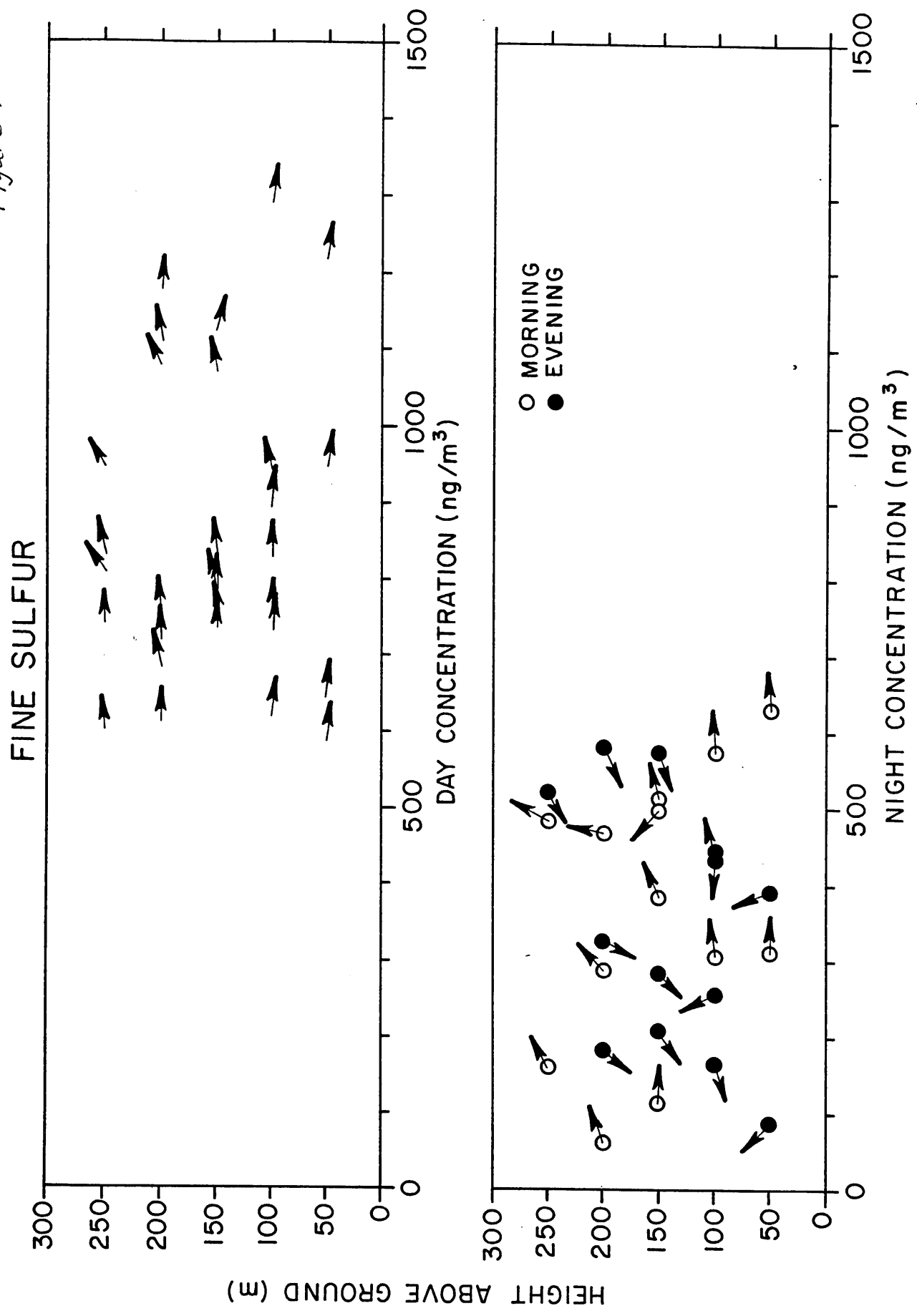
Figure 9. Fine sulfur transport flux at Wolverton
Direction of arrow corresponds to compass heading.
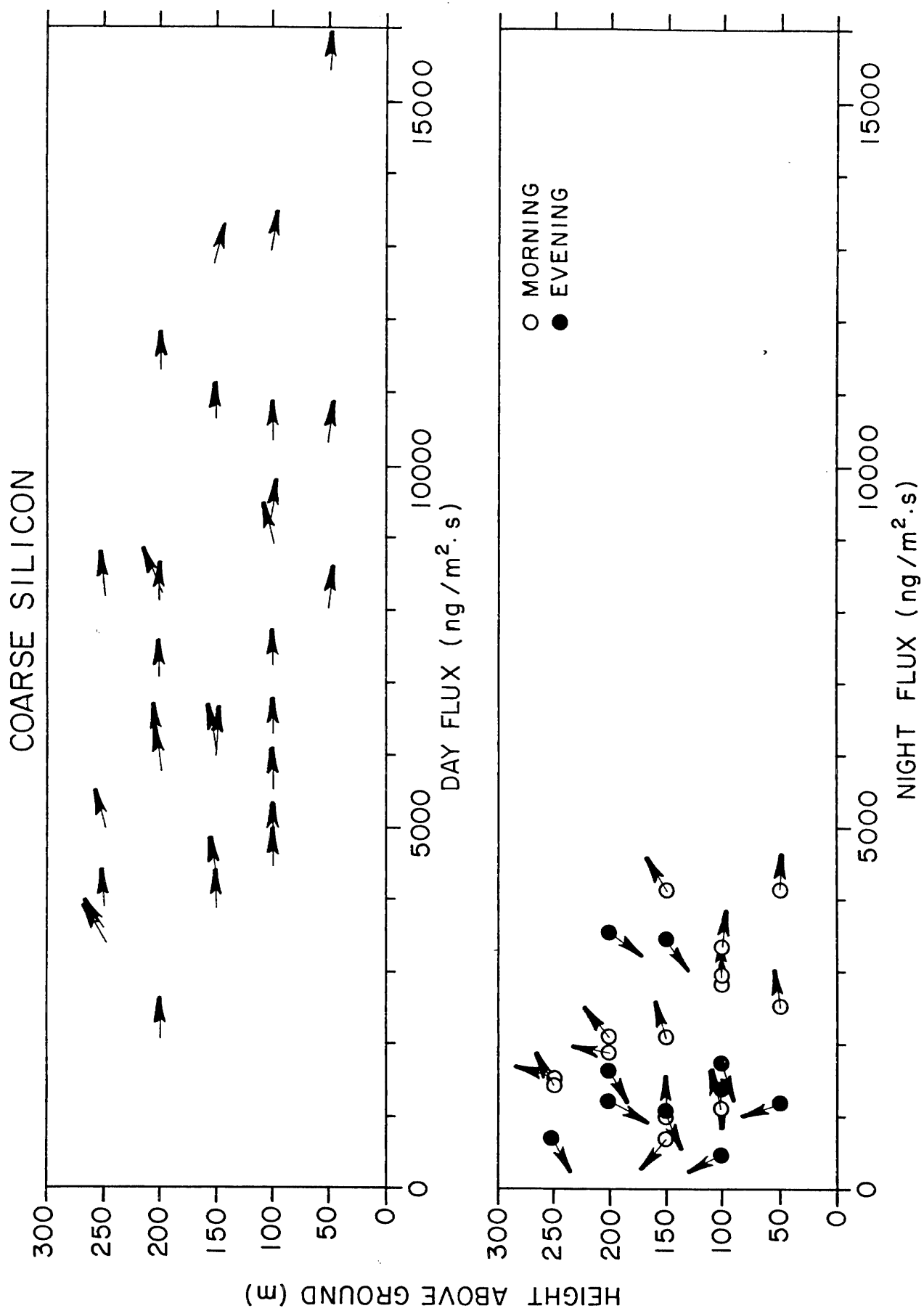
Figure 10. Coarse silicon transport flux at Wolverton
Direction of arrow corresponds to compass heading.

D.   Aerosol Fluxes

The particulate data concentration profiles described in the previous section can be used to compute an upslope or downslope flux. This flux is the product of the concentration and the wind speed measured at the appropriate height. All flux profiles are shown in the Appendix I. Figures 9 and 10 are shown because of their striking features. The sulfur fluxes are divided into day and night regimes. This corresponds to an upslope/downslope characterization. It is clear from the diagram that the fluxes are considerably higher during the day or upslope periods. The same conclusion can be drawn for potassium although the results are perhaps not as striking.

IV.   Pibal Winds

Pibal winds were measured at Ash Mountain, Wolverton Meadow, and Emerald Lake six times a day for the period August 13 through August 22, 1986. The observation times were 0400, 0700, 1100, 1600, 1900, and 2300PDT. The maximum height the balloons were tracked was 5500m above mean sea level.

These data are shown in Appendix II-E plotted as east-to-west cross sections which also include the National Weather Service pibal data at Fresno. These plots are useful for putting the circulation of the Sierra slopes into a larger perspective which includes synoptic variation and the meso-scale wind regime in the San Joaquin Valley.

Comparing the three mountain sites, shows clearly that the upslope/downslope regime is both deeper and more intense at Ash Mountain than at the higher locations. This is true for both the upslope and downslope winds; in each case the winds at Ash Mountain are

usually stronger and extend to greater heights than at Wolverton and Emerald Lake.

It is conceivable that the winds at the Ash Mountain site are stronger and deeper because this location shares in the San Joaquin Valley meso-scale circulation. By examining Fresno pibal data we can make some conclusions in this regard. The 1600PDT soundings suggest that the afternoon San Joaquin Valley west-northwest winds are connected to strong upslope winds at Ash Mountain. Both flows are about 1000m thick and the speeds are comparable. Figure 11 shows an example of this situation; however, by 2300PDT the downslope winds have usually appeared at Ash Mountain whereas at Fresno the northwesterlies have usually accelerated. At this time, these two systems are clearly decoupled. In the morning hours, the upslope flow starts early and is vigorously developed by 1100PDT. At this time, the northwesterly flow at Fresno is only weakly developed.

During the night, these data usually suggest a pronounced convergence in the wind field between Ash Mountain and Fresno. Based on experience in Southern California, the situation is one that often creates a "smog front." A possible sequence that might lead to the formation of a smog front in the Sierra foothills is as follows. During the night, pollutant-laden air flows up the San Joaquin valley and towards the foothills. These winds are opposed by the downslope flow of clean air from the mountains, creating a zone of horizontal convergence and mean rising motion. By morning, the boundary zone between the polluted and clean air is compressed into a narrow zone or "front." As the upslope wind develops, the smog front is swept along
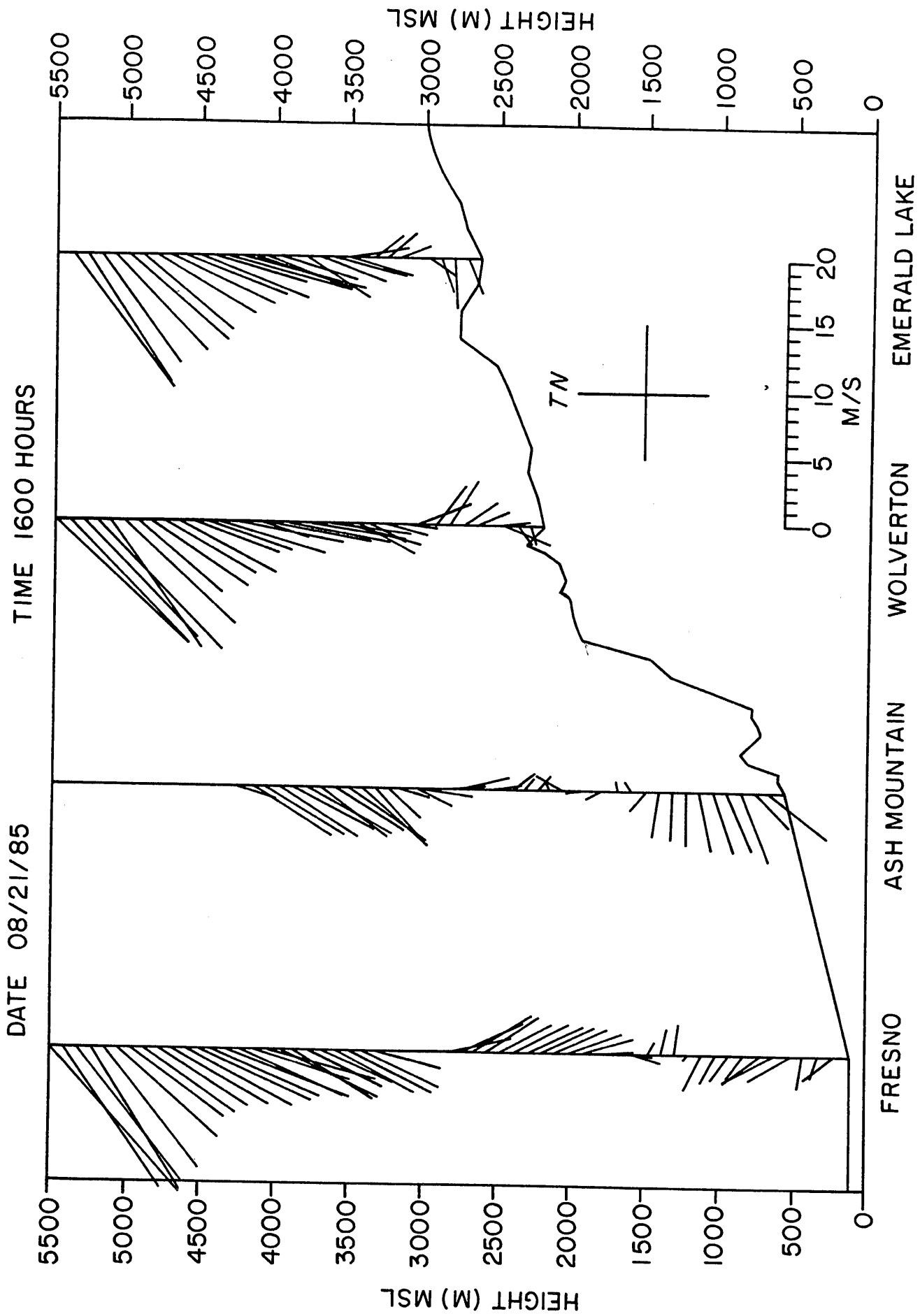
Figure 11. Pibal winds showing direction of flow as a function of altitude at study site.

with the general flow. The result at a fixed location would be a sudden increase in pollution sometime during the morning or early afternoon as the smog front passes over. This event may not yet have been observed in the Sierra foothills. As development proceeds in the San Joaquin Valley, it may become common. Figure 12 shows an example of a convergence zone between Fresno and Ash Mountain.

The passage of synoptic weather systems is obvious on these plots. The trough which passed through the area August 16-17 appeared first as middle-level southeasterlies on the 15th. By 1600PDT on the 16th, strong southeasterlies are found at all levels above the boundary layer. However, even under these conditions, the Valley northwesterlies and Sierra upslope flows are well developed. By the 18th, the upper air flow has become westerly to southwesterly.

The cross sections reveal three wind regimes. One is the lower, boundary-layer flow system which is found from 100 to 1000m above the surface of the earth. This regime is dominated by a very regular oscillation of upslope and downslope winds controlled by the diurnal variation of solar heating of the Sierra slopes.

The second regime is the meso-scale San Joaquin valley wind system. This circulation sweeps up the Valley in a northwesterly current which reaches its maximum strength in late evening. The valley circulation has two specific features which may be significant to air quality meteorology in Sequoia National Park. One is the nocturnal jet, which is strongest about midnight. The jet may be an efficient means to transport pollution from Central California to the southern San Joaquin area. The second feature of interest is the Fresno Eddy.
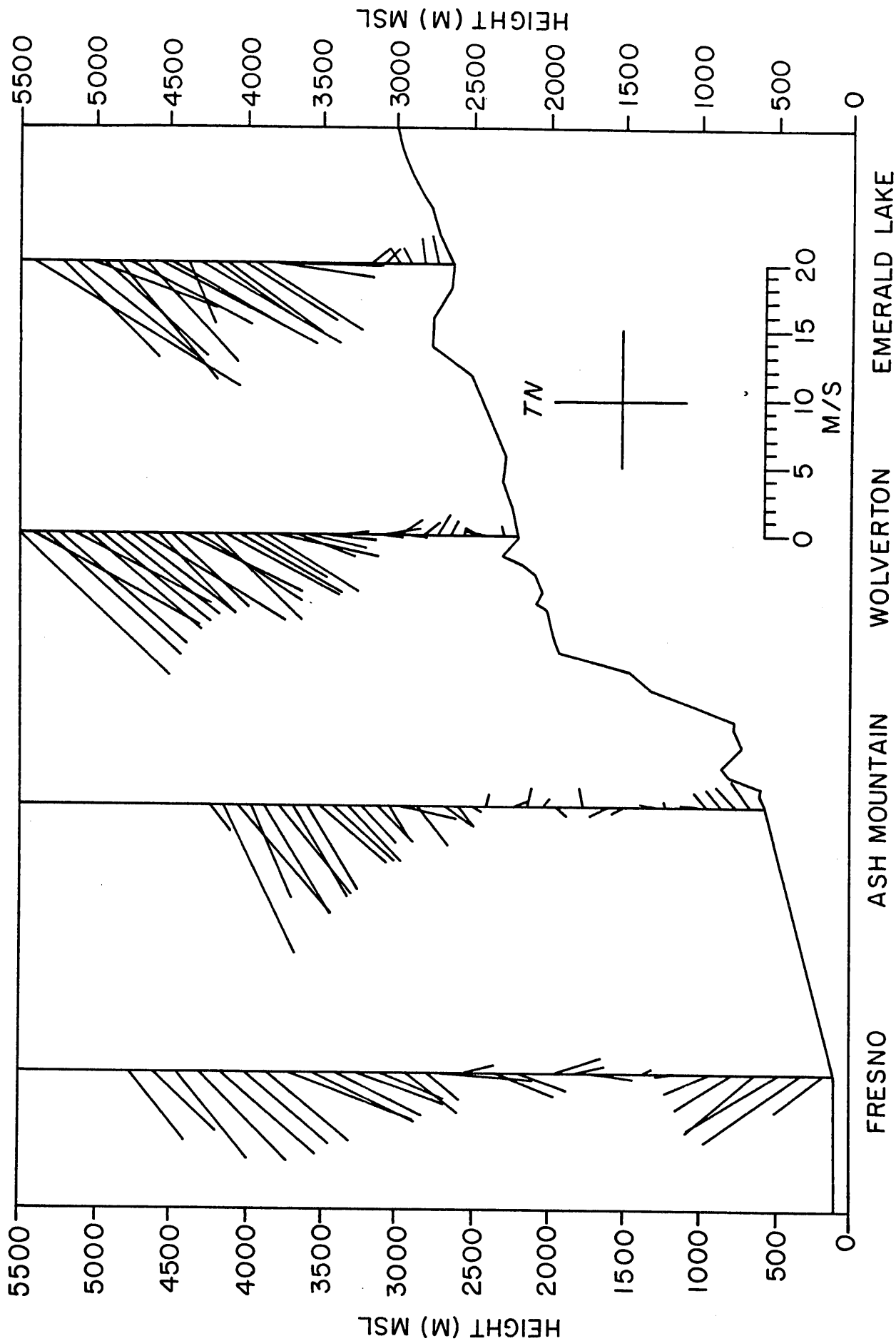
Figure 12. Pibal winds at study sites showing convergence zone between Fresno and Ash Mtn.

This flow feature may be a significant mechanism for transport of pollution from the oil fields of Kern County to the Sequoia area. The meso-scale system is represented in these analyses only by the Fresno pibal.

The third system is associated with synoptic-scale variation. These fluctuations are seen most clearly at upper levels and are irregular in their occurrence. The synoptic scale controls long-range transport, particularly the transport of sulfur-rich air from regions to the south of Sequoia National Park.

V. Surface Station Data

The equipment used in collecting surface data is described in Appendix II-A. Plots of the data, given by hour to emphasize diurnal variation, are given in the same appendix for the three sampling sites. These data will be valuable for further analysis that may emphasize deviations from normal conditions. For the most part the data for the sampling period are consistent.

VI. Summary and Conclusions

Based on the data collected and presented in this report we make the following conclusions.

1. When averaged over the entire observation period, the concentration of all five elements is higher in the afternoon (upslope) than in the nighttime or early morning (downslope) hours.

2. The concentration of some of the coarse elements, including silicon, iron, and calcium shows a strong tendency to increase with height in the lower 200m during nighttime hours.

3.   The fluxes of most elements show larger values during the afternoon (upslope) period in comparison with other times of the day.

4.   The fluxes of some of the elements such as fine and coarse silicon and fine mass show less of an upslope/downslope contrast.

5.   The potential for "smog front" phenomena seems to exist in the lower regions of the park due to convergence in the meso-scale wind field.

6.   The upslope/downslope boundary-layer, meso-scale, and large-scale winds interact in a complex fashion to produce the observed aerosol transport.

VII.   Recommendations

In future transport experiment in the Sierra Nevada region it will be important to obtain soundings that include the entire boundary layer.   This could be done with an instrumented aircraft with sufficient power to operate at high elevation.

The value of the aerosol profile data would be greatly enhanced if they were obtained in conjunction with three-dimensional meso-scale trajectories.

Questions regarding the complex interaction of meteorological phenomena of different scales remain unanswered.   For example, the Fresno Eddy may play a major role in transporting pollution into the Sequoia region from the south.   Is this a simple transport process operating "down-the-gradient" or are there more subtle three-dimensional and counter-gradient processes at work?

In future experiments we recommend a more integrated approach to the meteorology of the region. This would include observation periods in various synoptic situations, estimation of three-dimensional meso-scale trajectories, and measurements of the entire boundary layer.

We also suggest that since pronounced horizontal divergence exists in the wind field between Fresno and Ash Mountain, "smog fronts" may form in this region. This possibility of such fronts should be investigated.

VIII. References

Cahill, T.A., L.L. Ashbaugh, J.B. Barone, R.A. Eldred, P.J. Feeney, R.G. Flocchini, C. Goodart, D.J. Shadoan and G.W. Wolfe, 1977. Analysis of respirable fractions in atmospheric particulated via sequential filtration. J. A.P.C.A., 27(7):675-678.

Cahill, T.A., R.A. Eldred, J. Barone and L.L. Ashbaugh, 1979. Ambient Aerosol Sampling With Stacked Filter Units, Final Report. Prep. for Federal Highway Administration, Office of Research and Development, Washington D.C., Rep. No. FHWA-RD-78-178, by the Air Quality Group, Crocker Nuclear Laboratory, University of California, Davis, February, 1979.

Cahill, T.A., R.A. Eldred, D. Shadoan, P.J. Feeney, B.H. Kusko and Y. Matsuda, 1984. Complete elemental analysis of aerosols: PIXE, FAST, LIPM, and MASS. Nuclear Instruments and Methods in Physics Research B3

Feeney, P., T.A. Cahill, J. Olivera and R. Guidara, 1984. Gravimetric determination of mass on lightly loaded membrane filters. J. A.P.C.A., 34(4):376-378.

Flocchini, R.G., 1984. A particle sampler for tethered balloon systems (extended abstract). Presented at the 1st International Aerosol Conference on Aerosols Science, Technology and Industrial Applications of Airborne Particles. September 17-21, 1984, at Minneapolis, Minnesota, Liu, Pai and Fissan (Eds). Elsevier Science Publishers B.V. pp. 321-324.

Morris, A.L., D.B. Call and R.B. McBeth, 1975. A small tethered balloon sounding system. Bull. Amer. Meteor. Soc., 56(9):964-969.

Ryan, B.C. and J.G. Brown, 1978. Influences on winds in mountainous terrain. Conference on Sierra Nevada Meteorology. June 19-21, 1978, South Lake Tahoe, California. Sponsored by the American Meteorological Society, Boston, Massachusetts, and U.S. Dept. Agriculture-Forest Service. pp. 46-52.

Ryan, P.W., C.D. Tangren and C.K. McMahon, 1979. A balloon system for profiling smoke plumes from forest fires. Presented at the 72nd Annual Mtg. of the A.P.C.A. Cincinnati, Ohio, June 24-29, 1979. pp. 2-24.

Swanson, R.N., M.L. Mooney and L. Langan, 1981. Pibal ascent rate uncertainties in the planetary boundary layer. Presented at the 5th Symposium on Turbulence, Diffusion, and Air Pollution. March 9-13, 1981, Atlanta, Georgia. Sponsored by the American Meteorological Society, Boston, Massachusetts. pp. 63-64.

Taylor, S.R., 1964. Abundance of chemical elements in the continental crust: A new table. Geochimical et Cosmochimical Acta, 28:1273-1285.

Whiteman, C.D., 1980. Breakup of Temperature Inversions in Colorado Mountain Valleys. Doctoral Dissertation, Atmos. Sci. Pap. No. 328, Colorado State University, 250 pp.

Whitman, D.C., 1981. Temperature inversion buildup in valleys of the Rocky Mountains. 2nd Conference on Mountain Meteorology. Nov. 9-12, 1981, Steamboat Springs, Colorado. Sponsored by the American Meteorological Society, Boston, Massachusetts, and the U.S. Agriculture-Forest Service. pp. 276-282.

Whiteman, D.C., 1982. Breakup of temperature inversions in deep mountain valleys: Part I; Observations. J. Appl. Meteor., 21:270-289.

Transport of Atmospheric Aerosols Above
the Sierra Nevada Slopes

Final Report on Research Contract A4-127-32

APPENDIX I

A Masters Thesis by D.E. Ewell, 1987 "Meteorology and Aerosol
Transport in the Southern Sierra Nevada as Measured with
Tethered Balloon Systems"

Meteorology and Aerosol Transport in the Southern Sierra
Nevada as Measured with Tethered Balloon Systems

By

Diane Marie Ewell
B.S. (University of California, Davis) 1983

Thesis

Submitted in partial satisfaction of the
requirements for the degree of

MASTER OF SCIENCE

in

Ecology

◆   in the
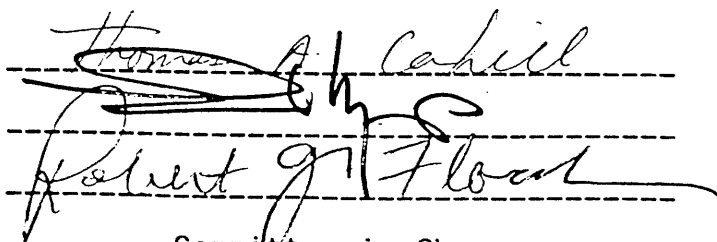
GRADUATE DIVISION

of the

UNIVERSITY OF CALIFORNIA

DAVIS

Approved:

Committee in Charge

1987

(i)

ACKNOWLEDGEMENTS

weather and air quality data.

TABLE OF CONTENTS

TABLE OF CONTENTS (Cont'd)

*Note that these are included as Appendix II.A-E of Transport of Atmospheric Aerosols Above the Sierra Nevada Slopes.

List of Figures

List of Tables

CHAPTER I

INTRODUCTION

The San Joaquin Valley of California is surrounded to the east, west and south by mountains which act to restrict the movement of pollutants from the urban, agricultural and industrial activities of the San Joaquin Valley, foothills and coastal areas. Typically during a summer day, the wind flow in the valley is from the northwest. The winds travel eastward through the Carquinez Strait near San Francisco Bay and sometimes through other coastal gaps. The winds then turn to the southeast and head up the San Joaquin Valley towards Bakersfield. The probable residence time for pollutants in the San Joaquin Valley in the summer is approximately two days (Blumenthal et al. 1985). The major escape routes for pollutants out of the San Joaquin Valley during the day are over the Tehachapi Mountains to the south or up the Sierran slopes to the east. Typically, a nocturnal inversion will form which traps the pollutants remaining in the valley after sunset. Various mechanisms such as the Fresno eddy and the low-level jet act to redistribute the pollutants within the valley during the night (Smith et al. 1981). The summer wind flow patterns are the same day after day unless disrupted by larger, synoptic scale meteorological events.

While the Los Angeles basin and the San Bernadino Mountains to the east have been reporting pollution problems since before 1953, the first report indicating

pollution problems in the San Joaquin Valley and Sierra was not until 1969 (Miller et al. 1969). Miller et al. conducted a survey of oxidant air pollution damage to various tree species in the forests of California. Since then, many studies have verified this and documented that the problem is worsening. While meteorology and air pollution go hand in hand, very few studies have focused on both in the Sierra. It is extremely important to know air pollution concentrations but without meteorological data it is impossible to determine the origins of the air pollution.

The goal of this thesis was to gain a better understanding of the aerosol transport and meteorology in the southern Sierra by conducting aerial measurements of meteorological parameters and aerosols. Upper air wind data and surface meteorological data were collected along an elevational gradient (560 to 2720 meters elevation). Boundary-layer meteorology and aerosol concentrations were collected at one site (2222 meters elevation). In the following chapters are an extensive literature review and description of the experimental design followed by the data analysis and summary. The data analysis includes the data collected during ten days in August, 1985. This includes 17 aerosol and 23 meteorological profiles for one site, approximately 50 wind speed and wind direction profiles for four sites and continuous ground meteorological data for three sites.

CHAPTER II

REVIEW OF PREVIOUS RESEARCH

A. Tethered Balloon Systems

This section will review studies which have used tethered balloon systems to measure pollutant concentrations. An extensive review on this subject was done by Armstrong et al. (1981). Armstrong also described several sampling systems that they developed at the Denver Research Institute. One of these systems was used to sample particle emissions downwind from two Hayden coal-fired power plants in Colorado from morning to midday on November 29th, 30th and December 1st, 1977 (Armstrong and Russell 1979). Some earlier field tests were conducted at Arapahoe power plants, also in Colorado. The balloon suspended a single 1200 gram sampling package within the power plant plume; horizontal and vertical gradients were not measured. The sample surface was a 0.4 micron nucleopore strip filter attached to a plate. The sampling head, attached by a flexible tube to a pump, moved across the filter powered by three silver cell batteries. A ground based radio transmitter controlled the sampling head, pump operation and emergency flight termination. The filters were analyzed using a scanning electron microscope with a KEVEX energy dispersive X-ray analyzer. Although the samples were amenable to bulk sample X-ray excitation analysis, this was not done. The appropriate sampling time for the X-ray analysis was dependent on the horizontal distance

from the power plant. A 15 minute sample at a distance of 150 meters was considered adequate while a 120 minute sample was needed with a distance of 1000 meters. A 1175 gram battery powered transmitting meteorological package (Atmospheric Instrumentation Research, Inc.) was carried by a second identical balloon to measure dry and wet bulb temperature, horizontal wind speed and direction and pressure (change). Results were presented on particle size and composition of the plant emissions.

A tethered balloon system with a 16 kilogram transmitting instrumentation package (including temperature, wind speed, pressure, humidity and aerosol concentrations) was operated up to 500 meters to study aircraft noise propagation (Sentell et al. 1976). Aerosols were measured using a sizing aerosol counter (light forward scattering). Calibration size categories were ≥ 0.3, ≥ 0.5 and ≥ 3.0 microns. Balloon height was determined by the pressure transducer in the instrument package, which was temperature compensated. Sampling was conducted starting at sunrise for four hours on June 29, 1976, at Wallops Island, Virginia. The ≥ 3.0 micron aerosol count was less than 0.9 per cubic centimeter and showed a slight increase by the last sounding (0900 EDT). At sunrise and for an hour after, the ≥ 0.5 and ≥ 0.3 micron aerosol concentrations were less at the ground level (40 and 250 per cubic centimeter, respectively) becoming constant above the inversion top at approximately 100 meters (200 and 800 per

cubic centimeter, respectively). As the temperature inversion broke up and the temperature profile became isothermal, aerosol counts became constant with height. The particle counts increased by 100 to 200 (0630 EDT) as a result of increased mixing and then decreased by 100 (0800 EDT) with the establishment of an adiabatic lapse rate.

Three grab samplers and a radiosonde unit (temperature and humidity), both timer-activated and battery powered, were attached to a tethered balloon system over Cincinatti, Ohio (Cleeves et al. 1966). Grab samples had to be removed before the one-hour timer recycled. A hand-operated ground grab sampler was also used collecting samples at the five foot level. Profiles were collected up to 275 meters at various times during ten days in July and August, 1962. The two liter grab samples were only analyzed for methane (parts per million (ppm)) but analysis of carbon monoxide, carbon dioxide and light hydrocarbon gases up to propane would have also been possible. Had the collector bag been inert, additional gases could have been determined. The weight of one grab sampler unit was 900 grams. The weight of the radiosonde was not given but was less than or comparable to one grab sampler unit. The approximate balloon height was determined by the elevation angle and the length of the tether line. Results indicated that methane concentrations at the five foot level were higher at night and early morning (2 to 6 ppm) and morning surface concentrations (before 0500 EST) were higher (2 to 4 ppm)

than those at 100 meters or above (≤ 2 ppm). By early afternoon the concentrations were generally constant with height up to the maximum height sampled with values around one to two ppm.

Vertical profiles of two types of pollen (40 and 13 micron diameter) and one type of fungal spore (10 micron diameter) were measured from ground level up to 800 meters over an agricultural field in the Po Valley near Bologna, Italy, during September 1975 and May and July, 1976 (Mandrioli and Tampieri 1978). Profiles were made once a day (19 days total) between the hours of 0900 and 1530 using four radio controlled impactor type sampling units and a radiosonde. The batteries supplied a constant voltage for each motor for at least 45 minutes. The sampling surface was a plastic strip (Melinex) 1 millimeter thick coated with silicone grease. The weights of the instrument packages were not indicated but they were lifted by a 14 cubic meter tethered balloon. This size balloon would have had a lift of aproximately 15 kilograms at mean sea level (standard atmospheric conditions) not including the weight of the balloon (Warren et al. 1971). The grass pollen and fungal spores were from local sources whereas the chestnut pollen was transported from 40 kilometers to the south. The typical midday temperature profile was neutral to slightly unstable up to 300 meters then slightly stable to the maximum height of sampling. In general, the local source pollen and fungal spores decreased rapidly

with height to 100 meters and then increased back to ground concentrations or slightly less above 100 meters. The authors hypothesized that during unstable conditions the two layers were independent and seperated at the level of maximum eddy vertical velocity variance which corresponded to a minimum in the concentration profile. The authors theorized that these two layers sometimes mixed giving profiles that were somewhat uniform with height. Since the chestnut pollen was from a remote source, its midday profiles did not show a simple correlation to the local temperature profiles. The concentration profiles were probably the result of re-entrainment during windy conditions or due to varying advective conditions. Profiles for all three sources during elevated inversion conditions tended to show a peak at the base of the elevated inversion above which the concentrations varied widely. In addition to the ground being a source, it was thought that particles aloft from previous days may have also been trapped in the stable layer. In summary, they stated that the ground layer was strongly influenced by emission rates whereas the layer aloft was constant with height over a period of a few days and mainly influenced by "random intakes" from the air below. The authors acknowledged that their interpretation was made without data on the dynamic structure of the atmosphere.

A tethered balloon system equipped with a Mast-Brewer ozonesonde (MAST Development Co., Davenport, Iowa) was used

to measure ozone profiles up to 200 meters in the rural town of Hay in New South Wales (Galbally 1968). Information was not given on the balloon dimensions but the weight of the ozonesonde was less than one pound. The sonde was designed to operate for four hours using water-activated batteries. Data was presented for sounding profiles performed during a 24 hour period starting 1600 August 22nd, 1967. Before the onset of the nocturnal inversion, the concentration profile was constant with height (23 parts per billion (ppb)). Inversion formation began after 1600 local time and a gradient was established where ozone concentrations increased with height from the ground up. The gradient was sustained until the morning inversion break up at 0900 (local time). Surface concentrations were less than 8 ppb throughout the night and the same as the 200 meter level by mid-afternoon. The concentrations during the 24 hours at 200 meters varied from 23 to 28 ppb. Calculated flux values using wind data from an airfield 6 kilometers away ranged from 14 to 36 billion molecules per square centimeter per second agreeing with values from a previous independent study.

A similar study done in Tateno, Japan, also found the upper layers to be largely conservative (30 to 40 ppb) with little variation in the ozone concentrations (Sekihara et al. 1977). A total of 25 tethered balloon profiles were conducted between May and November, 1976. No surface ozone was detectable when a very stable nighttime surface layer

prevailed. Ozone concentrations increased after sunrise even before the inversion had broken. In a few cases, the surface and upper level ozone concentrations were unusually high (70 ppb). In these cases, transport of ozone or oxidizing substances from the surface upward was suggested.

In Japan, three types of ozonesondes have been developed and one has been used in the Antarctic since 1966 (Kobayashi and Toyama 1966a, 1966b; Kobayashi et al. 1966). The optical type can be used only in the daytime and at levels above 15 kilometers. The two electrochemical types (using either the potassium-iodide or the carbon-iodine titration method) can be used at heights below 30 kilometers. Test flights for these two ozonesondes have shown them to be accurate to ±two percent in comparison to each other and to other methods. The optical type ozonesonde had a lower accuracy of ±15 percent below 15 kilometers. The ozonesondes were constructed to be "low cost and small weight" although specifics were not given. The electrochemical ozonesondes were approximately 12 by 23 centimeters in size as illustrated in a cross-sectional diagram.

Regener (1960, 1963, 1964) describes a 1 kilogram chemiluminescent ozonesonde that is powered by 3-1.5 volt dry cells connected in series and can be directly connected to conventional radiosondes without modification. The sonde is calibrated with an ozone generator before each flight. This type of ozonesonde has been used by the Air

Force Cambridge Research Laboratories and the U.S. Weather Bureau.

A program entitled "Atmospheric Studies in Complex Terrain" conducted nocturnal tracer releases in the coast range of northern California in September, 1980 (Dickerson and Gudiksen 1983). Part of the tracer sampling network (five experiments) were tethered balloons collecting tracer samples up to 500 meters above ground level. Two perflourocarbon tracers were released at five meters simultaneously from half way up the slopes of two adjacent drainages (Anderson and Gunning Creeks). While the horizontal distribution was similar for all five releases, the vertical distributions were not. One experiment (#4) showed that the tracer decreased rapidly with altitude indicating vertical stability. Another experiment (#2) resulted in lower concentrations that were homogeneous with altitude. The other experiments were intermediate to these two. Heavy methane tracers were released at two heights simultaneously (5 and 60 to 75 meters above the ground) near the ridge top of a drainage (Anderson Creek). The vertical distributions were much like the perfluorocarbon distributions except the bulk of the tracer was within the lowest 200 meters. Sulfur hexafluoride tracer was released in the upper part of a narrow and steep drainage at five meters (Putah Creek). While the average transport speed for the previously mentioned tracers was one meter/second, in this drainage the average was two to four meters per

second. One experiment (#4) showed high elevated concentrations with no surface impact and another (#2) showed high surface concentrations. Tracer plumes were first detected at an elevated level with the bulk of the tracer arriving at the surface within one to two hours over the valley basin. The various tracer plumes all merged over the basin at approximately the same altitude during the one experiment (#4), with sulfur hexafluoride passing through first, while they all merged at the same time and altitude for another experiment (#2). The various differences between the experiments were attributed to the influences of the regional scale flows in the vicinity of the release sites. During one experiment (#4), the regional flow was in the direction of the general drainage flow while during another (#2), the regional flow was directly opposite the drainage flow direction. Streamfunction analyses showed recirculation patterns which seemed to explain the vertical variability remarkably well.

Perroud et al. (1973) used captive balloons to measure sulfur dioxide, chlorine and hydrocarbon concentrations as well as meteorological variables such as humidity, pressure, temperature and wind speed. Depending on the load, five different sized-blimp shaped balloons were used. Sulfur dioxide and hydrocarbon concentrations had similar profiles under no inversion conditions. The concentrations decreased rapidly from the surface to 400 to 600 meters above ground level after which they increased again. The

chlorine increased from very low values up to 400 meters above ground level and then remained constant. Under inversion conditions, the sulfur dioxide profile was very different. The concentrations were three times higher than the maximum values in the former case below the inversion level but near zero at the surface. Above the inversion the concentration dropped to zero and then increased again. The chlorine and hydrocarbon profiles were similar to the no-inversion condition except the chlorine levels were 50 percent lower and the hydrocarbon concentration decreased to near 0 at 400 meters. Since only the abstract and figure labels had english translations, a more detailed review was not possible.

A study to determine the sulfur dioxide mixing height was conducted from April to October, 1974, at a location five kilometers southeast of the city of Bedford, Great Britain (Garland and Branson 1976). The main sources of sulfur dioxide were two brickworks to the west-southwest of the study area. Sulfur dioxide bubblers were placed at five levels on a balloon (powered from the ground through a metal cable tetherline) at varying intervals ranging from 150 to 1200 meters and sampled for one hour periods. No information was given on balloon dimensions but a single sampling package weighed nine kilograms. Meteorological variables (temperature, relative humidity, wind speed and direction) were measured on the same balloon before or after the sulfur dioxide profiles were taken. The paper

presents data for 15 profiles: 10 during the late afternoon, 4 during the late evening and 1 during the mid-morning. The shape of the individual profiles exhibited large variability which was attributed to the differences in meteorology and sources. From the limited number of profiles during stable conditions, it was suggested that the inversion did not always limit the upward spread of pollutants as observed by other authors. Height versus average concentration was plotted for selected profiles (profiles with local influences or with samplers in the clouds were excluded). The plot showed an increase of concentration with height (20 percent) up to 500 meters with a more distinct decrease above. The mixing height was estimated by extrapolating the sulfur dioxide concentration to zero and was determined to be 1200 to 1500 meters above the ground.

A lightweight sampling package (2.3 kilograms) was designed by the U.S. Forest Service for monitoring smoke plumes from forest fires (Ryan et al. 1979). Twelve sampling packages were carried on a 99 cubic meter balloon with 45 kilograms available lift at sea level (15 kilograms at 3000 meters above sea level). Packages included temperature and wind speed sensors and particle and gas-grab samplers. They were powered by three nine volt batteries (eight hour capacity). Both the grab and particle samplers were activated and deactivated at the ground by audio tones fed through a hard-wire control line.

Interrogation of all 48 sensor positions (4 sensors per package) was accomplished every 36 seconds and transmitted via hard-wire line as well. The particles were sampled through a teflon filter with a pump that could sample at constant flow rates of 0.5 to 4 liters per minute (loading compensated). The grab sample was collected in an aluminized five liter bag, although other types of bags could have been used. The pumps had a glass pre-filter and sampled at 0.05 to 0.2 liters per minute. This system was developed for sampling carbon monoxide, carbon dioxide (for forest fuel consumption estimation) and nitrogen oxides. They suggested that the balloon be positioned above the unstable region when samplers were located close to the surface to ensure balloon stability. When the balloon was near the surface under unstable conditions, the instrument packages were observed to swing 15 to 20 meters on either side of an imaginary center line with the balloon making figure eight movements. They found that the battery powered pumps which could normally run for 5 to 6 hours only ran for 30 minutes at near zero degrees celcius and quit at sub-zero temperatures. Results were not reported for the field tests and subsequent reports have not been published (McMahon 1986).

Large 10 and 20 meter diameter manned "balloon-borne Lagrangian measurement platforms" (LAMP) were used to investigate the conversion rate of sulfur dioxide gas to sulfate aerosol at the edges of power plant plumes (Forrest

et al. 1979; Zak 1981). They found an average conversion rate of 5.5 percent per hour with a range of 1.1 to 8.5 percent. The lower range was from a nighttime experiment over Alton-Wood River refinery area, Missouri, and the upper range was during the afternoon over St. Louis, Missouri. Conversion rates were on average much lower between the stack and the first measurement. From previous work and the results of the LAMP study, it was suggested that the key factors determining the conversion rate were the degree of mixing with background air, the chemical composition of the background air, the intensity of sunlight and the concentration of ozone. Ozone may have acted as a surrogate for free radical concentrations during the daylight hours resulting in higher conversion rates. Plume edges showed higher conversion rates than plume centers and were comparable to rates found in urban atmospheres.

Several studies have used tethered balloon systems to address meteorological topics such as turbulent fluctuations in wind, temperature and humidity over the Sea (Thompson 1972) and land (Yokoyama 1969; Haugen et al. 1975) and inversion breakup in mountain valleys (Whiteman 1982). The study by Haugen, et al., investigated the feasibility of turbulent measurements using balloon systems as measurement platforms and is discussed in more detail in the methods section of this paper. Whiteman used the same meteorological package used during this study to

investigate the morning inversion destruction in several
valleys in Colorado and developed a thermodynamic model for
the same. The model was able to simulate the temperature
structure evolution in a wide range of valley topography
without accounting for the along-valley wind systems (up-
slope mass transport was implicit). The simulations for
two of the three inversion breakup patterns observed were
obtained by fitting two constants related to the surface
energy and energy partitioning. This study will be dis-
cussed further in the next section.

B. Topographic Wind Systems

1. Introduction

This section will begin with an overview of the major
meteorological influences in the San Joaquin Valley of
California and a summary of the presently accepted theory
on topographic circulations with a brief description of
their general characteristics. Several wind patterns that
complicate the typical day/night topographic flow structure
are then presented. The various field studies which
describe the wind and temperature regimes observed in
mountainous terrain follow. Finally, the processes related
to nocturnal inversion breakup and formation as studied by
Whiteman are presented (1980, 1981, 1982).

There is a large body of literature on meso-scale
circulations in mountainous terrain beginning in the early
1800's and only the most relevant features can be presented
here. Several authors have presented reviews covering the

literature at various times (Hawkes 1947; Defant 1951; Orgill 1981; Whiteman 1980). The proceedings of many conferences and symposiums are available with abundant papers presented on mountain meteorology and related subjects (American Meteorological Society 1974, 1976, 1978a, 1978b, 1979, 1981, 1983, 1984; Reiter and Rasmussen 1967). Several of the papers presented at these meetings are discussed below.

2. Overview

Wind patterns in the mountains during the summer are necessarily complex due to the rugged and non-uniform terrain and intense daytime solar radiation. To the west of the southern Sierra Nevada are the San Joaquin Valley and the coast range and to the east are the Owens Valley and the Inyo mountains (see Figure 2). The western slope of the southern Sierra Nevada begins at the foothills of the eastern San Joaquin Valley and, for more than 60 kilometers, rises from 100 meters to over 4400 meters above sea level at the crest. In contrast, the eastern slope rises abruptly from the Owens valley (1000 meters above sea level) to the Sierran crest in only 24 kilometers (75 percent of the rise is within 10 kilometers of the crest).

During the summer months, the dominant wind direction in the San Joaquin valley is from the northwest to southeast or "up-valley" from Stockton toward Bakersfield. This flow results from a combination of the land-sea breeze, the Pacific coast summer monsoon and the topo-graphical

constraints of the coastal and Sierra Nevada mountain ranges. Marine air flow observations for the Pacific coast have been numerous (Fischer 1960; Edinger and Helvey 1961; Pearce 1962; Frenzel 1962; Lowry 1963; Edinger 1963; Fosberg and Schroeder 1963, 1966; Staley 1957).

Many theoretical papers and reviews on the land-sea breeze have been published (Defant 1951; Pearce 1955; Palmer 1957; Fischer 1961; Estoque 1961, 1962; Schroeder et al. 1967). The land-sea breeze cannot be discussed without the summer monsoon. The summer monsoon lasts from late spring to fall. The land-sea breeze is a local, small scale convection wind often limited to the east by the low coast range. The summer monsoon is part of the general circulation in that it is part of the semi-permanent subtropical high pressure belt and it is limited to the east by the Sierra mountain barrier (Schroeder et al. 1967). The summer monsoon winds travel inland off the ocean and do not reverse at night as the land-sea breeze does. The land-sea breeze is the result of differential heating of the land and water. Since water retains heat longer than land, the land is heated by day and cooled by night whereas the temperature of the ocean remains relatively constant. The ocean is at its lowest temperature in the summer due to it slowly cooling throughout the winter months. The ocean temperature is further cooled by summer upwelling of cold bottom waters. During the daylight hours, the sun warms the land and the

land warms the air above it. As the buoyant air rises, it is replaced by the cooler and denser air from over the ocean resulting in an onshore flow or "sea-breeze". To compensate for the surface movement of air from the ocean, air above the land moves toward the ocean and subsides creating a closed circulation cell. The reverse or "land-breeze" occurs at night but rather than offshore flow, what is observed is a decrease in speed of the onshore flow (Frenzel 1962). This is because the sea-land breeze is superimposed on the Pacific coast summer monsoon with each modifying the other. Schroeder et al. (1967) point out that because of the monsoon, the sea breeze has no significant moisture across its front unlike those found elsewhere.

Schroeder et al. (1967) classified the marine air flow into "warm" and "cool" days. Warm days (offshore gradient) occurred when the temperature in Sacramento was greater than 38 degrees celcius. These days were characterized by an intense sea breeze "front", little inland penetration, shallow sea breeze depth, weak sea breeze flow and shallow marine layer. Cool days (onshore gradient) occurred when the temperature in Sacramento did not exceed 32 degrees celcius. These days were characterized by a weak sea breeze front, far inland penetration, deep sea breeze depth, strong sea breeze flow and deep marine layer. Marine air is able to flow through gaps or low ridges in the coast range into the Central Valley. Different

synoptic patterns result in conditions in between the two extremes described above.

The timing of the northwesterly flow of "marine air invasion" can be seen from Fresno wind data (Smith et al. 1981). During the morning the flow is frequently from the south or from the west (toward the Sierra) and characterized by light wind speeds. By afternoon, however, the winds are stronger and from the northwest peaking between 1600 and 1700 PDT (4 to 5 meters per second). The strongest wind speeds, however, are observed near midnight due to the formation of a low-level nocturnal jet. When the nighttime inversion begins to form, the layer of cooler air next to the ground is decoupled from the warmer air above. As a result, the northwesterly wind just above or at the height of the nocturnal inversion top is released from the frictional effects of the ground surface and accelerates to supergeostrophic speeds as high as 20 meters per second (Smith et al. 1981). The average height of the low-level jet maxima is around 300 meters. In the northern half of the Valley the jet is stronger, develops later and is centered at a higher level than in the southern half of the Valley (Willis and Williams 1972; Morgan 1974). Almost every day of the year, a nocturnal inversion forms in the San Joaquin Valley (Lorenzen 1979). There is a tendency for the jet to form on all nights yet high velocity jet occurences (greater than eight meters per second) are less frequent (Smith et al. 1981). There have been some summers

when the jet did not occur very frequently. This was probably due to the lack of gradient between the coast and inland areas which is necessary to set up the northwest air flow up the San Joaquin Valley (Morgan 1987). The jet is less developed when the marine air inversion is deep enough to allow the cool marine air to flow over the coast range into the Valley and weaken the thermal low and hence, the northwest flow (Willis and Williams 1972).

The southerly flow observed in the morning hours is due to a wind pattern referred to as the "Fresno eddy" and occurs regularly during the summer (Smith et al. 1981, Blumenthal et al. 1985). When the Valley nocturnal inversion top is below the surrounding topography and the flow is northwesterly, the Tehachapi Mountains to the south block the air flow causing it to stagnate and be diverted cyclonically back to the north. The vertical extent of the Fresno eddy is on average 1000 meters, begins close to midnight and is observed in Fresno by 0900 PDT the following morning. The eddy center is generally located west of Visalia near Highway 99 with Fresno being the northern limit. On rare occasions, however, the Fresno eddy has extended as far north as Manteca (Smith et al. 1981). The eddy is usually restricted to the eastern side of the Valley causing a funneling of the northwesterly flow down the western side of the valley in the morning hours. On one of these occassions, velocities as high as 16 meters per second at 500 meters above ground level were observed

on the western side. The eddy wind speeds are generally
less than five meters per second. The days the eddy was
absent were characterized by a cold air trough moving over
the area causing cooler air temperatures aloft. During
these times, air continued to flow over the Tehachapi
Mountains for most of the night. During a study in 1979,
both the Fresno eddy and the low-level jet occurred
approximately 80 percent of the time in July and September
(Smith et al. 1981). While the jet provides a mechanism to
rapidly transport air pollutants from north to south, the
eddy effectively transports pollutants throughout the
southern part of the Valley and possibly upwards to higher
altitudes. The section in this paper on Pollutant
Transport Studies in the San Joaquin Valley describes a
conceptual model of the Fresno eddy.

3. Topographic and Slope Circulation

 Topographic winds include daytime up-valley and upslope
winds, nighttime down-valley and downslope winds and
associated compensation winds. For the purposes of this
report, compensation winds will be discussed seperately
from topographic winds although compensation winds are part
of the topographic wind system. During the daytime, flow
in the mountains is directed upslope and up-valley
("valley" wind), often like clockwork, usually beginning
a few hours after sunrise and ending near sunset. During
the nighttime, the flow is reversed to downslope and down-
valley ("mountain" wind). Commonly, return currents exist

above the valley and mountain winds. The terms used in the literature for the return flows include anti-winds, anti-mountain and anti-valley winds, counter-flows and compensation winds. The literature is replete with departures from the basic valley, mountain and slope (upslope and downslope) wind patterns due to the variety of valley orientations, shapes and sizes and the complex interactions with gradient winds and adjacent valleys and ridges. Invariably, for every generalized trend reported, there are cases that support the opposite trend.

Although not completely understood, the slope, valley and mountain winds are the result of a baroclinic condition due to temperature gradients from unequal heating. The thermal upslope flow results from the sun warming the sloping ground which in turn warms the air next to the slope. A horizontal pressure gradient away from the slope results between the warmer air next to the slope and the cooler air at the same height away from the slope. Due to the confines of the slope and the buoyant character of the heated air, the air is forced upward and along the sloping sidewall. Very small temperature differences between the slope and the free air over the valley can initiate the upslope flow (Atkinson 1981). The reverse situation occurs at night. Once the slope no longer receives solar heating, the air adjacent to the slope is cooled faster than the air further away over the valley. A pressure gradient toward the slope results but since the cooler air is heavier, it

moves downward along the slope by gravity flow.

The valley and mountain winds are thermally induced as well. The distinction lies in the difference of scale. Considering a horizontal plain that is adjacent to a valley, both receiving solar radiation during the daylight hours, the volume of air over the plain is much larger than the volume over the valley. The valley sidewalls offer more surface area for heating the air as well as an additional mechanism for distributing the heated air (upslope flow). As a result, the air temperature over the valley becomes warmer than the air over the plain at the same level creating a horizontal pressure gradient toward the valley. The resulting flow is toward the valley (up-valley). At night, the pressure gradient reverses and the resulting flow is toward the plain (down-valley).

The mechanism by which the slope winds transfer heat to and from the valley atmosphere, as mentioned above, remains somewhat unresolved. In the following discussion only daytime flows will be mentioned since nighttime flows are simply the reverse of daytime flows but at a lower magnitude. It is clear that, at the ridge level, there are vertical currents that carry the slope flow upwards during the day. Wagner (1938) theorized this air is subsequently transported over the center of the valley and is mixed downward back into the valley. Few observations have documented this type of vertical motion or convergence zone over the center of a valley (Hindman 1973; Myrup et al.

1983). Scorer (1958) speculated that the air moves horizontally to the valley center at various levels along the slope. This theory would not allow the depth of the upslope flow to increase toward the ridge as observed. The various evidence points to the importance of the valley sidewalls in the valley and mountain wind systems with some authors stating valley and mountain winds are the consequence of the slope winds (Thyer 1966). Sterten and Knudsen (1961) theorized that after sunrise, as drainage flow ceases at the head of the valley but continues at the other end of the valley, the resulting pressure gradient would initiate the up-valley flow. Poor understanding of the various mechanisms involved and their relative importance that has contributed to the difficulty in modeling mountain meteorology.

Although exceptions can be found for every rule, some characteristics of slope, valley and mountain winds appear repeatedly in the literature (Defant 1951; Thyer 1966; Buettner 1967; Whiteman 1980; Orgill 1981). In general, they found the upslope flow is thicker and greater in magnitude than the downslope flow and both increase in depth downwind. Downslope wind speed has been reported to be both proportional and inversely proportional to the slope of the valley sidewall. This was also true for the slope of the valley floor and the valley and mountain wind systems. The cross sectional shape of the valley, however, does not seem to influence the valley and mountain winds.

Valley size appears to affect the timing of the flows; wind systems develop sooner and more rapidly in smaller valleys. Both the depth and magnitude of the valley and mountain flows have been found to decrease with distance up-valley. The depth of the valley wind flow tends to be close to the ridge height whereas the depth of the mountain wind flow is below ridge height. Both the slope, valley and mountain winds have wind speed maxima above the surface where frictional forces are reduced. Slope winds are easily modified by changes in topography, solar insolation, vegetative cover and weather conditions. Compensation winds have been both observed and not observed. When they occur, they are usually as thick as the mountain or valley wind layer underneath but can be reduced below ridge level or entirely suppressed with strong gradient winds. Compensation winds form later and end sooner than the corresponding valley and mountain winds. Qualitatively, the above characteristics are most likely observed under light to moderate gradient winds and clear skies in a close to "ideal" valley which is, as described by Buettner (1967), closed at the head (not a pass), slopes down to and opens into an adjacent plain and is large, dry, straight and steep but not canyon-like.

4. Other Wind Flow Patterns

The basic valley, mountain and slope flows interact with other commonly observed wind flow patterns in complex ways. Complicating the general picture are cross-valley winds,

nocturnal airfalls, jets and surges, wind profile
instabilities and "maloja" type winds. Cross-slope flow
results from the unequal heating of the opposite valley
sidewalls resulting in a wind flow towards the more heated
slope. For example, in a north-south oriented valley
after sunrise, a circular flow develops with winds flowing
up the heated east facing slope, crossing below ridge level
to the shaded west facing slope and then down the west
facing slope. The opposite would occur once the east
facing slope was heated in the late afternoon while the
west facing slope became shaded. During midday or
midnight, these patterns would be dimished due to the
heating and cooling becoming more evenly distributed
throughout the valley. Interaction of the slope flows with
the valley and mountain wind systems and overlying winds
makes the cross-valley flow difficult to observe in its
pure form. Wanta and Lowry (1976) have presented, in
theory, circulations resulting from various combinations of
valley orientations and upper-level gradient winds, some of
which are relatively complex. McHattie (1968) observed
considerable cross-valley component in a north-south
oriented valley in Kanasis Valley of southwestern Alberta,
Canada.

Nocturnal airfalls have been observed by Morgan and
Slusser (1979) in the southern Sierra Nevada of California
and are the result of terrain channeling. From their
ground observations, they found that these winds occurred

at the bottom of steep canyons that drained large
watersheds. One site showed maximum wind speeds of eight
meters per second, averaging around six meters per second.
These airfalls developed a few hours after sunset and ended
abruptly one hour after sunrise. In the mountains, the up-
valley nocturnal low-level jet has received little
attention but results from the same mechanisms (although on
a smaller scale) responsible for the low-level nocturnal
jets observed all over the United States at all seasons of
the year (Blackadar 1957). As the nocturnal inversion
forms, the late afternoon up-valley flow is decoupled from
the surface resulting in increased wind speeds. This
phenomenon has been observed in the Sacramento Valley
(Myrup et al. 1986) and the San Joaquin Valley (Giroux et
al. 1981; Smith et al. 1981; Blumenthal et al. 1985).
Whiteman (1982), during an investigation of the inversion
formation period in Colorado Rocky Mountain valleys, did
not observe an increase in up-valley wind speeds but rather
a decrease. Nocturnal surges have been widely reported in
the literature (Buettner and Thyer 1966; Tyson 1968;
Dickerson 1980). Surges result from adiabatic heating of
the air as it moves downslope or down-valley which weakens
the pressure gradient responsible for its movement. The
downslope or down-valley flow slows down until the air is
cooled enough to produce the pressure gradient that drives
it downslope or down-valley again. These wind speed
oscillations have been observed in the mountain wind (down-

valley) with periods ranging from one to three hours. Similar oscillations in the daytime valley winds have not been reported (Orgill 1981).

Wind profile instabilities occur in the mountain wind profile within the inversion layer. Davidson and Rao (1963) observed wind speed deformations below the level of maximum wind speed possibly initiated at the ground by sudden large wind shears which then propagated upwards. It was noted, however, that wind shears observed near the surface did not always lead to profile deformations. Whiteman (1980) observed temperature profile deformations that corresponded to wind shifts or directional wind shears within the inversion layer prior to sunrise. He suggested a similarity of these deformations with those observed by Petkovsek in Yugoslavia. Petkovsek (1973) attributed the deformations to downslope flow penetrating horizontally into the valley after being heated adiabatically. The flow was restricted to a thin 30 to 180 meter layer due to intense temperature gradients within the inversion layer. Petkovsek found 97 percent of the deformations occurred at night. A study conducted in the northern Sierra Nevada observed multiple layers within a surface based inversion by acoustic radar (echosonde) (Dunsmore and Fransioli 1978). The layers were attributed either to slope advection of cooler air near the valley floor displacing warmer air upward or advection of warmer air into a level above the valley floor. These differences in air

temperature probably originated from the unequal cooling near sunset of opposite slopes. They found that under the influence of strong gradient winds, the thin layers exhibited internal gravity waves which propagated at near Vaisala-Brunt frequency (3 to 24 minute periods). When temperature data were available, the temperature variations corresponded to the echosonde records. The layers were shear zones with vigorous mixing and were not associated with updrafts. A study conducted at Kirkwood Meadows near Lake Tahoe, California, also found evidence of gravity waves within the inversion layer at Vaisala-Brunt frequencies (three to five minute periods) which were attributed to the winds aloft (Palmer and Watrous 1978). The "sloshing" back and forth across the valley was observed by filming the movement of smoke. The transverse gravity wave enhanced the mixing of the smoke along and near the bounding slopes. Later in the morning, during another smoke release, the waves were gone and general mixing prevailed. There was evidence of interaction between the gravity wave oscillations and the up-down valley velocity fluctuations.

Winds that are down-valley during the daytime have been observed in many mountain regions of the world and have frequently been called "Maloja" winds after a mountain pass between Engadine and Bergall Valleys in Switzerland (Huschke 1959). This unusual wind pattern is characterized by down-valley flow during the day. In Switzerland, the

stronger daytime valley-wind from the Bergall Valley flowed over the pass and continued down the Engadine Valley. DeMarrais et al. (1968) frequently observed up-valley winds from the Camas Valley flow over the pass and down into the valleys to the north in Sawtooth National Forest, Idaho. Buettner (1967) observed Maloja type winds in two valleys of Mount Ranier in Washington. These valleys showed "correct" up-valley winds in the morning and/or afternoons with Maloja type winds the rest of the time. These winds were observed at some sites but not others, apparently influenced by the glaciers, adjacent valleys and timing of insolation down-valley from the sites. Somewhat related are the downslope winds observed on the east side of the Coast Range in San Diego, California, during the afternoons resulting from marine air "spilling" over the coastal mountains (Schroeder 1961). The down-valley winds occurred both when the marine inversion was deep (cool weather type) and when it was shallow or absent (warm weather type). The down-valley winds tended to be stronger than the up-valley winds and generally replaced the up-valley winds before noon causing a 180 degree wind shift. These unexpected wind shifts were most likely the cause of many fire fighter fatalities on several wildfire incidents. These down-valley winds have been observed all along the eastern side of the California coastal mountains, on east-draining valleys in the foothills of the Sierra Nevada and on eastern slopes of the Santa Ana Mountains of southern

California (Countryman and Schroeder 1959a, 1959b,
Schroeder 1961). A similar wind pattern but on a larger
scale, are the Foehn-like Santa Ana winds which blow warm,
dry air over southern California from the Great Basin
(Sommers 1978). Although the mechanism is very different,
the effect is to dominate the local wind patterns in a
frequently unexpected and unpredictable manner.

5. Complex Terrain Field Studies

Intense local meteorological studies such as those
reported by Countryman and Schroeder (1959a, 1959b), Ryan
and Brown (1978) and Dickerson and Gudiksen (1983) are very
informative on the range of complex interactions that can
occur given the variation in weather and topography. For
example, Countryman and Schroeder documented the hourly
wind flow variations on an easterly draining mountain in
the Sierra Nevada with 20 meteorological stations. In the
early morning, west-facing slopes were showing down-valley
and downslope flow while eastern slopes were already up-
valley and upslope. By mid-morning the western slopes of
the Sierra Nevada had heated sufficiently to cause a
westerly (down-valley) flow throughout the study area.
More topographically sheltered slopes, however, maintained
upslope flow. The afternoon pattern was similar to the
mid-morning except for the area around the south-facing
slopes of a prominent ridge where the flow was upslope.
Late afternoon showed stronger westerly winds which caused
winds in the study area to be less variable. An eddy

circulation that had been observed since early morning at one station was less pronounced as well. After sunset, flow for all the stations was downslope and down-valley. This area was studied in preparation for a prescribed burn. During the burn, a firewhirl developed at the same location as where the eddy circulation had been observed. Firewhirls have been well documented on the lee side of ridges and behave like dust devils except that they carry burning debris which can cause fires to spread more rapidly by spotting (Graham 1955).

An on going research program entitled "Atmospheric Studies in Complex Terrain" (ASCOT) began in 1978 with a major emphasis on studying nocturnal drainage flow (Dickerson and Gudiksen 1983). The field research thus far has been carried out in mountain regions of four states: Mayacmas Mountains (coast range), California; Rattlesnake Mountain, Washington; Pajarito Mountain, New Mexico; and Brush Creek (Rockies), Colorado. The majority of the research was conducted at Mayacmas Mountains in California. A high density of direct and remote sensing meteorological instrument systems were used in a relatively small area for each major experiment including instrumented towers, tethered sondes, mini-sonde equipped balloons, optical path anemometers, optically-tracked pilot balloons and doppler sodar. Several atmospheric tracer systems were used in the California experiments as well. Although the data analysis is far from complete, results that have been published to

date are extremly informative. Dickerson and Gudiksen
(1983) are the editors of a progress report that summarizes
the program over four and one half years and includes
extensive references. The following is a very brief
summary of some of the results from the ASCOT studies.

Interaction of drainage and upper level wind fields
created complex flow patterns. In the coast range of
California, there were three larger-scale winds that
affected the local drainage winds: winds from migratory
synoptic disturbances, seasonal onshore flow of marine air
or afternoon sea-breezes and descending upper-level
easterly winds. In summertime, when the migratory synoptic
features were less frequent, strong drainage flows occurred
over 50 percent of the time. Although cooling occurred
before the local sunset, downslope flow did not begin until
the ambient winds were light enough and an adequate surface
inversion formed (3 to 30 degrees celsius over few tens of
meters or less).

The inversion depth was observed to range between 3 and 7
percent of the vertical drop (for all experiments) from the
top of the slope. Although the inversion depth increased
linearly with distance down the slope, the strength of the
inversion and the wind speed increased at a lesser rate. A
low-level "jet" occurred at approximately one half of the
inversion height that was associated with the drainage
winds. Vertical profile data of tracer concentrations from
Mayacmas Mountains showed the tracer plumes to arrive first

a few hundred meters aloft and then later at the surface over the valley basin because of the increase in wind speed with height. Wind speed and drainage layer depth decreased with time during "good" drainage nights probably due to a decline in the influence of higher level winds from increased stratification.

The tracer experiments at Mayacmas Mountains indicated that surface drainage flows at and below mid-slope were fairly well decoupled from the upper level winds whereas there was considerable mixing between the transition layer (60 to 75 meters above ground level) and the drainage layer higher up on the slopes. Even when there was mixing, the tracer was confined to the lowest 200 meters indicating vertical stability. Meteorological and tracer concentration profiles indicated the existence of "recirculation" systems or compensation winds. Tracer experiments within the forest canopy showed that the canopy inhibited dispersion and slowed the transport speed.

6. Inversion Breakup and Formation

Whiteman (1980, 1981, 1982) has investigated both the breakup and formation of inversions in seven Colorado mountain valleys for both winter and summer seasons using a balloon-suspended meteorological sounding package. He described three patterns of inversion breakup, two of which only occurred once or twice out of 64 days of experimental data. The first pattern shows the convective boundary layer growing upward into the inversion. This pattern has

been most frequently observed over flat terrain.   In
pattern two, the convective boundary layer begins to grow
but ceases after a shallow height is attained.   The major
path of inversion destruction is accomplished by the
descent of the inversion top.   The most frequently
observed, third, inversion breakup pattern during this
study was a combination of the first two patterns.   Both
the growth of the convective boundary layer and the descent
of the inversion top acted to break up the inversion.

A subset of 21 cases in 4 different valleys under clear,
undisturbed weather conditions were chosen to demonstrate
the main features of the inversion breakup.   Overall,
inversion depths, as determined by the potential
temperature inflection point, were roughly the height of
the surrounding ridges but were lower than the height of
the regional terrain.   On average, inversion breakup was
completed 3.5 to 5 hours after sunrise.   The ratio of
inversion depth to valley depth ranged from 0.53 to 1.75
with and average of 1.10.   The inversions occurring above
the ridge height were probably regional, covering more than
one valley.   The inversions occurring below the ridge top
were probably due to terrain constriction upstream or
widening of the valley downstream.   The inversion depth had
a limited effect on the inversion strength; the deeper the
inversion the weaker was the inversion strength.

During the inversion breakup (after sunrise), five layers
were identified with characteristic temperature and wind

profiles. The two diagrams in Figure 1 show the typical wind and temperature patterns during valley inversion breakup (Whiteman 1982, Figs. 8 and 9). (1) A convective boundary layer was present immediately above the valley floor and (2) valley slopes with up-valley and upslope winds, respectively. (3) Above the convective boundary layer but within the valley, was a stable core region with down-valley winds. (4) The neutral layer over the inclined slopes of the Rocky Mountains and above the inversion top contained up-incline winds. (5) Above this layer were the gradient winds of the stable-free atmosphere. The subsidence of the stable core was attributed to the divergence of mass by the upslope flow. The average ascent rate of the convective boundary layer and descent rate of the inversion top were approximately equal (71 and 79 meters per hour, respectively).

After the inversion breakup, up-valley flow prevailed up to ridge height throughout the valleys. From limited observations of the cross-sectional structure, it was observed that the isotherms in the inversion layer were horizontal across the valley except for the cool, shallow down-slope wind layer near the slope. Although the convective boundary layer began to grow sooner over the sunlit slope, the growth rate was similar to that over the valley floor. The slope convective boundary layer showed temperature deformations and large down-valley wind components not observed in the valley floor convective
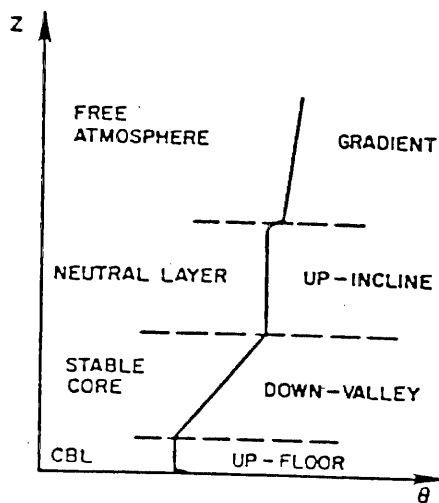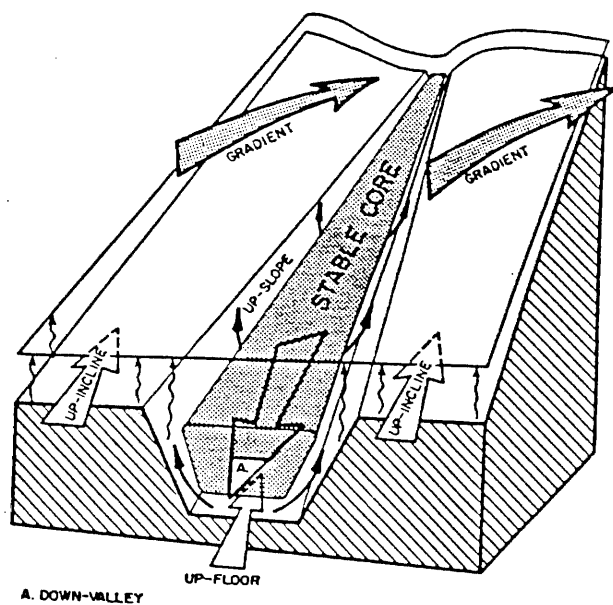
Figure 1: (Top) Typical correspondence between temperature and wind structure during inversion destruction and (Bottom) typical wind system development during inversion destruction (from Whiteman 1980).

cross-valley wind components were disorganized and showed multiple layering.

The evening inversion formation was initially characterized by four layers. From the ground upwards were a surface (inversion) layer, a constant theta (potential temperature) layer, an inversion cap (strong jump in potential temperature) and an isothermal layer. By approximately four hours after sunset, the surface layer had grown to the entire depth of the valley. Winds were down-valley within the surface layer and up-valley in the isothermal layer. Wind shear and cross-valley wind components were characteristic of the constant theta layer (the top portion of the down-valley flow regime). Winds within the inversion cap (50 meters thick) were weak and exhibited appreciable cross-valley components as well. The inversion depth initially grew rapidly for several hours (170 to 210 meters per hour), beginning 30 minutes or more before the sites were shaded. Down-valley winds were established below the inversion cap layer and increased in depth and speed. This was followed by a period of slower growth and wind development until sunrise. The maximum height of the inversion was approximately ridge height by sunrise. Both the constant theta layer and the inversion cap lasted until the inversion top reached a height of 500 to 600 meters above the site approximately two hours after sunset. The rise of the inversion cap was attributed to mass convergence from adiabatic vertical advection of the

down slope flow below the inversion top. The down-valley winds, unlike the up-valley winds, showed maximum speeds (eight to nine meters per second) in the center of the layer and decreased toward the ground and inversion top. Unlike a nocturnal jet, the maxima occur throughout the nocturnal period, are in the down-slope direction and are related to the decrease in frictional forces above the ground surface rather than from the top of the temperature inversion.

C. Pollutant Transport Studies in the San Joaquin Valley of California

1. Introduction

Numerous studies have investigated the flow patterns and associated pollutant transport in the San Joaquin Valley and Delta regions (northwest end of the San Joaquin Valley). These studies are particulary relevant since the pollutant distribution within the San Joaquin Valley determines the source strength of pollutants available for transport into the Sierra Nevada. To date, no summary exists for these large and informative studies. The various studies have measured vertical profiles and ground transects (width and length of the valley) of various meteorological variables and pollutant and tracer (from tracer releases) concentrations (Miller et al. 1972; Lamb and Shair 1977; Unger 1978; Carroll and Baskett 1979; Lehrman et al. 1980; Smith et al. 1981; Blumenthal et al. 1985). The studies by Lehrman et al. and Smith et al. extended their networks into the Sierra. Carroll and

Baskett and Miller et al. used aircraft and ground stations on selected days to specifically investigate the transport into the Sierra.

2. Review

A 1976 study in the San Francisco-Bay Area region completed 8 tracer releases from August 31 through September 14 (Lamb and Shair 1977). Two types of tracers were sampled by automobile, aircraft and automated ground stations from Sacramento to Manteca to the north and south of the release site, respectively. The releases were conducted during all hours of the day to investigate the various phases of the sea-breeze cycle. Of the eight releases, five were at Montezuma Hills (north of Antioch in the Delta region), one at Martinez and two at Pinole. On the average, the tracer was transported southeast over Stockton. It was apparent that material emitted from the northern portions of the Bay area followed trajectories south through Stockton and Tracy into the San Joaquin Valley although sampling stopped 17 kilometers south of Manteca.

The study by Lehrman et al. (1980) was conducted from the foothills to the upper reaches of the San Joaquin River Valley northeast of Fresno during the summer and fall of 1979 (see Figure 2). Tracer was released from Friant Dam (300 meters above sea level) August 25th and 28th, 1979, from 1200 to 1530 PDT and sampled by automobile and aircraft from 1530 to 1700 PDT. The aircraft was
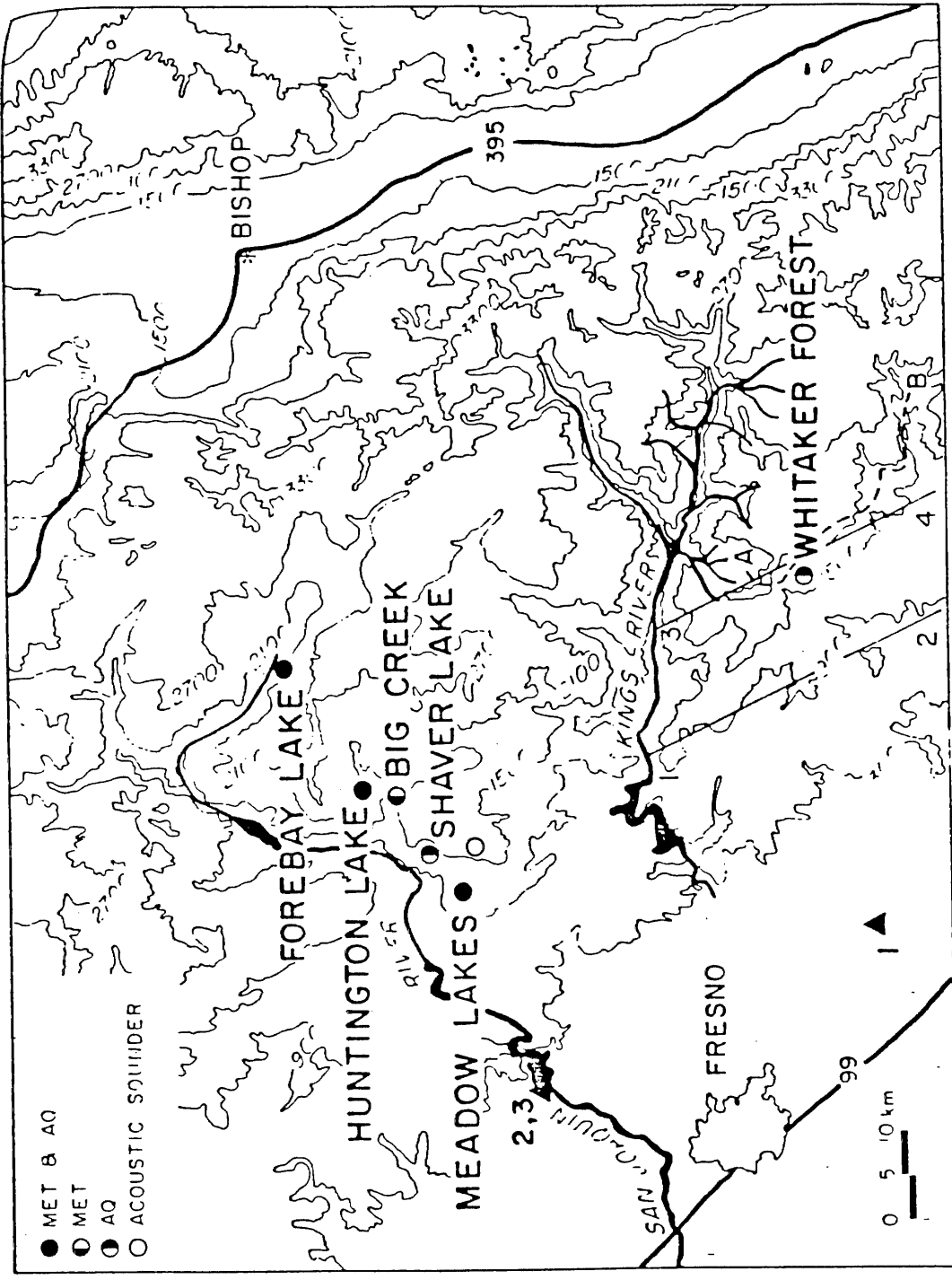
Figure 2: Map of study area for the Upper San Joaquin River Valley Impact Study (from Lehrman et al. 1980).

instrumented with a temperature probe. Additional
afternoon aircraft flights on July 27th and September 23rd
measured ozone, turbulence, dry-bulb and dew-point
temperature, nitrogen oxides, sulfur dioxide and
condensation nuclei. Ground stations were located along
the San Joaquin River at Meadow Lakes, Shaver Lake,
Huntington Lake and on the South Fork of the San Joaquin
River at the Forebay (1365, 1676, 2132 and 2184 meters
above sea level, respectively). These stations were
instrumented to measured ozone, particle light scattering
coefficient (indicates degree of light scattered away from
the line of sight by gases and particles), wind speed, wind
direction and temperature. Ozone data from the Forebay
site were not available due to equipment problems and
additional ozone data were available from Whittaker's
Forest (5360 meters elevation) in Kings Canyon National
Park. Pilot balloons were released frequently July 26 to
27, August 25 to 28 and September 23. An accoustic sounder
was operated at Shaver Lake from August through October to
obtain surface mixing depths.

At Shaver Lake, the mean nighttime mixing depth, as
determined from the accoustic sounder, was less than 25
meters and the afternoon depth exceeded 500 meters. The
afternoon mixing depths, as determined from the pilot
balloon observations, at Huntington Lake and Meadow Lakes
reached 400 to 600 meters above ground level while at
Millerton Lake the mixing depth often extended to 1000

meters above ground level. Little correlation was observed
between the daily surface maximum ozone concentrations at
Fresno and the mountain sites. Shaver Lake, however,
showed higher values during an extended period of high
ozone concentrations in Fresno. The mountain sites showed
a downward trend toward the end of the sampling period
while Fresno did not, indicating reduced slope transport.
Day/night ozone and scattering coefficient patterns
suggested transport from the valley with peaks occuring
later in the day and lower in magnitude at the mountain
sites than at Fresno. Ozone concentrations at the mountain
sites were relatively uniform throughout the day with a
less dramatic peak as compared to Fresno. The day/night
scattering coefficient at Forebay showed the least
variation and lowest median values indicating significant
dilution of the valley air mass. A high correlation
between the ozone concentrations and the scattering
coefficient at 1100 and 1700 hour (PDT) observations for
Huntington Lake indicated a well-aged pollution source.
Lower correlations were observed for 0500 and 2300 PDT
indicating local sources during the night and early morning
periods.

Aircraft traverses and spirals on July 27th showed the
mixing layer to be 1470 meters above the foothills and at
or above the surrounding ridge level for the mountain
sites (600 to 900 meters above ground level). Within the
mixing depth, the ozone concentration and scattering

coefficient were constant with height except over the Sierran crest where multiple layering of pollutants and meteorological parameters indicated less efficient mixing. Above the mixing height, the air was less polluted. Aircraft traverses indicated pollution levels decreased with increasing distance from the valley. On September 23rd, the afternoon mixing layer was 300 meters deeper over Huntington Lake and the same over the foothills as compared to July 27th. This difference was attributed to a cutoff low pressure area aloft off the central coast of California causing considerable instability. The ozone concentrations and scattering coefficient were much lower on the September flight.

On the day of the August 25th tracer release, the mixing height was 1290 meters above ground level over the foothills. Over Shaver Lake a neutral lapse rate extended to 760 meters above the ground capped by a weak inversion with a stronger inversion 180 meters higher. The South Fork aircraft spiral showed an even more complex temperature structure. The estimated path of the tracer plume was initially up the San Joaquin River but at 1500 PDT, the plume separated with one branch continuing up the river while the other headed to the east due to a wind shift. Tracer material was detected in low but significant levels at Forebay but not at Huntington Lake, which is up a small side drainage of the San Joaquin River. Initially, the plume was 26 kilometers wide but once the wind shift

occured, it was wider than the length of the 100 kilometer automobile traverse. The second tracer release was made under similar synoptic conditions as the first except with less cloud cover. Up to 1040 meters above the foothills, the temperature profile showed several alternating stable and unstable layers and above this the profile was more stable. Tracer concentrations peaked at Huntington Lake at 1800 PDT, beginning at 1700 PDT, and dropped to zero by 1900 PDT. A similar wind shift from west to northwest occured as in the previous tracer release but due to the sampling plan, the data only suggested a separated plume. Again the plume was widely dispersed and the tracer material above the foothills reflected the layering of the temperature profile. The South Fork was not sampled during this release. From the tracer tests, it was concluded that air reaching the mountain slopes originated from north of Fresno and the Fresno urban plume did not frequently impact the San Joaquin River Valley.

Smith et al. (1981) presented the results from six summer and six fall tracer releases in the San Joaquin Valley during July and September, 1979. The three releases to characterize transport from the San Fransisco-Bay area (Manteca and Livermore) showed preferential transport down the western side of the San Joaquin Valley during the day with no tracer detected in Fresno. The eddy circulation on the east side of the valley restricted the tracer to the west side during the two morning releases in Manteca.

During the afternoon Livermore release, the majority of the
tracer was restricted to the west side probably as a result
of the channeling by the strong, valley-wide northwest
flow. The morning after the two Manteca tracer releases,
low levels of tracer (less than 10 parts per trillion
(ppt) were widely dispersed north, east and west of Fresno
which indicated transport by the Fresno eddy. Most of the
tracer from the Livermore release remained in the valley
spread out north of Fresno (10 to 20 ppt) the following day
probably due to the later release time (1510 to 2030 PDT)
restricting the transport south. Tracer was not sampled
further south than Fresno during these three releases. An
afternoon release from Reedley in the Sierra foothills 30
kilometers south-southeast of Fresno (1200 to 1700 PDT)
resulted in two tracer plumes moving east and northeast due
to the upslope windshift during the release. The tracer
plume was detected at 1830 PDT (85 ppt) between Whittaker's
Forest and Lodgepole in Sequoia National Forest and Sequoia
and Kings Canyon National Parks, respectively (transport
speed of 8 kilometers per hour). The tracer remained in
that area the entire night dropping to zero the next day
during the afternoon upslope flow. Since little of the
tracer was transported out of the valley by upslope flow
during the day of the release and trace levels of tracer
material were found the next day in the valley, it was
uncertain whether the bulk of the tracer on the following
day was transported upslope and out of the valley or was

merely highly dispersed within the San Joaquin Valley. A significant amount of tracer (31 ppt) was detected at 0500 PDT at Huron on the west side of the San Joaquin Valley indicating downslope and eddy transport. Results from a tracer release 2 days later indicated 25 percent of the Reedley tracer release was possibly still in the valley giving the tracer an approximate 2 day residence time within the valley. An aerial nighttime release into the nocturnal jet (at 400 meters above ground level) along Highway 99, north of Fresno, showed that the majority of the tracer was transported south to Bakersfield and remained aloft. Unfortunately, tracer sampling ended at 1500 PDT the following day while the tracer was still aloft and the subsequent path of the tracer was unknown. It was suggested that, as the mixing depth developed, the tracer would have been mixed downward to the ground in the southern end of the valley. An afternoon release in the coast range west of Highway 152 resulted in the tracer being carried aloft and out of the valley in a convergence zone of the upslope flows from both sides of the coastal mountains.

Two of the six fall releases were from Oildale, north of Bakersfield, to document transport from the San Joaquin Valley into the Mojave Desert and are discussed later. A release from Fellows on the east side of the coast range in the southwestern valley had similar results as the summer release in the coast range. The release, however, was in

the morning hours (0700-1220 PDT) and the flow on this day
in the low levels was easterly. The next release from
Fellows four days later was conducted shortly after
midnight (PDT) and downslope drainage flow (until 0900 PDT)
transported the tracer eastward and subsequently into the
Mojave Desert the following day. A release from Oildale,
north of Bakersfield, just before midnight (PDT) resulted
in the tracer being transported to the northwest in the
drainage flow and then upslope into Sequoia National Forest
the next day with none detected in Bakersfield. A morning
release from Manteca was directed south along Highway 99
unlike the July Manteca releases which were transported
further west. Tracer was detected in Bakersfield beginning
25 hours after the release (16 kilometers per hour
transport speed). The following day, the majority of the
tracer was still in the east-central valley until midday
when afternoon instability began.

The extensive project by Blumenthal et al. (1985)
included continuous measurement of ozone (25 sites),
surface winds (32 sites) and upper-air wind data (2 sites)
and periodic aircraft soundings (morning and midday), pibal
or airsonde wind measurements (4 sites plus airport),
hydrocarbon sampling (surface and aerial) and tracer
measurements (3 Bakersfield releases, surface and aerial)
throughout the southern and central San Joaquin Valley from
July 15 through August 18, 1984. The midday median mixing
heights (above ground level) were found to be 60 percent

deeper at the edges of the valley (Fresno, Wonder Valley, Oildale, Bakersfield and Arvin) than in the center (Sierra Sky Park, Selma and Buttonwillow) possibly from the upslope flow on the valley sides causing compensating sinking motions in the valley center. The mixing depth was typically 200 meters greater in the Bakersfield area than the Fresno area probably due to the narrowing of the valley in the southern end. During the study period, the mixing height (determined from afternoon temperature profiles from aircraft spirals) at any one site varied between 15 and 20 percent and in the Fresno and Bakersfield areas, median mixing heights ranged from 600 to 925 and 1100 to 1125 meters above ground level, respectively. Wind speed turned out to be a more important factor than the mixing height in the day/night ozone variation. The average wind run was 50 percent higher on low ($\leq$12 parts per hundred million or pphm) than on high ($\geq$12 pphm) ozone days.

The Fresno "plume" (peak hour concentrations) impacted areas from northwest to southwest of the city and most frequently impacted areas directly to the east. These directions were determined by aircraft spirals and traverses, surface ozone monitoring stations and surface streamlines constructed from the 32 surface wind stations. In general, the maximum ozone concentration in Fresno occurred between 1500 and 1700 hours (PDT) and a lesser peak frequently occurred in the late morning. The morning peak was probably from the recirculation of the Fresno air

mass carried north in the morning by the Fresno eddy and then returned when the winds shifted to the upslope or up-valley (toward Bakersfield) direction. The afternoon pollutant-laden air mass probably reached Visalia by the evening (2000 to 2100 PDT) and continued on to the southeast during the night. As in a previous study (Smith et al. 1981), occasionally more than one ozone plume was observed due to the southeasterly to westerly wind shift. The afternoon ozone peak in Visalia (1500 PDT) was not associated with the afternoon peak in Fresno and was attributed to emissions from Highway 99 by calculation of back surface trajectories. The Bakersfield afternoon plume impacted areas to the east-southeast or southeast. As observed in Fresno, pollutants were recirculated back to Bakersfield from a mid-morning southeast to northwest wind shift. The eddy at Bakersfield, largely a result of the downslope winds from the mountains to the southeast, was smaller and less well defined than the Fresno eddy. A tracer release conducted 18 kilometers southeast of Bakersfield at 1630 to 1830 PDT was initially transported out of the valley but close to 10 percent returned in the nocturnal drainage flow and was detected at Delano (30 miles north-northeast of Bakersfield) at 0600 PDT the following morning. Tracer was also detected at Lake Isabella (800 meters elevation) in the Sierra to the northeast at 0100 PDT (no additional samples were taken after this time).

After analyzing various correlations and back-
trajectories, the sources of morning ozone background
levels were uncertain. It was suggested that the morning
background ozone levels were determined by the regional
ventilation rates and were probably transported from the
north or northwest of the region in question. Residence
time for pollutants was estimated to be no more than two
days within the valley agreeing with the previous study by
Smith et al. (1981). The morning and afternoon average
background values upwind from Fresno and Bakersfield were
eight pphm. Fresno and Bakersfield, on average, added 40
percent (5 to 6 pphm) to the afternoon background levels
resulting in average downwind ozone concentrations of 13 to
14 pphm.

In 1973, Carroll and Baskett (1979) investigated two
episodes of pollutant fumigation in Yosemite National Park
following persistent periods of stagnation in the Central
Valley. Synoptic conditions favoring an extended sea
breeze brought the elevated pollutant concentrations into
the mountains. Evidence of counterflow was observed in the
vertical profiles of oxidant and water vapor over Yosemite
Valley. The scenario of a period of stagnation followed by
an extended sea breeze was estimated to occur less than
three times per month in the summer.

A 10 day study conducted in 1970 by Miller et al. (1972)
used aircraft and ground stations to trace oxidant
transport into the Mineral King Valley (upper East Fork of

the Kaweah River) of Sequoia National Park. They found
that nighttime oxidant concentrations were preserved in the
mountains whereas in Fresno, oxidant concentrations fell to
zero. They attributed this to the lack of fresh sources of
nitric oxide in the mountains which converts ozone to
nitrogen dioxide and oxygen. The report concludes that
Fresno is probably the geographic origin of the daily
oxidant peaks observed at Hammond at 1800 PDT and the
following day in the Mineral King Valley at 1700 PDT.
Hammond is 20 kilometers west of the Mineral King Valley at
the confluence of the East Fork and the Middle Fork of the
Kaweah River. The aircraft flights showed a distinct
elevated oxidant layer over Three Rivers (5 kilometers
southwest of Hammond at 260 meters elevation) between 350
and 1570 meters above ground level at midday and in the
afternoon but not in the early morning .

A tracer study was conducted in Sequoia National Park
during the summer of 1985 (Shair 1986). The preliminary
results of three daytime tracer releases from Woodlake (17
kilometers northeast of Visalia) showed tracer transported
to Emerald Lake 45 kilometers to the northeast at 2800
meters in elevation. The transport speed varied from 10.5
kilometers per hour (3 meters per second) during a frontal
storm to less than 1 kilometer per hour (0.3 meters per
second) under clear sky conditions. The previously
mentioned report by Lehrman et al. indicated a transport
speed of 8 kilometers per hour from Reedley in the

foothills to Grant Grove in Kings Canyon National Park.
Using 8 kilometers per hour as an approximate transport
speed from Fresno to Hammond, an air parcel beginning in
Fresno at 0900 PDT would reach Hammond by 1930 that
evening. The more probable case would be a transport speed
of less than 5 kilometers per hour beginning at 1100 PDT
which would transport the Fresno parcel to Hammond by 0300
PDT the next morning. Since downslope winds begin near
sunset, an air parcel from Fresno would never arrive at
Hammond. The oxidant peak in Hammond occurred at 1800 PDT
(Miller et al. 1972). A more likely source for the Hammond
ozone peak would be the upwind areas westward as far as and
including Visalia (40 kilometers east-southeast of
Hammond).

The results of the transport studies above do not resolve
the relative importance of the two major ventilation
mechanisims for the San Joaquin Valley during the summer,
namely, the daytime upslope flow over the Sierra and the
up-valley flow over the Tehachapi Mountains. Smith et al.
(1981) suggested the flow out the southern end of the
valley was the major mechanism whereas Blumenthal et al.
(1985), indicated the Sierran upslope flow was the more
important mechanism. Pilot balloon observations in the
Sierra and San Joaquin Valley showed the mixing depth was
greater at the higher elevations compared to the valley
(Smith et al. 1981). To account for the increased
horizontal flux, air was assumed to be drawn in laterally

from layers above the valley floor. The air drawn in
laterally was estimated to account for 70 to 80 percent of
the total upslope flux. The relative importance of the
upslope ventilation was stated to be further reduced by the
return of pollutants in the nocturnal drainage flow.
Tracer releases also indicated only air at the edges of the
valley was effectively transported upslope into the Sierra.
The calculated flux (volume of air per unit time) for July
from Fresno to Bakersfield (below 1200 meters) indicated
that upslope flow may have accounted for half of the flux
but insignificantly contributed to the flux between
Stockton and Fresno. The flux above 1200 meters in
Bakersfield may have accounted for half of the excess flux
in Fresno due to the low-level nocturnal jet indicating the
northwest flow was diverted over the blocked air mass in
the southern valley and transported over the Tehachapi
Mountains.

A conceptual model was developed to integrate the results
from one of the San Joaquin Valley studies (Smith et al.
1981). They suggested that the excess flux from the
nocturnally blocked northwesterly flow forms a convergent
zone in the southern portion of the valley resulting in
small compensating upward vertical motions within the
Fresno eddy with a divergent zone above. This type of
circulation would transport pollutants from lower levels to
levels where they could be transported by winds aloft.
This is one explanation for the complex layering aloft

frequently seen in aircraft spirals over the valley. The many possible mechanisms for the pollutant layering preclude simple explanations. The decoupling of the surface layer with the layer aloft by the nocturnal inversion acts to conserve the pollutant layer above while the surface pollutants are subject to surface and chemical destruction mechanisms. The decoupling is underscored by the low-level nocturnal jet which frequently forms at or above the inversion top. Another mechanism would involve winds above the mixing layer or inversion layer which move in a different direction than the surface winds thus transporting air aloft from a different origin. During more stable synoptic conditions, the mixing layer within the valley may never develop enough during the day to mix in the layers aloft thus conserving the pollutant layering. One early morning profile over the southern San Joaquin Valley showed high concentrations at the base of an elevated temperature inversion (1200 meters above ground level) which most likely represented the maximum mixing depth from the previous day . Another profile made shortly after midnight the next day showed higher concentrations in an elevated layer isolated from the surface but trapped by the nocturnal stable layer (Blumenthal et al. 1985). These layers were probably mixed to the surface the following day during unstable afternoon conditions.

Although probably much less significant, the importance of nocturnal ventilation over the Tehachapi is relatively

unknown as well. One early morning aircraft spiral made to the south of Bakersfield found peak ozone concentrations at the ridge level and it was speculated that some of this was probably transported over the mountains into the Mojave Desert (Blumenthal et al. 1985). A paper by Giroux et al. (1981) discussed results from two nights of aircraft sampling in the southern San Joaquin Valley. He found, during one of the nights, a nocturnal "ozone reservoir" over Bakersfield which was decoupled from the surface by the nocturnal jet flow. At 2000 PDT, the vertical profile showed ozone concentrations increasing from 2 pphm at the surface to 10 pphm at 100 meters and 12 pphm at 2000 meters (above ground level). At 0345 PDT, the ozone concentrations were less than 2 pphm at the surface increasing to 8 pphm at 1000 meters and beginning to decrease above 1600 meters (above ground level). Since the average Tehachapi ridge elevation is approximately 1500 to 1800 meters elevation (Tehachapi Pass and Tejon Pass are approximately 1200 meters elevation), it was probable that with the northwesterly flow, the ozone reservoir was not only being depleted at the ground but also being transported over the mountains.

An investigation of transport into the Mojave Desert reported an association of nighttime particulate lead concentrations with winds from the direction of the San Joaquin Valley at a site eight kilometers east of Tehachapi Pass in the Mojave Desert (Flocchini and Myrup 1986).

Nighttime particulate lead levels were thought to be higher than the daytime levels due to the concentrating effect of the stable, shallow nocturnal drainage flow as compared to the dispersing effect of the unstable afternoon flow. Two of the tracer tests during the study by Smith et al. (1981) were morning releases from Oildale (just north of Bakersfield) to investigate transport to the Mojave Desert (1981). Both releases indicated the high nighttime levels of pollutants were associated with the afternoon upslope flow in the southern end of the San Joaquin Valley impacting the Mojave desert between 2000 and 2100 PDT. Initially, southeast winds transported the tracer to the northwest but when the winds shifted beginning at 1100 PDT, the tracer was transported out of the valley. Tracer was transported to the northeast through southeast over the southern Sierra and Tehachapi Pass. From a mass balance calculation it was estimated that 70 to 80 percent of the tracer was transported into the Mojave desert by the night following the release with 10 to 20 percent transported to the southern half and the rest transported to the northern half. An estimated 15 percent remained in the southern San Joaquin Valley the same night and 5 percent the next day. The dilution factor from Bakersfield and Oildale to the Mojave was only two to three and agreed well with the conserved aerosol dilution factors. Comparing these factors to the unconserved aerosol species indicated that sulfates were created and nitrates were scavenged from the

valley to the Mojave. A release from the Los Angeles Basin allowed comparison of the sulfate mass distribution between the Los Angeles and San Joaquin Basin air masses. The Oildale aerosol mass was distributed around 0.1 to 0.2 microns aerodynamic diameter indicating homogeneous gas phase conversion of sulfur dioxide. The Los Angeles aerosol mass distributed around 0.5 microns aerodynamic diameter indicating heterogeneous droplet phase conversion. It was determined from Mie scattering calculations that the air mass from the Los Angeles Basin would degrade visibility more than the San Joaquin Valley air mass. Although the release times for the two Oildale releases were different (0700 to 1200 PDT and 0200 to 0700 PDT), the similarity of the results demonstrated that the time of maximum impact of sources in the southern San Joaquin Valley upon the Mojave Desert occurred during the late evening corresponding to the afternoon upslope flow in the San Joaquin Valley. The peak in visibility degradation, as measured by particle absorption, corresponded to the peak in tracer concentration. Visibility was aproximately 100 kilometers between 1600 and 1800 PDT and was 60 kilometers between 2200 and 2300 PDT. The degraded visibility continued until 1000 PDT the next day indicating pollutant impact the entire night and next morning. This timing corresponded to the wind shift to southeasterly or upslope as seen at the Tehachapi site in the previously mentioned study (Flocchini and Myrup 1986). These two tracer releases contrasted with

results from a nighttime Oildale release (2200 to 0337 PDT)
11 days later. During this test, the tracer was wholly
transported during the day to the northeast into the Sierra
where only low levels were detected due to rapid dispersion
by unstable afternoon conditions. No tracer samples were
taken in the Mojave Desert, however.

3. Summary

Smith et al. (1981) first reported on the Fresno eddy
circulation in the San Joaquin Valley. The San Joaquin
Valley nocturnal jet has been documented by several authors
(Willis and Williams 1972; Morgan 1974; Smith et al. 1981;
Blumenthal et al. 1985). The land-sea breeze and summer
monsoon in California have also been well studied (Cramer
and Lynott 1961; Scroeder et al. 1967; Carroll and Baskett
1979; Lamb and Shair 1977). The complex mountain and
valley air flows have been studied to some extent in the
Sierra Nevada (Countryman and Scroeder 1959a; Miller et al.
1972; American Meteorological Society 1978a; Carroll and
Baskett 1979; Lehrman et al. 1980; Shair 1986). While the
individual subjects have been studied in some cases
extensively, no single study has ever attempted to study
the interaction between the various phenomena and how they
are influenced by synoptic weather patterns.

Lamb and Shair showed that pollutants are transported
from the bay area into the northern San Joqüin Valley.
Smith et al. (1981) showed that pollutants were
preferentially transported down the west side of the San

Joaquin Valley that originated from the north. They also showed that the Fresno eddy and the nocturnal jet occurred frequently during the summer. Blumenthal et al. (1985) could not identify the sources of morning ozone levels and concluded that they were determined by regional ventilation rates. Lehrman et al. (1980) indicated the Fresno pollutant plume impacted areas to the east and southeast while Blumenthal et al. found the plume impacted areas northwest to southwest of Fresno with the most frequent direction being east. Smith et al. associated the Visalia afternoon peak ozone levels to emissions from Highway 99. Both Blumenthal et al. and Smith et al. agreed that the overall summer residence time of pollutants in the San Joaquin Valley was less than two days. While Blumenthal et al. contributed the major ventilation mechanism to upslope flow over the Sierra, Smith et al. contributed it to upslope flow over the Tehachapis. The importance of nocturnal ventilation over the Tehachapis was also inconclusive from the various studies.

Carroll and Baskett (1970) observed synoptic conditions favoring an extended sea breeze which, when preceeded by periods of stagnation in the San Joaquin Valley, brought elevated pollutant concentrations into the Sierra. Miller et al. (1972) attributed afternoon ozone levels in Hammond and Mineral King to ozone transport from Fresno. The timing of the peak ozone levels, however, did not correspond as reported by Miller et al. when compared to a

tracer study by Shair (1986).

A conceptual model was developed by Smith et al. for the Fresno eddy circulation. They suggested that a convergent zone in the southern portion of the valley resulted in small compensating vertical motions within the Fresno eddy with a divergent zone above allowing transport of pollutants from lower levels to levels where they could be transported by winds aloft. A model is currently being developed for the National Park Service by Systems Application, Inc., in San Rafael, California, to model ozone concentrations in the San Joaquin Valley for impacts on the western slopes of the Sierra using large urban areas in the San Joaquin Valley and Bay Area as source regions (Henderson 1987). A draft of the first phase has been completed which modeled ozone concentrations for two summer days in 1984 for which an extensive data base was available. This phase focused on Sequoia and Kings Canyon National Parks. The next phase will include a larger area and a longer and more varied meteorological period. The model being used is a modified version of an established regional transport model (RTM-3) that has been used extensively in Canada, Europe and eastern United States. The model was originally used for sulfate and sulfur dioxide and has been modified to include ozone. A draft report of the second phase should be completed by fall of 1987.

The immense data sets from some of the larger studies

(Smith et al. 1981, Blumenthal et al. 1985) have produced much information and probably much more information could be extracted with further analysis of these data sets. At the same time, these studies have had spread out networks, not included the mountain areas and operated under limited synoptic weather conditions. Important questions remain unanswered. It may be necessary to conduct a valley-wide sampling network, including the Sierra Nevada and coast range as well as the San Joaquin Valley and foothills, with a grid spacing of 10 kilometers as suggested by Myrup et al. (1983) for the Sacramento Valley. There is presently a project being planned which will investigate the air pollution/meteorology of the entire San Joaquin Valley including from the Delta region to the north to the Tehachapis to the south and from the coast range to the west to the Sierra (up to 9000 feet elevation) to the east (Ranzieri 1987). This project will probably begin in 1989 with some preliminary work possibly in 1988. The project will involve monitoring ozone and possibly PM-10 (respirable size particulate matter) pollutants. A 20 member Policy Committee with representatives from all participating agencies together with the Valley County Board of Supervisors (8 counties represented) will direct the contracted studies. The five to seven year project will investigate pollutant transport in light of questions based on policy concerns on growth and clean air in the San Joaquin Valley.

CHAPTER III

EXPERIMENTAL DESIGN

A. Introduction

The field data were collected at three sites in Sequoia National Park during two ten day intensive sampling periods in July and August of 1985. The data from the July intensive were incomplete due to equipment problems. At all three sites single theodolite tracked pilot balloons were released 4 times a day and twice nightly 50 percent of the time. The calculated ascent rate was 3 meters per second (30 gram free-lift weights). Observations were recorded every 30 seconds yielding wind observations every vertical 90 meters. The Atmospheric Science Department of Fresno State University also released 4 balloons per 24 hour period in Fresno which roughly corresponded to the release times used in the Park. For the three sites in Sequoia National Park, a pre-addressed and pre-stamped post card was placed in each pilot balloon requesting information on date and place found. Only one post card was returned out of approximately 50. The post card found was released in Ash Mountain at 0700 PDT on August 15th, 1985, and found in the Tablelands between Pear lake and Moose Lake on September 1st, 1985 (approximately 19 kilometers to the northeast, 2730 meters higher in elevation).

At all three sites, ground weather stations were set up with instrumentation measuring wind speed, wind direction,

relative humidity and temperature at five meters and temperature again at two meters. Every 30 minutes mean relative humidity, temperature and wind speed, mean wind vector magnitude and direction and standard deviation of direction were recorded.

In addition to the above, two large tethered balloons were operated at the middle elevation site. On one balloon was attached a meteorological sounding package (tethersonde) which measured pressure (change), dry-and wet-bulb temperatures, wind speed and wind direction. On the tether line of the other balloon, two-staged stacked filter unit aerosol samplers were attached at intervals of 50 meters up to 250 meters above the ground. The filters were analyzed for elements sodium to lead using an alpha particle induced x-ray emission (PIXE) technique developed at the Crocker Nuclear Laboratory at the University of California, Davis (Cahill et al. 1984). In addition, the filters were weighed using a Cahn electrobalance and the fine filters were analyzed for carbon soot and elemental hydrogen.

This study was the first time the aerosol sampling balloon system was employed in the field to collect real time data. The system was, however, tested prior to the present study at the University of California, Davis, for short periods. A total of five morning, nine afternoon and three evening aerosol profiles were made during the August field period. A total of 7 morning, 15 afternoon and 7

evening meteorological profiles were made as well. The
date, time and duration of each aerosol sampling period or
tethersonde ascent and descent for July and August are
presented in Table 1. For the aerosol samplers, the listed
time is when the first sampler began and total minutes is
the longest sampling time usually corresponding to the
highest level. For each sampling level, the total time was
5 minutes , on average, less than the level above it. If,
for example, all 5 levels were operating, then the sampling
time difference between the lowest and highest level would
have been approximately 20 minutes. Also included in Table
1 are the Fresno temperature, dewpoint temperature and
station pressure.

B. Location

The three experimental sites were located at or near
Sequoia National Park's long-term primary acid deposition
research sites established in 1982 through funding from the
congressionally mandated 10 year National Acid Deposition
Assessment Program. A map of California with the study
area outlined is shown in Figure 3. Figure 4 is a map of
the Marble Fork of the Kaweah River watershed drawn from 15
minute quadrangles (1:62,500 scale, 80 foot contours) with
contour intervals at every 400 feet. The heights shown are
in hundreds of feet above mean sea level. On the south
side of Elk Creek at the 2400 foot contour level (24) is
the Park's lower elevation research site. The Park's mid-
elevation research site is in the Giant Forest area (GF)

Date	SAMPLERS Time	Tot. Min.	Levels	TETHERSONDE Time (PDT)	Min. Up	Min. Down	FRESNO deg. C T	DT	mb P
7/25	0934	59	0,1,2	1005	34	--	30.0	17.8	997.8
7/26*	0920	70	0,2	0959	23	--	28.3	16.7	1001.2
7/26	1242	72	0,1,2,3	1300	09	--	35.6	15.0	1000.2
7/26*	1426	34	0,4	1440	09	--	36.7	15.6	999.2
7/27				1354	08	17	37.8	12.8	999.2
7/28				0838	26	18	26.7	13.9	999.8
7/28				1101	15	08	31.7	12.8	999.5
7/28				1143	12	05	33.9	11.1	999.2
7/28				1220	12	10	36.7	10.0	998.8
7/28				1647	22	14	38.3	8.9	996.4
7/28				1818	17	15	37.8	8.3	996.1
7/28				2224	22	14	26.7	13.9	997.5
7/29				0411	13	10	18.9	10.6	998.5
7/29				0624	27	20	16.7	11.1	1000.5
7/29				0746	20	15	17.8	11.1	1001.2
7/29				0857	20	12	19.4	11.7	1001.5
7/29				1132	09	12	26.1	11.1	1001.2
7/29				1255	18	13	28.9	10.0	1000.8
7/30				0743	17	17	17.2	12.2	1002.5
7/30				0855	19	12	20.0	12.8	1002.9
7/30				1114	17	27	23.9	12.8	1003.2
7/30				1510	13	18	30.6	12.8	1001.5
7/30				1805	14	11	31.7	10.6	999.5
7/30				2208	14	09	25.0	12.2	999.8
7/31				0727	12	07	17.7	11.7	1002.5
7/31				1138	13	16	25.0	12.2	1003.2
8/13	1020	83	1,2,3				23.3	12.2	1003.9
8/14	1416	92	1,2,3	1445	37	17	32.2	10.6	1000.8
8/15	0902	96	1,2,3	0845	45	16	22.2	12.2	999.5
8/15*	1446	97	1,2	1450	16	13	33.9	11.7	997.0
8/16	0859	128	1,2,3,4	0923	11	24	23.9	13.3	997.1
8/16				0958	25	20	23.9	13.3	997.1
8/16	1643	134	1,2,3,4	1649	18	17	34.4	12.8	994.4
8/16				1656	16	15	34.4	12.8	994.4
8/16				1811	17	20	33.9	12.2	994.1
8/17				0824	28	28	17.8	13.9	1001.5
8/17	1627	134	2,3,4,5	1629	46	40	29.4	15.6	1000.8
8/17				1755	16	17	29.4	15.6	1000.5
8/18	0936	134	2,3,4,5	0954	22	30	20.0	12.8	1006.3
8/18				1127	27	28	25.0	15.0	1005.9
8/18	1648	102	2,3,4,5	1640	25	13	31.7	14.4	1003.2
8/18	2301	109	2,3,4,5	2324	21	17	22.8	11.7	1003.2
8/19				0002	39	22	22.8	11.7	1003.2
8/19	1443	115	1,2,3,4,5	1448	29	35	30.6	12.8	1003.2
8/20	1002	106	2,3,4,5	1056	38	32	26.7	14.4	1003.2
8/20				1206	26	30	29.4	13.9	1002.9

Table 1: Schedule of tethered balloon systems (see next page).

	SAMPLERS			TETHERSONDE			FRESNO		
Date	Time	Tot. Min	Levels	Time (PDT)	Min. Up	Min. Down	deg. C T	deg. C DT	mb P
8/20*	1638	106	2,3,4,5	1639	31	20	33.3	10.6	1000.2
8/20				1730	22	06	33.9	9.4	999.8
8/21*	0406	112	1,2,3,4	0414	20	23	18.9	8.9	1002.5
8/21				0457	22	21	18.3	8.9	1002.5
8/21				1402	48	28	32.8	12.2	1003.6
8/21	1656	112	2,3,4,5	1704	31	40	34.4	11.1	1001.9
8/21				1900	43	29	33.3	11.7	1001.5
8/21	2216	121	1,2,3,4	2053	36	29	28.9	13.3	1002.2
8/21				2251	43	33	25.6	12.2	1002.9
8/22*	1349	114	2,3,4,5	1456	22	15	35.0	10.6	1002.9

* 7/26: (0920) 100m batteries exploded at unknown time, 70 minutes estimated.

7/26: (1426) 200m batteries exploded at unknown time, 29 minutes estimated.

8/15: 50m sampler brought down early due to high windspeed, total time was 32 minutes.

8/20: 250m intake tube came off at unknown time, 106 minutes estimated.

8/21: 50m batteries quit at unknown time, 97 minutes estimated.

8/22: 100m batteries quit at unknown time, 102 minutes estimated.

Table 1 (cont'd.): Schedule of tethered balloon systems. For samplers, time indicates when the first pump began and total minutes indicate the longest sampling time usually corresponding to the sampler at the highest level (except where indicated). The levels 0, 1, 2, 3, 4 and 5 correspond to 0, 50, 100, 150, 200 and 250 meters, respectively. The sounding schedule shows the starting time and indicates the duration of the up and down soundings. Also listed are Fresno temperature (T), dewpoint temperature (DT) and station pressure (P).

Figure 3: Map of California.

FIGURE 3: Map of California.

Site Locations:
AM-Ash Mountain (560m)
WV-Wolverton (2222m)
EL-Emerald Lake (2633m)

Other Land Marks:
GF-Giant Forest (1950m)
LP-Logdepole (2073m)
MR-Milk Ranch (1900m)

Figure 4:
Map of the Kaweah River
Marble Fork drainage,
Sequoia National Park.
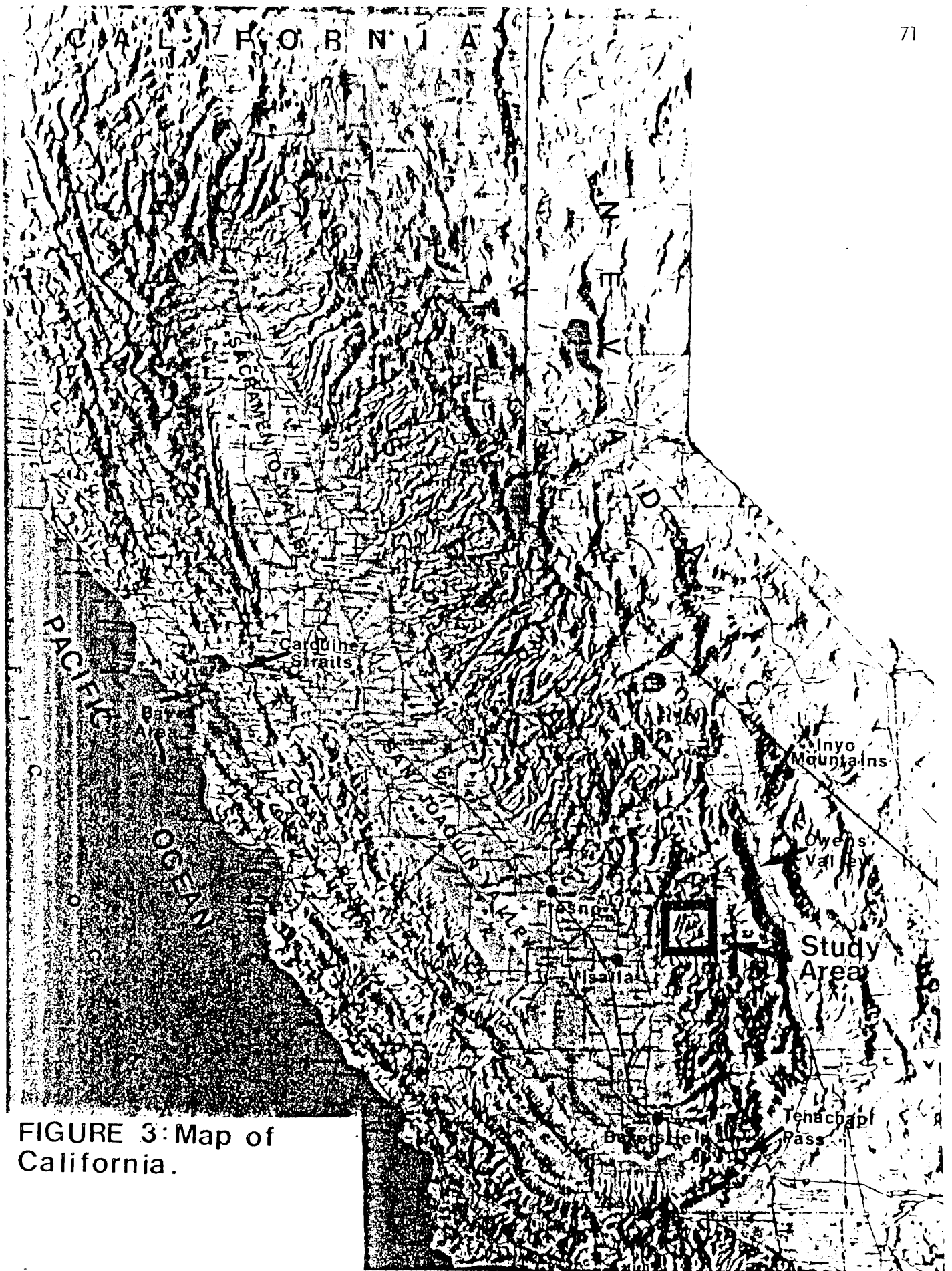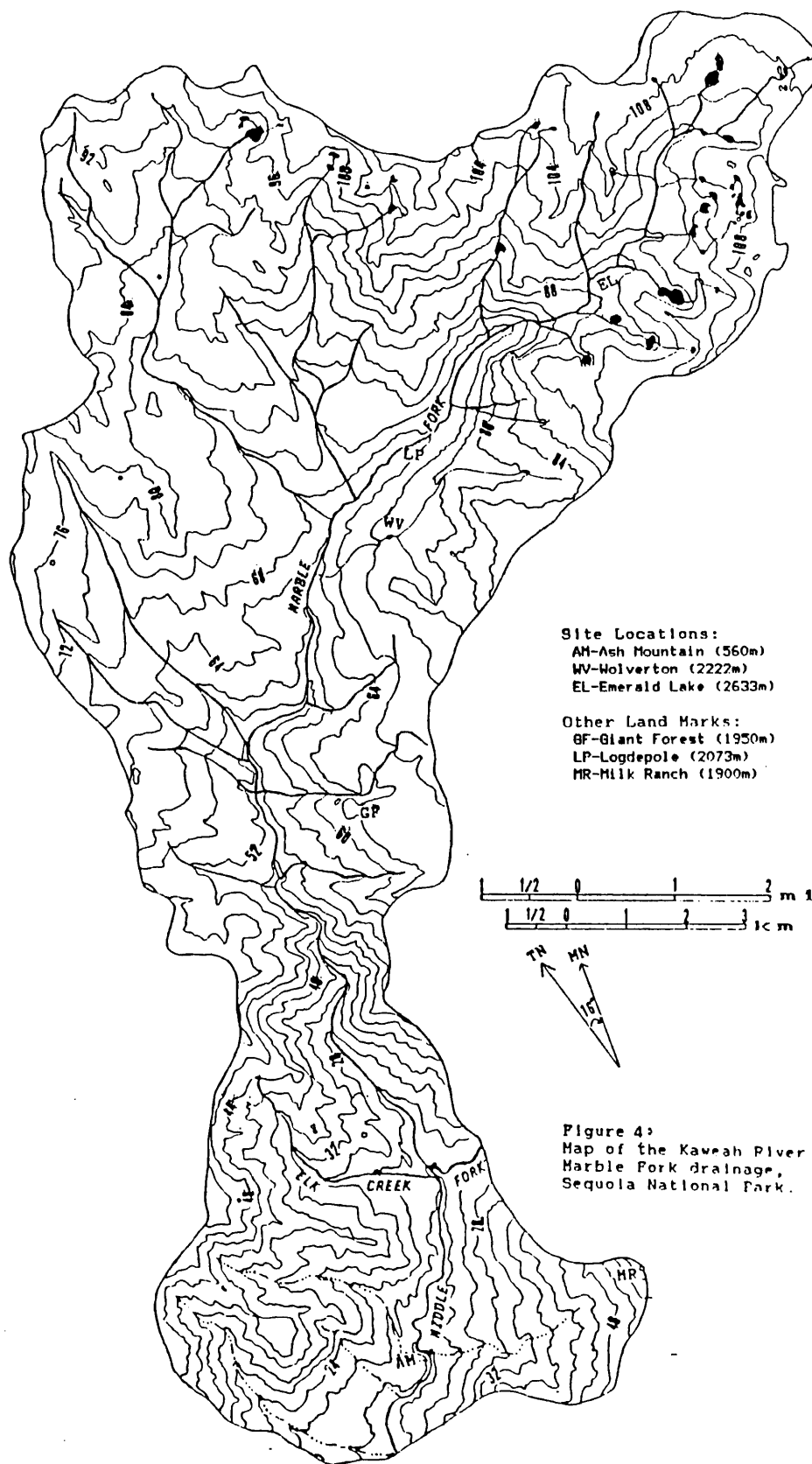
near Log Meadow (not shown). The Park's upper research station is at Emerald Lake proper (second lake up creek that is directly below (south) "EL" in Figure 4).

For this study, the lower elevation site, Ash Mountain (AM), was 125 meters northwest of and 30 meters above the Park Headquarters area at 560 meters elevation. The site was located on a east-southeasterly facing slope in the chaparral community vegetation type. The mid-elevation site, Wolverton (WV), was 1.5 kilometers southwest of the Lodgepole campground and 1 kilometer from the General's Highway by road at 2222 meters elevation. Balloons were launched in the middle of Wolverton Meadow which is surrounded by mixed-conifer community vegetation type. The upper elevation site, Emerald Lake (EL), was 3.5 kilometers east of the Lodgepole campground along the Marble Fork below Pear Lake (large lake to right (east) of "EL" in Figure 4) at 2719 meters elevation. The site was located on a flat granite area sparsely vegetated with sub-alpine community type species. The weather stations were located near the balloon release sites. At Ash mountain, the weather station was located at the Park Headquarters area. The instrumentation was located at seven and ten meters on the Park's meteorological tower instead of at two and five meters above the ground as the other two stations because of the tall oak trees surrounding the area. The weather station at Wolverton was near a maintenance road directly across Long Meadow from the ski resort/trail head parking

lot and was surrounded by low-lying meadow vegetation. At
Emerald Lake, the weather station was located on a large
granite outcrop using a limb on a dead standing tree as the
instrument tower. The "two meter" temperature probe was on
a rock on the ground and the "five meter" instruments were
on a limb four meters above the ground. Regretfully, the
relative humidity probe did not function properly. The
data were recorded on CR21 microloggers (Campbell
Scientific, Inc., Logan, Utah) and transcribed manually
twice a day. A description of the instrumentation is in
Appendix II-A.

The special requirements of the tethered balloon systems,
namely storage area and electricity, greatly limited the
possible locations for the mid-elevation site. Electricity
was not required but was convenient for charging the 12
volt batteries needed for the winch operation and was used
to operate the receiver and printer ground station. It was
for these reasons that the Wolverton site was chosen and as
a result, the features of this location are slightly
different from those at the Park's research site at Log
Meadow in the Giant Forest area (4.5 kilometers to the
south, 150 meters lower in elevation). The other two sites
are more comparable to the Park research sites. The
Wolverton Meadow is in a bowl that faces to the north and
for this reason it is a ski area during the winter season.
Localized inversions are frequent and break up late
morning. The topography has more gradient and is more

complex than in the gently rolling Giant Forest area, a
favored area for the giant sequoia trees.

In Figure 4, the flow is from the top to the bottom of
the page. The Marble Fork drainage meets the larger Middle
Fork drainage in the lower portion of the figure. Below
this, the figure shows a portion of the Middle Fork
drainage where the lower elevation site is located. The
Middle Fork flows to the west before joining the Marble
Fork and subsequently flows to the southwest. Elk Creek
joins the Middle Fork immediately south of the confluence
with the Marble Fork.

The topographic features for the three sites are
presented in Table 2. Fresno is included for comparison.
The values were estimated using 15 minute quadrangle maps.
Directions are from true north and indicate the direction
toward the specified parameter. For example, the up valley
direction for Emerald Lake is 90 degrees. This indicates
that the Marble Fork valley rises toward the east near the
Emerald Lake site. Since the topography is variable and
does not follow a straight line, an imaginary line was
drawn perpendicular to the valley axis and through the site
representing a cross section of the valley at the site.
The direction of a line perpendicular to this at the valley
floor was the recorded up-down valley direction. Valley
floor width was measured by the distance between the two
intersection points of the lowest contour line and the
cross section line. The distance between the first contour

Feature	Emerald Lake	Wolverton	Ash Mountain	Fresno State
Longitude	118.68	118.73	118.83	119.75
Lattitude	36.62	36.60	36.50	36.93
Township	15S	15S	16S	13S
Range	30E	30E	29E	20E
Section	24W	29NE	33E	5SE
Elevation (m msl)	2719	2222	560	100
Height Above Valley Floor (m)	10	200	50	0
Up/Down Valley (degrees)	090/270	080/260	030/210	135/315
Valley Floor Width (m)	250	100	125	100 km
Ridge Height (m msl)	3400 SE 3400 NNW	2750 SE 2450 NW	1900 E 1080 W 1600 NW	1200 W 4000 E 2000 SE
Ridge Height Above Site (m)	680 SE 680 NNW	530 SE 230 NW	1340 E 520 W 1040 NW	1100 W 3900 E 1900 SE
Distance Ridge To Ridge (km)	5 N-S	11 NNW-SSE	7 NW-SE	200 SW-NE
Valley Floor Slope (%)	5	6	5	~0
Upslope/Downslope (degrees)	150/330	135/315	300/120	090/270
Slope Inclination (%)	18	10	23	--

Table 2: Topographic features for study sites.

above and below the valley axis line were used to measure
the valley floor slope. Distance ridge to ridge was
measured by a cross section of the valley perpendicular to
the orientation of the highest ridges on either side of the
valley which was not always the same as the cross section
through the site. To determine the general slope
orientation surrounding the site, the ground weather
station wind directions were also considered in addition to
the maps. Slope inclination was then calculated by a line
drawn from the site to the second 400 foot contour line
above the site using the up-slope direction. For Fresno,
the valley floor was approximated by the distance between
the beginning of the coastal range to the west and the
foothills to the east at the 1000 foot contour levels. The
distance ridge to ridge was taken along the same line but
extended to the Fresno County line on either side. Slope
of the San Joaquin was considered approximately zero.

C. Equipment

1. Aerosol Sampling Unit

The weight of each sampling unit including batteries and
filter cassette assemblage was less than one kilogram. A
review of the aerosol sampling system may be found in
Flocchini (1984).

a. filter cassette assemblage

The stacked filter cassette design is described in
Cahill et al. (1977). The only differences in the
configuration for this study were that an intake manifold

was not used and the filter cassette hung downwards toward the ground from the tether line. For the coarse and fine particle modes, 8.0 micron coated nuclepore filters and 3 micron teflon filters were used, respectively, which were both 25 millimeters in diameter. The manufacturer's filter specifications are listed below.

Filter Type	Mfg. Code	Pore Dia. μm	Pore Dens. pores/cm^2	Filter Thick. μm	Porosity %	Filter Dia. mm	Filter Area cm^2
Teflon[1]	PTFE	3	1×10^5	25	75-85	25	1.1[2]
Nuclepore[4]	N800	8	--	10^3	5	25	3.8

1. Gelman Science, Ann Arbor, Missouri.
2. Masked filter area.
3. Values are for uncoated filters. Apeizon-L grease coated filters (lot 51A8B2) were used during this study which increase the thickness by 30 to 65 μm (actual value unknown).
4. Nuclepore Corporation, Pleasanton, California.

b. motor and pump assemblage

The motors employed (Astro Challenger Cobalt 05 motors designed for model airplanes by Astro Flight) to drive the pumps (modified GAST rotary vane vacuum pumps) were powered by two lithium cell batteries (50 ampere-hour) which lasted approximately 3 to 4 hours without an appreciable decline in output.

During the July field program, it was discovered that the pumps were running at too high a rate and the gear ratio between the motor and pump was reduced by one third for the August field program. This reduced the average flow rate from 11.9 ±1.7 to 10.5 ±1.8 liters per minute but improved the battery performance remarkably resulting in only one

case of battery explosion during the August period rather than a 30+ percent failure rate during the July period.

Flow rates were measured at the beginning and end for each sample and flow volumes were estimated as described in Appendix II-B.The cut-point calculations are also described in Appendix B. The fine particle cut-point was estimated to be between 1.0 to 1.5 microns aerodynamic diameter. The coarse filter probably had no upper cut-point due to the high face velocity (46 centimeters per second) and the absence of an intake manifold. The upper cut-point was calculated to be approximately 123 microns aerodynamic diameter which includes most coarse particles suspended in the atmosphere!

2. Tethersonde

Specifications for the tethersonde package and balloons are contained in Appendix II-C.The meteorological package is described in Morris et al. (1975). Since barometric pressure at the site was not measured, pressure was calculated using Fresno airport hourly station pressure observations and the hydrostatic equation. The equation for this calculation as well as equations for calculating potential temperature, mixing ratio, absolute humidity and other secondary meteorological parameters are presented in Appendix II-D.

D. Filter Analysis

The fine teflon filter was used with a mask to decrease the sample area by 70 percent thus increasing the

sensitivity of the elemental analysis. The samplers were run from one to two hours allowing detection of major elements (present at higher concentrations in the atmosphere) whereas minor elements such as lead and vanadium were frequently below the threshold value. The accuracy of the PIXE elemental analysis, determined by regular re-analysis of filters, is reported as 4 percent for sulfur, 6 to 9 percent for silicon, potassium, calcium, iron and zinc and 10 to 15 percent for copper, lead and bromine (Cahill et al. 1986b). A new analytical method, proton elastic scattering analysis, was used to analyze the fine filters for elemental hydrogen as well. The current accuracy for this method is approximately 15 percent.

Filters were analyzed for gravimetric mass and carbon soot (fine filters only) using a Cahn 25 electrobalance and a laser integrating plate method, respectively (Cahill et al. 1984). The uncertainty associated with the Cahn electrobalance is on the order of two micrograms which would correspond on average to a six and seven percent uncertainty for the fine and coarse gravimetric mass concentrations, respectively. The uncertainty associated with weight gain is discussed below. For the carbon soot calculation, an absorption efficiency of 10 meters squared per gram is used to convert the coefficient of optical absorption to carbon soot concentration. The uncertaintly of the measurement technique is approximately six to seven percent (Cahill et al. 1986b). Table 3 lists the averages

and associated errors for the fine and coarse elemental, gravimetric mass and carbon-soot data.

Filter blanks were prepared and treated as the filters used for sampling except they were not loaded into the filter cassettes. The blank filters did not gain any significant weight. It is possible that the major weight gain for the teflon filters is through interaction with the plastic material of the filter cassettes (Feeney et al. 1984). Weight gain from contact of the teflon filters with the O-ring was avoided by using filter masks. The weight gain has been found to increase over time. Since the filters used for sampling were in the cassettes for no longer than a day and usually less than three hours, the weight gain was assumed negligible and thus no corrections were made to the gravimetric mass values. The weight gain, in general, is less for the nucleopore filter than it is for the teflon filter so corrections for the nucleopore gravimetric mass were also considered negligible.

E. Sources of Error

This section will discuss the various sources of error related to the pilot balloon observations and tethersonde data . These sources of error can only be discussed in light of findings from other studies since no attempts were made at their quantification. Also discussed are the problems associated with the aerosol sampling balloon and the possibility of contamination of the aerosol filters by the carbon vane pump.

1. Pilot Balloons

Wind speed error associated with single theodolite tracked pilot balloon observations was investigated by Swanson et al.(1981) using data from a study conducted in the Delta and Sacramento Valley of Northern California. Variations in ascent rate for the 4, 8 and 12 minute observations from 169 double theodolite profiles showed that some but not all releases had significant variability in ascent rates. No explanation was given as to why some of the releases showed more variability than others. Wind speed profiles were calculated using both theodolite observations and observations from just one of the theodolites and plotted in the same figure. It was evident that the single theodolite profiles showed areas of large, fictitious wind speed shear when the ascent rate was not constant. Some of the windspeeds were three to six times higher than the double theodolite calculated windspeeds. The ascent rate used for the single theodolite calculations was calculated from the computed height of the last double theodolite observation divided by the total time so that the error was minimized for the single theodolite computation. The ascent rate of 1.5 meters per second was also lower than routinely used so the uncertainty resulting from the assumed constant ascent rate as presented by Swanson et al. would be the lower limit in most cases. Wind direction error was not investigated.

The author has made some theoretical error calculations

based on the upper limit of vertical windspeeds found in the literature under normal conditions in mountainous areas (Davidson 1961, 1963). To estimate the possible error, calculations were made for conditions with 2 and 5 meters per second vertical windspeeds. On the average, vertical windspeeds are approximately two meters per second during unstable convective afternoon conditions and five meters per second represents the upper limit. Downdrafts of up to seven meters per second have been observed on the lee side of ridges with an ambient wind perpendicular to the ridge line (Davidson 1961). This effect is most prominent close to the ridge and damps out at horizontal distances three to four kilometers from the ridge line (Davidson 1963). The three sites for the present study were at least that far from the major ridge lines. The measured values in the table below are calculated using the assumed ascent rate of three meters per second and the actual values include the additional height due to the indicated vertical wind speed. The difference amounts to approximately 60 percent in every case. As the elevation angle approaches 90 degrees, the difference between the windspeeds becomes less than one (it is 0 at 90 degrees).

WIND SPEED	ELEVATION ANGLE (degrees)				
	15	30	45	60	75
Measured 2 m/s	11.4	5.3	3.0	1.8	0.8
Actual	18.8	8.7	5.0	2.9	1.4
Difference 5 m/s	7.4	3.4	2.0	1.1	0.6
Actual	30.1	13.9	8.0	4.6	2.2
Difference	18.7	8.6	5.0	2.8	1.4

Note: All values are in meters per second.

For updrafts, then, the wind speed is underestimated and for downdrafts the wind speed is overestimated. Wind speed error was apparent in the profiles from July during a thunderstorm when unrealistically large windspeeds and shear occurred in the data. The error under more normal conditions would be expected to effect only the boundary layer (lower 1000 meters or first 10 pilot balloon observations). This can be seen by comparing the tethersonde wind data with the lower observations of the pilot balloon data. There is good agreement for the morning and evening data and on some occasions the windspeeds are either higher or lower by no more than 2 meters per second during the daytime (especially during afternoon releases). During another study in Sequoia National Park in 1986, several double theodolite pilot balloon releases were made to determine vertical wind speed error for the single theodolite releases. Calculations were performed using a vector method developed by Thyer (1962). Afternoon releases had maximum vertical wind speeds of two meters per second (positive) within the boundary layer and were mostly less than one meter per second. During overcast, thunderstorm conditions, the maximum vertical wind speed still remained under four meters per second. The highest vertical wind speeds were within the first two observations after release. The wind direction should not be affected but since the observations are every 90 meters, small wind direction shifts contained

in layers less than 90 meters would be missed.

2. Tethersonde Balloon

There has been some investigation on balloon borne
instrumentation error. Whiteman (1980, 1981) used the same
meteorological package used in this study to investigate
breakup of inversions in Colorado Mountain valleys. He
conducted a series of tests at the National Center for
Atmospheric Research (NCAR) facilities in Boulder,
Colorado. The instrument package was tested in a wind
tunnel and some attempts were made to simulate the
conditions that might occur while the package was suspended
from a balloon. The standard instrument specifications
from the testing are included in Appendix II-C and will not be
discussed here. One test was to tilt the package 10, 20
and 30 degrees from the vertical and the resulting
wind speed was compared to the true wind speed. As
expected from theory, the package windspeeds were
consistently lower than the true air speed by approximately
the cosine of the angle. The balloon used for the project
was a lightweight (1.5 kilogram) 3.25 cubic meter blimp-
shaped balloon (Follmer Model 115). Field observations
were presented that give insight into the possible errors.
They observed that when the wind speed was greater than 5
meters per second, the balloon drifted downwind causing a
low wind speed on the ascent and a high wind speed on the
descent. A further complication was that on the descent,
the balloon maintained its elevation until nearly above the

winch, at which point it would descend straight down. For this reason, Whiteman did not average the up and down soundings in the data analysis. The balloon's response to changes in wind direction were discussed in view of its dimensions. The balloon was very responsive to light winds, pointing into the wind even when the cup-anemometer was stationary. It was theorized that the balloon would not respond to directional eddies smaller than half the length of the balloon. The balloon was observed to respond slowly to large stepwise changes in the wind direction, especially a 180 degree directional change. During turbulent, convective conditions, it was observed that the tethersonde package swayed as much as 20 degrees away from the balloon orientation. It was summarized that the accuracy was a complex function of the "response time and damping coefficient of the balloon, the response time of the tethersonde compass, the angle of attack of the sonde and the swinging and twisting of the tethersonde relative to the balloon."

They suspended the package below the tail of the balloon to achieve a 25 degree angle of attack under no wind conditions. This positioning was necessary so the balloon would be relatively level at higher altitudes with stronger winds since the tail expands with the increased inside pressure (Morris et al. 1975). During our study, we used balloons purchased from Pie in the Sky (San Mateo, California). The balloon used for the tethersonde package

weighed 6.8 kilograms and was 10.2 cubic meters (see Appendix II-C).Due to its different characteristics, its response was probably slower than the lightweight Follmer balloon but there were several reasons why we chose this balloon. During the July field season, we used the Follmer balloon for the tethersonde package. The balloon was very susceptible to damage, especially if moisture remained on the plastic for any length of time. For this reason as well as the problem of diffusion of air into the balloon, the balloon required constant recharging with helium and often became dis-inflated during a profile. The Pie in the Sky balloons, although heavier, were not as susceptible to damage and required little recharging. We also suspended the tether package differently due to the different lead line configuration. The package was suspended immediately below the front of the balloon. The problem of being in the wake of the balloon was avoided and the package was much more stable due to the reduced length of the suspension lines. Since the lift was greater than the Follmer balloon and the tether line came from the center of the balloon, the balloon was relatively level under no-wind conditions and the front end tilted slightly upwards at higher altitudes due to the expansion cords being located toward the front end of the balloon.

Another study in Florida compared data from ballon-borne (metal-cable tether) and from tower-mounted instrumentation including the mean horizontal wind speed and direction and

the fluctuating components of the horizontal winds, vertical winds and temperature (Haugen et al. 1975). The instrument package on the balloon was attached to a vane which kept the instrumentation pointed into the wind. The blimp-shaped balloon was much larger (1300 cubic meters) than the balloons used during the present study but some salient findings are of interest. The dominant motion of the balloon was lateral oscillation and this motion increased with increasing height above the tethering point. The sensors were located at 500 and 1000 feet with the balloon position varied at 1200, 2000, 3000 and 4000 feet above ground level. The mean horizontal wind speed was overestimated by the balloon instrumentation by 7 and 11 percent at 500 and 1000 feet, respectively. The balloon motion was tracked by two theodolites simultaneously. The average ratio of the standard deviation of the lateral motions of the cable at the two heights (500 and 1000 feet) and the ratio of the horizontal wind speed discrepancy were very close indicating the horizontal wind speed overestimate was largely attributable to the lateral motions of the balloon. It was stated that the effect of the lateral motion could be minimized by increasing the balloon-probe separation. Another study by Ryan et al. (1979) recommended a spacing of 100 to 300 meters between the instruments and the balloon when measurements were taken close to the ground since they observed the instruments swayed as much as 15 to 20 meters from an

imaginary centerline when the balloon was close to the ground. During the present study, the balloon acted as the wind vane and it was not possible to increase the distance from the package to the balloon.

3. Aerosol Sampling Balloon

The balloon used for aerosol sampling during the August field season was a spherically-shaped Pie in the Sky balloon which had more lift than the blimp shaped (JK20) balloon used in July (same balloon used for the meteorological package during August). The JK20 balloon lifted only 3 of the packages whereas the spherical balloon lifted 5 packages. The only problems encountered with the aerosol sampling balloon was at the point of attachment of the sampler on the tether line and the sampling height. During the July period, a JK20 balloon was lost due to the line being cut by the plate edge on which the pump and motor were mounted. In August, the samplers were attached in such a way that the plate could not contact the tether line. Another added feature in August was attachment of the exhaust line to the tether line away from the filter inlet to avoid contamination from the outlet. The aerosol samplers were placed every 50 meters along the tether line. During windy afternoons the balloon tether line was not vertical and sometimes the lower portion of the tether line had an angle greater than 45 degrees from the vertical. No attempt was made to estimate the actual height of the samplers. Much calmer conditions prevailed during the

morning and night so that the tether line was mostly vertical.

4. Filter Contamination

A test was run connecting the exhaust of the pump to the filter inlet to determine if "blow-by" contamination was occuring. Data from one 33 minute sample was used to obtain the ratio of each major element (and carbon-soot) to silica. In the table below are the ratios from the exhaust filter sample (test), balloon data (1) and 24-hour particle samples (2) collected during the same time at Giant Forest (Cahill et al. 1986a). Elements that are not listed but occured in the exhaust sample are fine Mg, Mn, Zn, Br, Cl and Pb and coarse Mg, Mn, Cu, Zn, Cl and Br. These elements were not presented because they are not of interest and most of their concentration errors were larger than 50 percent due to their being trace elements in the atmosphere. The calcium ratio is listed but calcium did not occur in the test sample. The 24-hour samples were from a similar stacked filter unit which was operated at a lower face velocity using an electric pump. The coarse filter collected particles between 2.5 and 15 microns and the fine filter collected particles smaller than 2.5 microns. The sampler height was approximately 2 meters above ground level. The reason the data are presented as ratios is to render the data directly comparable. The exhaust sample was concentrated exhaust whereas the data

FINE

	K/Si	Al/Si	Fe/Si	
Test	.261	.207	8.867	
1	.248(58)	.640(30)	.279(58)	
2	.582(9)	.527(9)	.254(9)	
Soil	.070	.437	.202	
Crust	.074	.292	.200	
	C-S/Si	H/Si	S/Si	Ca/Si
Test	2.159	.156	.433	--
1	5.222(58)	2.359(57)	3.061(60)	.109(36)
2	1.790(9)	2.017(9)	2.850(9)	.136(9)
Soil	--	--	.008	.049
Crust	--	--	<.001	.147

COARSE

	Al/Si	S/Si	Ca/Si	Fe/Si
Test	.621	.141	.099	5.352
1	.657(46)	.207(14)	.151(52)	.294(59)
2	.465(9)	.051(9)	.120(9)	.257(9)
Soil	.433	.027	.070	.182
Crust	.292	<.001	.147	.200

Dashes indicate the numerator is not present in soil.

collected in the field, if contaminated, would show values including the ambient air as well. The values in parenthesis are the number of values that were averaged. Also presented are soil and average crustal (crust) ratios. The soil ratios are from the average of two soil samples collected near the Giant Forest area which were analyzed for elemental concentrations. The crustal values were taken from a report by S.R. Taylor (1964).

The ratio for fine carbon soot (C-S) is higher for Wolverton (1) than Giant Forest (2) indicating that it may be a contaminant from the exhaust. Table 3 gives the averages and associated error for the elemental, carbon-soot and gravimetric mass concentrations. The large standard deviation for the carbon-soot concentration (larger than half the average) indicates the large variability in the data. Considering that the standard

	FINE				COARSE			
	1	2	1	2	1	2	1	2
	Al		Fe		Al		Fe	
avg	189	139	71	69	1217	982	543	575
s	87	46	45	25	847	391	533	202
err	21	11	22	10	39	16	24	12
s	10	<1	10	<1	17	2	11	<1
up	19	9	34	9	29	9	34	9
down	11		25		19		27	
	Si		S		Si		S	
avg	260	268	630	713	1786	2235	320	89
s	136	90	299	123	1239	781	146	16
err	19	10	14	10	25	11	68	82
s	9	<1	8	<1	10	<1	22	7
up	33	9	33	9	33	9	8	2
down	28		29		27		6	
	K		Mass		K		Mass	
avg	61	143	36	14	284	262	27	14
s	33	29	33	2	199	71	15	3
err	33	10	6	1	51	18	7	1
s	19	<1	--	--	17	3	--	--
up	33	9	34	9	19	9	33	9
down	28		29		28		30	
	H		Ca		Ca			
avg	495	499	34	36	273	264		
s	179	76	19	11	194	82		
err	15	15	37	13	45	15		
s	--	--	11	1	17	3		
up	33	9	22	9	30	9		
down	26		15		22			
	C-S							
avg	1119	420						
s	616	108						
err	7	7						
s	--	--						
up	33	9						
down	27							

1. avg=average concentration; s=standard deviation of the concentration; err=average error for concentration; s=standard deviation of the error; up=number of afternoon concentrations in average; down=number of morning and/or evening concentrations in average.
2. 1: Tethered balloon data.
   2: Giant Forest 24-hour data.
3. Elemental concentrations and carbon-soot are in nanograms per cubic meter and gravimetric mass is in micrograms per cubic meter.

Table 3: Aerosol concentrations averaged over all profiles and heights for August 13th through 22nd, 1985.

deviation of the carbon-soot/silicon ratio is 3.9 (0.9 for Giant Forest), it is unlikely that carbon-soot is a real contaminant. The cabins located near the Giant Forest site are probably responsible for the large difference in the average fine potassium concentrations between Giant Forest and Wolverton.

For the coarse particles, the ratios for sulfur and aluminum appear to be higher for Wolverton than Giant Forest. Since the test ratio for aluminum is close to the Wolverton and Giant Forest ratios, it is not possible to determine whether it is a contaminant or not. The difference in the sulfur ratios between Wolverton and Giant Forest may be due to the different cut-points. The coarse filters used for the balloon samplers collected particles larger than 1 micron whereas the coarse filters used at Giant Forest collected particles between 15 and 2.5 microns. The fine sulfur ratios agree fairly well which indicates the discrepancy may be due to larger sulfur containing particles. Since the test sulfur ratio is so much smaller than the Wolverton ratio, if there is contamination, it is probably small. As with the fine carbon-soot concentrations, the standard deviation for the Wolverton coarse sulfur concentration is nearly half the average (Table 3) and the standard deviation of the sulfur/silicon ratio is 0.11 which indicates it is not significantly different from the Giant Forest ratio.